US Army Corps of Engineers

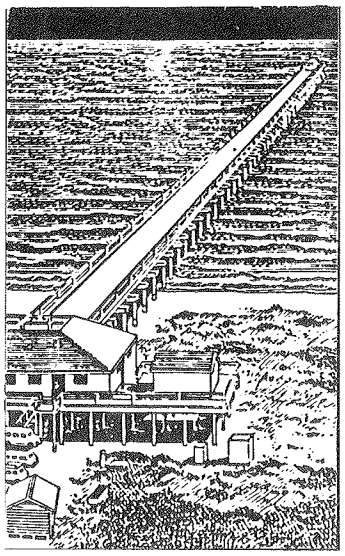

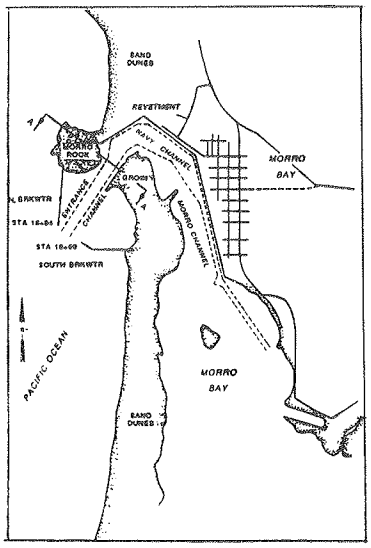

MISCELLANEOUS PAPER CERC-89-13

EFFECTS OF ENTRANCE CHANNEL DREDGING AT MORRO BAY, CALIFORNIA

by

James M. Kaihatu, Linda S. Lillycrop, Edward F. Thompson

Coastal Engineering Research Center

DEPARTMENT OF THE ARMY
Waterways Experiment Station, Corps of Engineers
3909 Halls Ferry Road, Vicksburg, Mississippi 39180-6199

September 1989
Final Report

Approved For Public Release; Distribution Unlimited

Prepared for US Army Engineer District, Los Angeles
PO Box 2711, Los Angeles, California 90053-2325
Under Intra-Army Order No. E86890007

Destroy this report when no longer needed. Do not return it to the originator.

The findings in this report are not to be construed as an official Department of the Army position unless so designated by other authorized documents.

The contents of this report are not to be used for advertising, publication, or promotional purposes. Citation of trade names does not constitute an official endorsement or approval of the use of such commercial products.

Unclassified

SECURITY CLASSIFICATION OF THIS PAGE

REPORT DOCUMENTATION PAGE

Form Approved OMB No. 0704-0188

1a. REPORT SECURITY CLASSIFICATION
Unclassified

1b. RESTRICTIVE MARKINGS

2a. SECURITY CLASSIFICATION AUTHORITY

2b. DECLASSIFICATION/DOWNGRADING SCHEDULE

3. DISTRIBUTION/AVAILABILITY OF REPORT
Approved for public release; distribution unlimited.

4. PERFORMING ORGANIZATION REPORT NUMBER(S)
Miscellaneous Paper CERC-89-13

5. MONITORING ORGANIZATION REPORT NUMBER(S)

6a. NAME OF PERFORMING ORGANIZATION
USAEWES, Coastal Engineering Research Center

6b. OFFICE SYMBOL (If applicable)

7a. NAME OF MONITORING ORGANIZATION

6c. ADDRESS (City, State, and ZIP Code)
3909 Halls Ferry Road
Vicksburg, MS 39180-6199

7b. ADDRESS (City, State, and ZIP Code)

8a. NAME OF FUNDING/SPONSORING ORGANIZATION
US Army Engineer District, Los Angeles

8b. OFFICE SYMBOL (If applicable)

9. PROCUREMENT INSTRUMENT IDENTIFICATION NUMBER
Intra-Army Order No. E86890007

8c. ADDRESS (City, State, and ZIP Code)
PO Box 2711
Los Angeles, CA 90053-2325

10. SOURCE OF FUNDING NUMBERS

PROGRAM ELEMENT NO.	PROJECT NO.	TASK NO.	WORK UNIT ACCESSION NO.

11. TITLE (Include Security Classification)
Effects of Entrance Channel Dredging at Morro Bay, California

12. PERSONAL AUTHOR(S)
Kaihatu, James M.; Lillycrop, Linda S.; Thompson, Edward F.

13a. TYPE OF REPORT
Final report

13b. TIME COVERED
FROM _____ TO _____

14. DATE OF REPORT (Year, Month, Day)
September 1989

15. PAGE COUNT
148

16. SUPPLEMENTARY NOTATION
Available from National Technical Information Service, 5285 Port Royal Road, Springfield, VA 22161.

17. COSATI CODES

FIELD	GROUP	SUB-GROUP

18. SUBJECT TERMS (Continue on reverse if necessary and identify by block number)
Harbors--California--Morro Bay--Hydrodynamics.
Channels (Hydraulic engineering)--California--Morro Bay--Evaluation. Morro Bay (CA).

19. ABSTRACT (Continue on reverse if necessary and identify by block number)

The US Army Engineer Waterways Experiment Station's Coastal Engineering Research Center was requested by the US Army Engineer District, Los Angeles (CESPL), to provide technical assistance in engineering analysis and evaluation of two proposed channel enlargement plans for Morro Bay, California. These plans were developed to alleviate the hazardous conditions present at the entrance. This report details the study and provides final results to CESPL.

Significant wave heights, periods, and directions taken from the Wave Information Studies' (WIS) hindcast data base were input into the Regional Coastal Processes Wave finite difference model and transformed to breaking conditions along Estero Bay. Southern swell data were taken from an offshore directional buoy moored near Los Angeles, California, during 1984-85 and similarly transformed. The resulting breaking wave heights, periods, and directions were used to calculate longshore flux factors for use in sediment transport computations.

(Continued)

20. DISTRIBUTION/AVAILABILITY OF ABSTRACT
☒ UNCLASSIFIED/UNLIMITED ☐ SAME AS RPT. ☐ DTIC USERS

21. ABSTRACT SECURITY CLASSIFICATION
Unclassified

22a. NAME OF RESPONSIBLE INDIVIDUAL

22b. TELEPHONE (Include Area Code)

22c. OFFICE SYMBOL

DD Form 1473, JUN 86 Previous editions are obsolete. SECURITY CLASSIFICATION OF THIS PAGE

Unclassified

19. ABSTRACT (Continued).

A set of 42 representative waves were input into the Harbor Wave Transformation finite element model to ascertain the increase in the level of wave action inside the harbor with improved conditions. The results were then used to compute the number of days of breaking which would occur at various locations throughout the harbor. Existing conditions were also calculated as a check on the procedure; the agreement with Morro Bay Harbor Patrol record was found to be adequate. Current-induced breaking was also analyzed by calculating the maximum entrance channel current during falling tide and then computing the amount of steepness-limited breaking at the entrance for existing and improved conditions.

The potential longshore sediment transport rate was calculated using the previously calculated longshore flux factors and techniques found in the Shore Protection Manual. The rate of transport toward the harbor was calculated and compared favorably with results of a prior study.

The final results of the study indicated that the frequency of wave breaking would decrease at the entrance after either improvement was implemented, However, the hazardous breaking wave conditions previously at the entrance would be present further inside the harbor. Additionally, these breaking waves would tend to be higher than those presently at the entrance, since increasing channel depth allows more wave energy to enter the harbor.

PREFACE

This study was authorized by the U.S. Army Engineer District, Los Angeles (SPL), through an "Intra-Army Order for Reimbursable Services", No. E86890007, dated 17 October 1988. It was conducted during the period January 1989 through May 1989 by personnel of the Coastal Oceanography Branch (COB), Research Division (CR), Coastal Engineering Research Center (CERC) of the U.S. Army Engineer Waterways Experiment Station (WES).

This report was prepared by Mr. James M. Kaihatu, Hydraulic Engineer, COB; Ms. Linda S. Lillycrop, Hydraulic Engineer, COB; and Dr. Edward F. Thompson, Research Hydraulic Engineer, CR. Mr. Kaihatu and Ms. Lillycrop were under the direct supervision of Dr. Jon M. Hubertz, former Acting Chief, COB, and Dr. Martin C. Miller, Chief, COB. All were under the direct supervision of Mr. H. Lee Butler, Chief, CR, and under general supervision of Mr. Charles C. Calhoun, Jr., Assistant Chief, CERC, and Dr. James R. Houston, Chief, CERC.

Ms. Panola Rivers, Civil Engineering Technician, COB, Ms. Beverly D. Green, Contract Student, COB, and Mr. William R. Tillman, Contract Student, COB, assisted in preparing various files, figures and grids for use in the study. The assistance of Mr. Paul D. Farrar, Research Oceanographer, COB, Ms. Jane M. Smith, Hydraulic Engineer, COB, and Dr. Lyndell Z. Hales, Research Hydraulic Engineer, Coastal Processes Branch, CR, is deeply appreciated. Mr. Peter L. Crawford, U.S. Army Engineer

District, Buffalo, and Dr. H.S. Chen, Marine Products Branch, Development Division, National Meterological Center, National Oceanic and Atmospheric Administration, provided valuable suggestions for implementing the finite element harbor model used in this study. Prof. Sam S. Y. Wang, School of Engineering, The University of Mississippi, was very helpful in the application of an automated finite element grid generation program.

Commander and Director of WES during publication of this report was COL Larry B. Fulton, EN. Technical Director was Dr. Robert W. Whalin.

CONTENTS

	Page
PREFACE	1
CONVERSION FACTORS, NON-SI TO SI (METRIC) UNITS OF MEASUREMENT	4
PART I: INTRODUCTION	
Background	5
Numerical Modeling Approach	11
PART II: OFFSHORE WAVE CONDITIONS	13
General Wave Climate	13
WIS Hindcast Data	14
Southern Swell	16
PART III: WAVE REFRACTION MODELING	18
Wave Refraction Numerical Model	18
Longshore Flux Statistics and Calculations	22
PART IV: WAVE ACTION AND WAVE BREAKING IN THE ENTRANCE CHANNEL AND THE OUTER HARBOR	25
Hazardous Conditions	25
Wave Breaking at the Entrance and in the Channel	25
Current-Induced Breaking Wave Climate Analysis	40
PART V: LONGSHORE SEDIMENT TRANSPORT RATE	45
Entrance Shoaling and Maintenance Dredging	45
TetraTech Study of 1975	45
Sediment Transport	46
PART VI: CONCLUSION	50
Need for Physical Model Study	50
REFERENCES	52
APPENDIX A: LONGSHORE FLUX FACTOR DISTRIBUTION: MONTHLY	A1
APPENDIX B: BREAKING WAVE CLIMATE ANALYSIS	B1
APPENDIX C: LONGSHORE TRANSPORT ANALYSIS	C1
APPENDIX D: NOTATION	D1

CONVERSION FACTORS, NON-SI TO SI (METRIC) UNITS OF MEASUREMENT

Non-SI units of measurement used in this report can be converted to SI (metric) units as follows:

Multiply	By	To Obtain
degrees (angle)	0.01745329	radians
feet	0.3048	metres
cubic yard	0.7646	cubic metres
mile	1.6093	kilometres
feet/second	0.3048	metres/second
nautical mile/hour	1.852	kilometres/hour

EFFECTS OF ENTRANCE CHANNEL DREDGING AT MORRO BAY, CALIFORNIA

PART I: INTRODUCTION

Background

Location

1. Morro Bay is a small craft commercial harbor located in San Luis Obispo County, California, approximately midway between San Francisco and Los Angeles. The harbor is located near the center of Estero Bay, a large shoreline indentation marked by Point Estero to the north and Point Buchon to the south. These bounding headlands limit direct wave attack to between 190 deg and 310 deg azimuth.

2. The harbor itself is protected from the open ocean by two rubble-mound breakwaters (Figure 1). The north breakwater is 1884 ft long and has an average crest elevation of +18 ft above mean lower low water (MLLW). The south breakwater is 1859 feet long with a crest elevation that varies between +14 ft MLLW to +18 ft MLLW. These breakwaters form a 900 ft wide opening. An entrance channel has been dredged there which is approximately 350 ft wide and 2700 ft long, and is maintained at a -16 ft MLLW depth.

Statement of the Problem

3. The primary problem at Morro Bay is the frequency of wave breaking at the entrance. This makes for extremely dangerous

---

* A table of factors for converting non-SI units of measurement to SI (metric) units is presented on page 4.

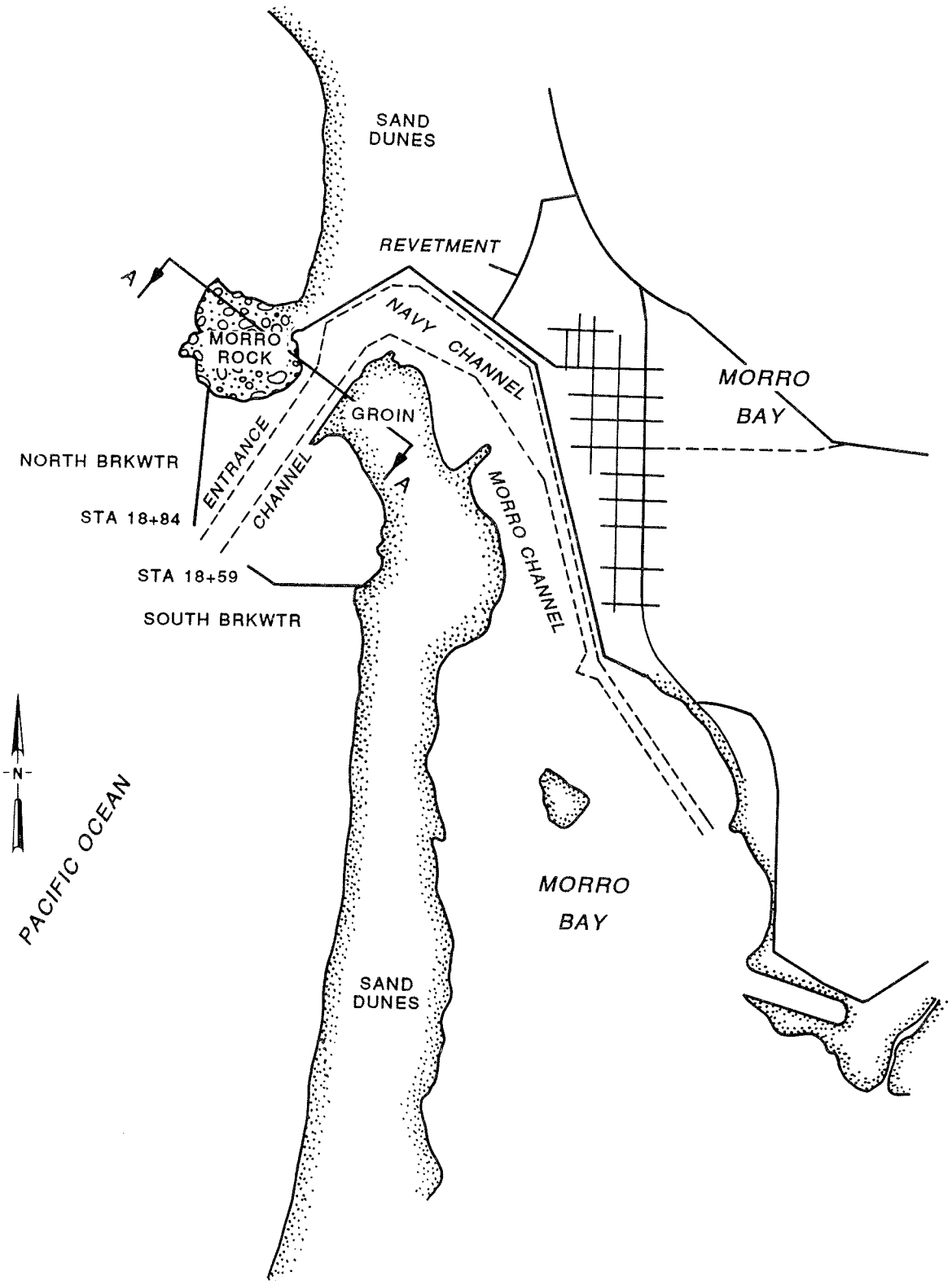

Figure 1. Morro Bay, California

entrance conditions which have led to a number of accidents. The most highly-publicized accident occurred in February 1983, when the 45-ft cabin cruiser San Mateo was capsized by high waves at the entrance. All 31 passengers were thrown into the water, including 26 schoolchildren. All passengers survived, but the captain of the vessel died a year later from injuries suffered during the accident. The most recent fatality was the drowning death of a very experienced fisherman in November 1987. His boat, the 42-ft Langosta II, was overtaken and capsized by what was described in newspaper accounts as "a tall wave" (U.S. Army Engineer District, Los Angeles 1988). This death was the 21st such fatality in eight years, making Morro Bay one of the eight most dangerous harbors in the United States.

4. The primary cause of this frequency of breaking at the entrance is believed to be the shoaling and steepening of waves as they approach the harbor. The breaking wave problem is compounded during ebb tide by an interaction with strong tidal currents. Local fishermen have also claimed that shoaling of the existing entrance channel has moved the "waiting area", where incoming fishing boats would wait and determine conditions, further offshore. This causes the boats to have to travel a greater distance through dangerous conditions. However, hydrographic surveys of the entrance channel have not revealed shoaling or bar formation at the entrance.

5. A resolution adopted by the House Committee on Public Works of the U.S. House of Representatives authorized study and review of possible modifications to the existing project at Morro Bay (U.S. Army Corps of Engineers, Los Angeles 1988). The project

authorization is contained in House Document No. 283, 77th Congress, 1st Session.

6. The U.S. Army Engineer District, Los Angeles (SPL) studied several structural and dredging alternatives to attempt to relieve this problem (U.S. Army Engineer District, Los Angeles 1988). They then selected two dredging alternatives which were to be considered during the feasibility phase of the project. The planforms for these alternatives are shown in Figures 2 and 3. They are referred to as Alternatives 5 and 6, and are described as follows (U.S. Army Engineer District, Los Angeles 1988):

> a. Alt. 5: This is a dredged channel with a final depth of -40 ft MLLW. The most seaward section of the channel faces west-northwest to reduce breaking of waves incident from this direction. This first section is 875 ft long. The second section is 437 ft long and is oriented west. The final 396 ft meets the existing entrance channel. The floor width is 215 ft.
>
> b. Alt. 6: This is a dredged channel with an extended width at the mouth. The project depth is -40 ft MLLW. The width of the most seaward section of the channel is approximately 1000 ft long. Its centerline is oriented west-northwest. This seaward section continues for 728 ft. The second section is 417 ft long and is oriented west to west-southwest. The innermost section is 387 ft long and meets the entrance channel, which has a floor width of 270 ft.

The bottom of the enlarged entrance was to slope at 0.05 from a transition point (marked "B-B" on Figures 2 and 3) to the existing channel bottom. Dredging quantities were estimated by SPL to be 190,270 cu yd for Alternative 5 and 276,720 cu yd for Alternative 6.

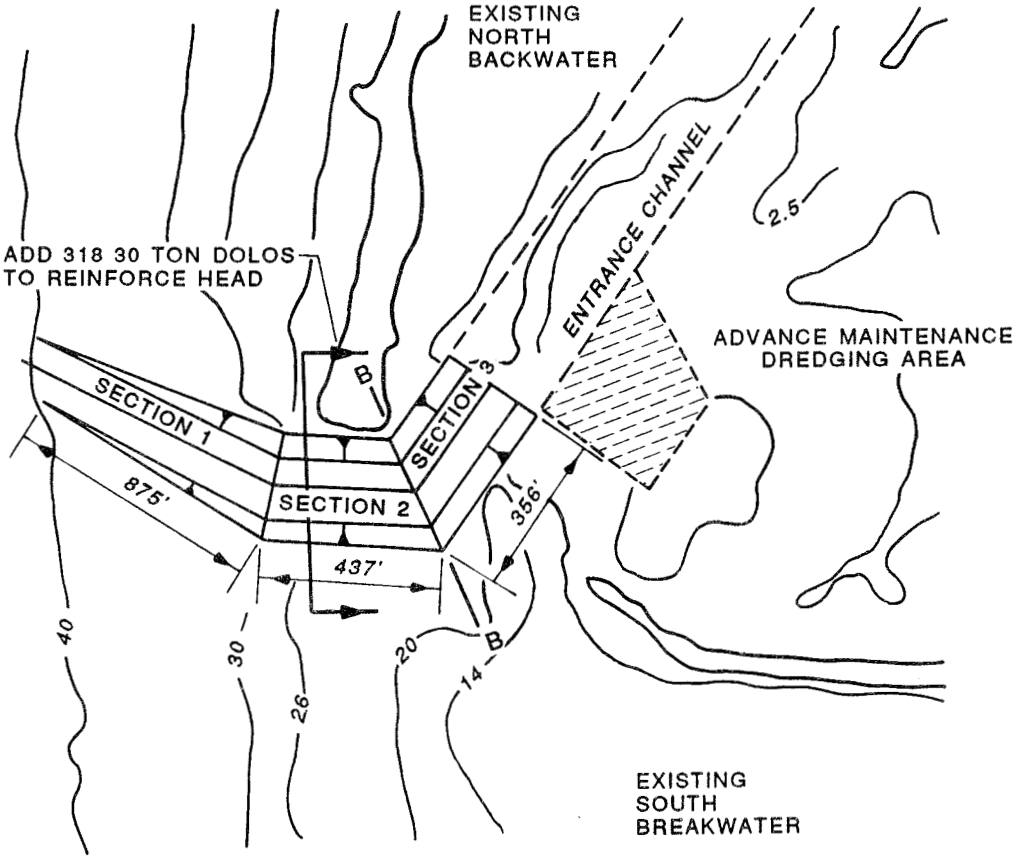

Figure 2. Dredging Alternative 5

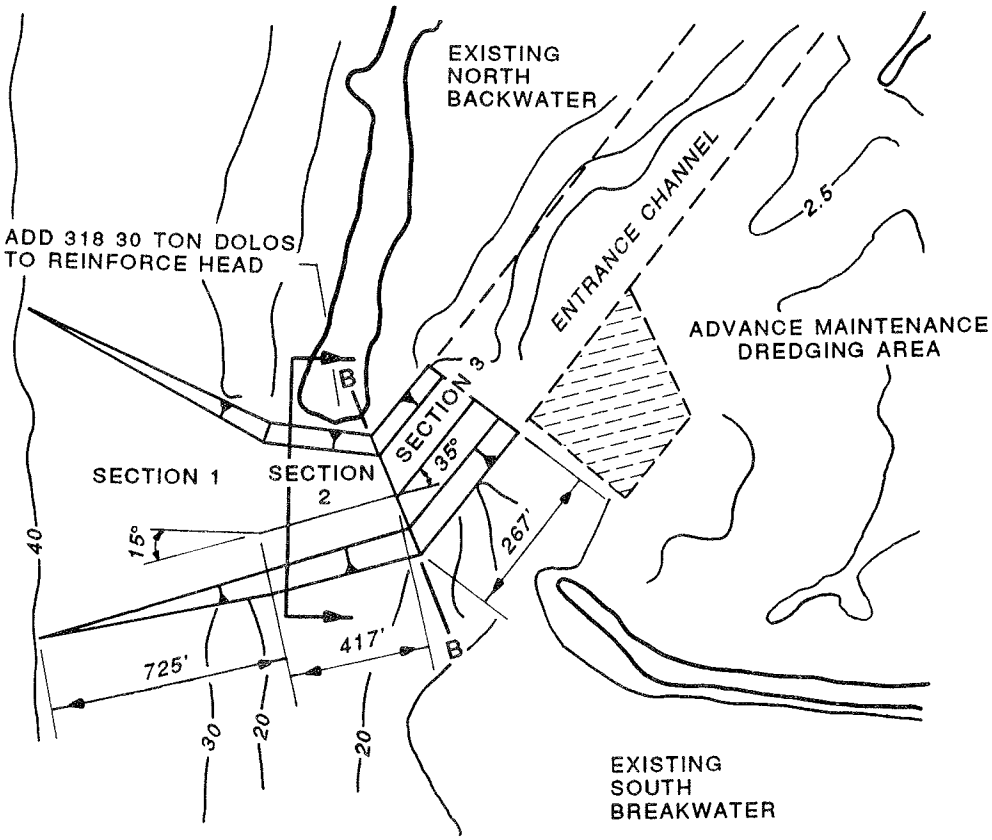

Figure 3. Dredging Alternative 6

Numerical Modeling Approach

7. The Coastal Engineering Research Center (CERC) of the U.S. Army Waterways Experiment Station (WES) is a major center for all areas of coastal engineering research. CERC has state-of-the-art techniques for field data collection and analysis, physical modeling, and numerical modeling of coastal processes. Numerical modeling, in particular, has experienced significant advances in the last decade, due primarily to the development of computer technology. Researchers at CERC have used this fast-growing technology to develop flexible, accurate and efficient numerical models which have seen widespread use in the coastal engineering community.

8. SPL requested CERC to evaluate the impacts their proposed improvements would have on the wave climate at Morro Bay. Specifically, CERC was to investigate the following:

a. The effect of the enlarged entrance on the breaking wave frequency inside the channel.

b. The effect of the enlarged entrance on the wave action inside the outer harbor.

c. The potential sediment transport rate toward the harbor in Estero Bay.

9. CERC developed a numerical modeling approach for this study consistent with SPL time and cost constraints. This approach allowed for optimum flexibility for changing improvement plans and modeling various wave conditions. The approach developed used two numerical models for determining the wave characteristics both at regional scale (Estero Bay) and local scale (Morro Bay Outer Harbor).

The sequence of events for this study is described in the following paragraphs.

10. CERC's hindcast wave data base was used to assemble the deep water wave conditions for input to the numerical models (Corson, et. al 1987). These hindcasted waves included sea and northern hemisphere swell. Southern swell, not presently a component of this data base, was taken from a deep water directional buoy located within the Southern California Bight.

11. These waves were input into the numerical model RCPWAVE, or REgional Coastal Processes WAVE Propagation Model (Ebersole, Cialone, and Prater 1986). The waves were transformed to shore, and the breaking wave heights and directions were saved to be used in sediment transport calculations for Estero Bay.

12. A set of 42 representative waves were input into the numerical model HARBD, CERC's harbor wave transformation model (Chen and Houston 1987). This numerical model determined the wave action near the entrance and inside the outer harbor for both existing and improved conditions. The output of HARBD was then used to estimate the breaking wave conditions through the channel for both existing and improved conditions.

13. The breaking wave heights and directions from the RCPWAVE calculations were used to estimate potential sediment transport rates toward the harbor in Estero Bay. Potential transport rates toward the harbor from the north and south beaches were calculated.

PART II: OFFSHORE WAVE CONDITIONS

General Wave Climate

Swell

14. Swell waves are ocean waves which have left their generating area and are propagating toward the coast, no longer coupled with the wind. They are usually smooth, round waves which have begun their transformation processes of sorting and decay. They tend to be of longer period than sea waves.

15. The general swell wave climate of central and northern California is quite different than that of southern California. This is due to the general orientation of the shoreline, with the point of demarcation between these orientations being Point Conception. Areas north of Point Conception such as Morro Bay are subject to the strong swells approaching from the west-northwest (Inman, et.al. 1986). These swells are usually caused by:

a. Intense extratropical cyclones which are generated near the Japanese and Aleutian Islands.

b. Steep pressure gradients around the Pacific high pressure cell.

Sea

16. Sea waves are waves which are still in the generating area. These waves have spiky forms with short crests and wavelengths. In general, coastal winds are stronger for the central and northern California coast than those in southern California. Estero Bay is sheltered from much of the strong northerly wind activity occurring in the northeast Pacific by Point Buchon to the north. Winds blowing near the coast from the

west-northwest direction, however, are not blocked. The resulting sea waves from this direction can be quite high.

WIS Hindcast Data

17. The offshore waves required as data input into the refraction modeling were taken from the Wave Information Study's (WIS) Pacific Ocean Phase II hindcasts (Corson, et.al. 1987). These hindcasts were generated from historical pressure field records for the years 1956-1975, and have been used as a primary data source for many previous CERC studies. Phase II hindcasts were generated on a moderately fine resolution grid, with the WIS Phase I hindcasts serving as a seaward boundary. Station P2012, located at 35.21N, 121.60W, was used as the deepwater station for this study. A wave rose for the data is shown in Figure 4.

General Characteristics of the WIS Hindcast Data

18. The WIS data taken from Station P2012 have the following general statistics associated with it:

a. Mean significant wave height: 2.6 meters
b. Mean peak period: 10.3 seconds
c. Most frequent (22.5° direction bands) wave direction: 292.5 degrees azimuth
d. Largest significant wave height: 8.9 meters
e. Peak period associated with the highest wave: 12.5 seconds.

Hindcast Sea and Swell Waves

19. The WIS hindcast data are usually in the form of a time history of significant wave height, peak period, and peak direction, covering the period of time needed. The data are compiled for sea waves alone, swell waves alone and the combined

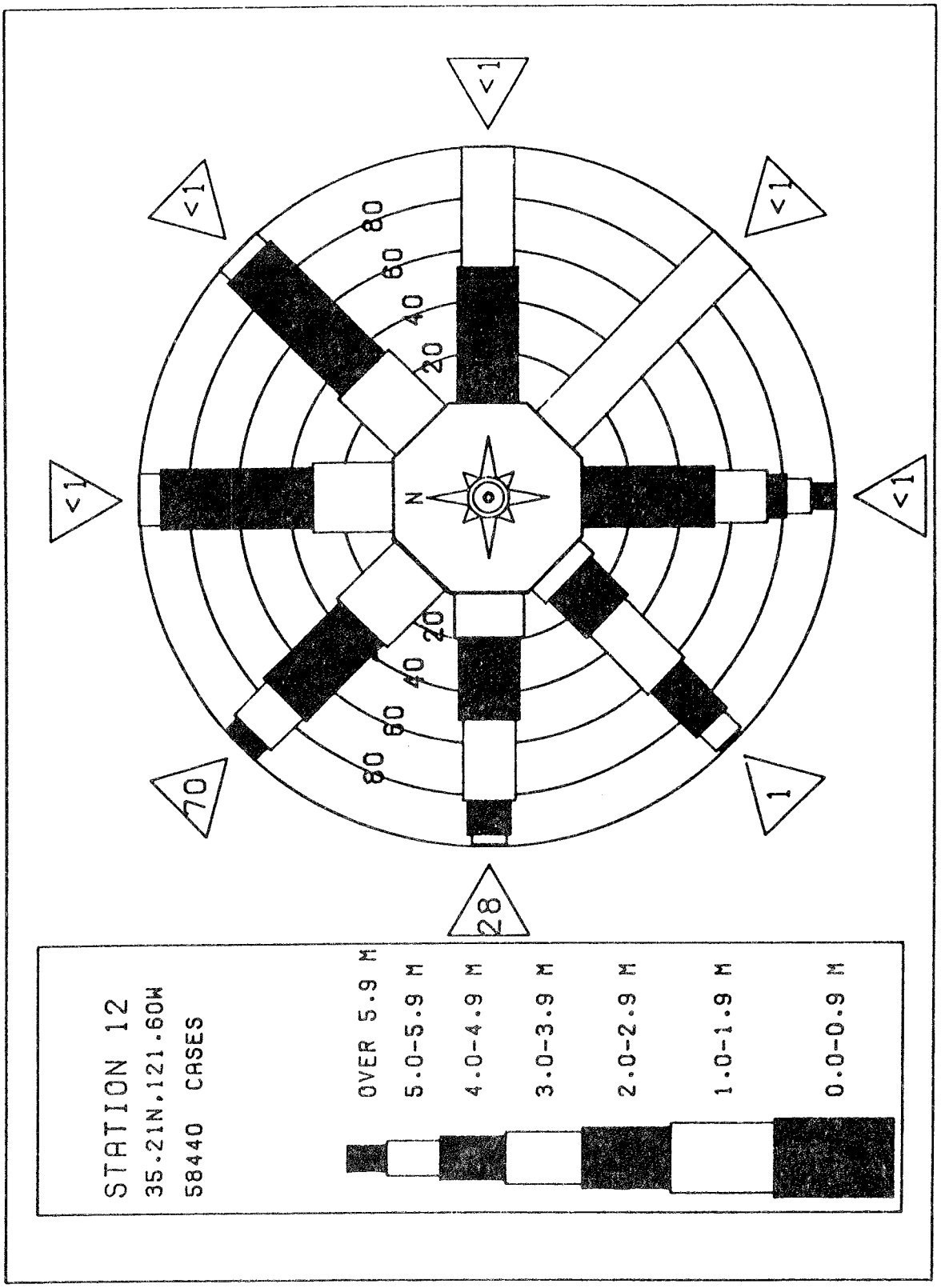

Figure 4. Wave Rose for WIS Station P2012

sea and swell. Sea and swell waves were treated separately for this study. Twenty years of hindcast data, covering the years 1956 through 1975, were divided into months and then processed through a percent occurrence program. This program analyzed the time series and separated the data into specific height, period and direction bands. Bands of 5 degrees azimuth and 0.5 meters height were used. Periods of 5.44, 7.57, 9.10, 10.02, 11.14, 12.54, 14.35, 16.77, 20.19 and 22.22 seconds were also used. Each of these periods represented the median value of a particular period band defined in the WIS data base.

Southern Swell

20. The WIS hindcast data provides an accessible and reliable input source for coastal engineering studies. It does not include southern swell in its Pacific hindcast data base at present, however. Southern swell includes not only southern hemisphere swell, but also swell generated by extratropical storms near equatorial zones.

21. The southern swell data used in this study were taken from the National Oceanic and Atmospheric Administration (NOAA) directional "Olympics" buoy, so named because it was moored approximately 65 miles southwest of Los Angeles (32.76 degrees north, 119.48 degrees west) during the time of the 1984 Los Angeles Olympic Games. It remained in the area for approximately a two year period (April 1984 through September 1985). The data were filtered to include only waves which:

a. Have a period of 6 seconds or more;
b. Have an approach angle of 135 degrees to 225 degrees azimuth.

Although the "Olympics" buoy was located well within the Southern California Bight region, it was in sufficiently deep water (approximately 4,500 feet in depth) to apply the data to the WIS Station 12, under the assumption that untransformed southern swell arrives at the California coast in a long-crested wave train. This time series was then run through the same percent occurrence program as the WIS hindcast data.

PART III: WAVE REFRACTION MODELING

Wave Refraction Numerical Model

22. The first step of the modeling process was to perform wave refraction calculations for the Estero Bay area. The wave refraction-diffraction model RCPWAVE was used to perform this task (Ebersole, Cialone and Prater; 1986). RCPWAVE is an iterative finite difference wave propagation model based upon the mild-slope equation, which describes combined wave refraction and diffraction by bathymetry (Berkhoff 1972):

$$CC_g \, \partial^2\phi/\partial x^2 + CC_g \, \partial^2\phi/\partial y^2 + (\sigma C_g/C)\phi = 0 \qquad (1)$$

where:

x,y = orthogonal horizontal coordinates, ft

C = wave celerity, ft/sec

C_g = group velocity, ft/sec

σ = wave frequency, radians/sec

ϕ = velocity potential, ft^2/sec

This velocity potential can be expressed in terms of an amplitude and phase:

$$\phi = ae^{iS} \qquad (2)$$

where:

a = wave amplitude function = $gH(x,y)/2\sigma$, dimensionless

$H(x,y)$ = wave height, ft

$s(x,y)$ = wave phase function, dimensionless

Substituting equation 2 into equation 1 and solving for real and imaginary parts separately yields:

$$1/a\{\partial^2 a/\partial x^2 + \partial^2 a/\partial y^2 + (1/CC_g)(\nabla a \bullet \nabla(CC_g))\} + k^2 - \nabla s = 0 \quad (3)$$

and

$$\nabla(a^2 CC_g \nabla s) = 0 \quad (4)$$

where:

$\nabla = (\partial/\partial x + \partial/\partial y)$, the gradient in two dimensions.

Pure diffraction can be recovered from equations 3 and 4 by setting h(x,y) constant, yielding the Helmholtz equation. Setting:

$$(\partial^2 a/\partial x^2) = (\partial^2 a/\partial y^2) = 0 \quad (5)$$

recovers a form of the ray equations for pure wave refraction (Berkhoff 1976). The breaking wave height decay scheme used in RCPWAVE is a two-dimensional expansion of the formulation of Dally, Dean and Dalrymple (1985), which has been used in many wave propagation models. RCPWAVE has been compared to laboratory data (Berkhoff, Booij and Radder 1982) with good results.

23. RCPWAVE is preferable to ray tracing methods because it can model the lateral flow of energy along the wave crest which occurs during, for instance, wave propagation over a shoal. It requires deep water wave height, period and direction as input, and gives as its output wave height, wave direction, wave number and breaker index over the entire grid. RCPWAVE operates under the following assumptions:

a. Linear, monochromatic waves.
b. No structures or currents.
c. Gentle bathymetry.
d. Negligible energy reflection.
e. Negligible energy loss due to bottom friction or waves breaking outside the surf zone.
f. Negligible energy input from the wind.

These assumptions are acceptable for the open coast areas in Estero Bay north and south of the harbor. However, they deviate from the actual conditions near the entrance mouth, which is marked by steep channel slopes, structures, currents and energy reflection from Morro Rock. Because of this, RCPWAVE could not be used to evaluate the breaking wave climate at the mouth. An alternative approach for evaluating the breaking wave climate is detailed in a later section of this report.

24. The grid over which RCPWAVE operated was a variable-spaced grid with over 4,000 cells (61 longshore cells and 68 offshore cells), encompassing approximately 13 miles of coastline and extending about 6 miles offshore. It was oriented to accommodate the extreme wave approach directions (190-315 deg azimuth). This grid is shown in Figure 5. The size of each cell varied in the x-direction (offshore direction) from 200 ft to 600 ft, while the cell size in the y-direction (longshore direction) remained constant at 1200 ft.

25. These refraction results were to be used in littoral transport calculations. Thus, the location of wave breaking was considered most important. However, the NOAA bathymetric charts used as a bathymetry source were lacking sufficient resolution to locate the exact point of breaking. To account for this, the version of RCPWAVE used in this study was modified to save wave information one cell seaward of RCPWAVE

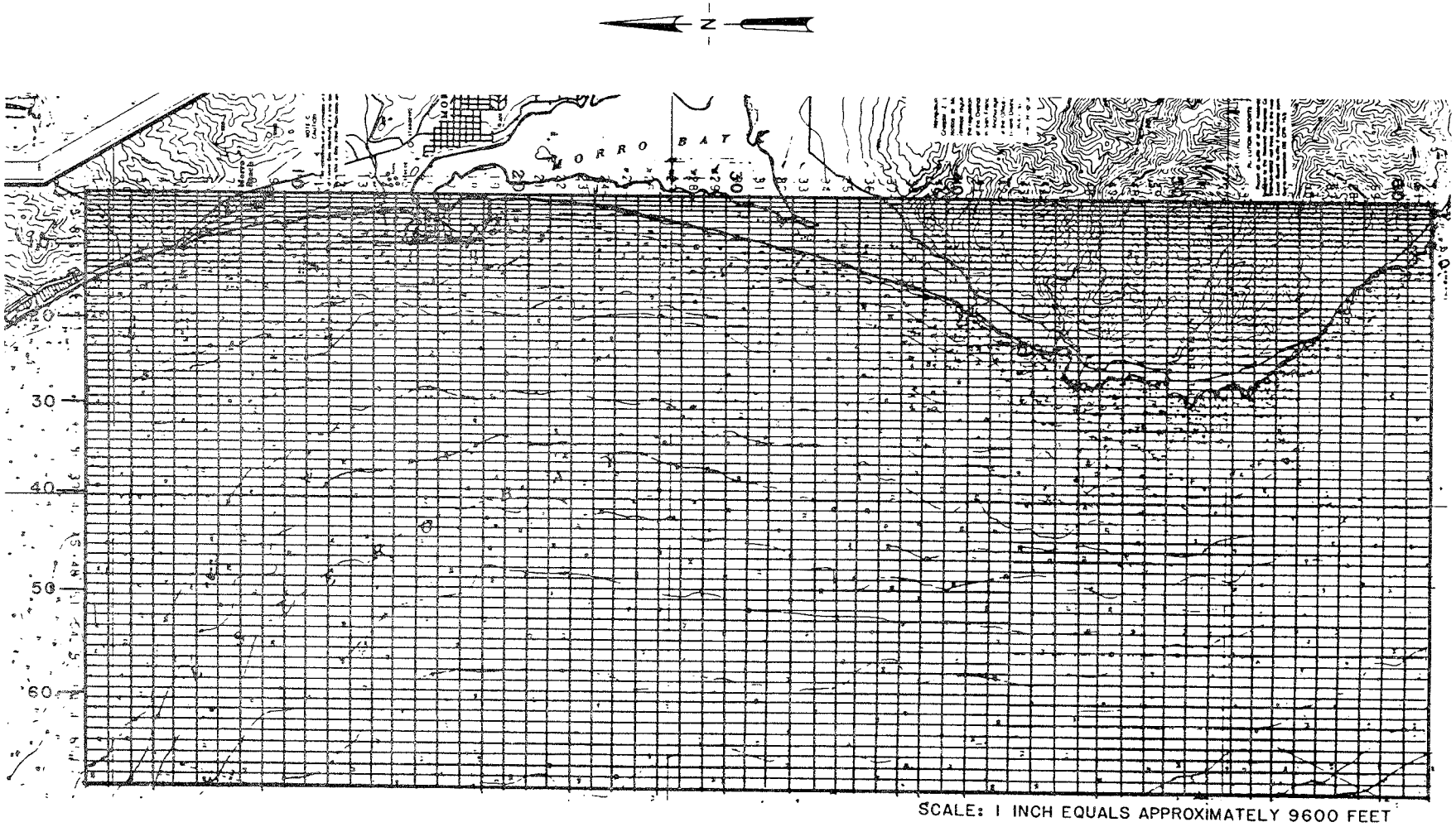

Figure 5. RCPWAVE Grid for Morro Bay

breaking. This information was refracted (using Snell's Law) and shoaled until the breaking criterion of (waveheight = 0.78*depth) was reached.

Longshore Flux Statistics and Calculations

26. One of the tasks of this study is to determine the potential longshore transport rate in Estero Bay. This involved using Shore Protection Manual (SPM) methods (SPM 1984) to determine potential longshore transport. The required wave climate information for this task is breaking wave heights, periods and directions. From this information, longshore flux factor was calculated, which would serve as a direct input into longshore transport calculations.

27. A subroutine was added within RCPWAVE to calculate longshore flux factor from the breaking wave heights, periods and directions. The equation used for this calculation was:

$$P_{ls} = (1/16)\ \rho\ g\ H_b^2\ C_g\ \sin(2\Theta_b) \qquad (6)$$

in which:

P_{ls}=longshore flux factor, ft-lb/sec-ft of beach

ρ = mass density of sea water, slugs/cubic ft

g = gravitational acceleration, ft/sec^2

H_b = breaking wave height, ft

C_{gb} = group velocity of breaking wave, ft/sec

Θ_b = breaking wave angle, deg between wave crest and shoreline

For each wave condition, the longshore flux factor was calculated at incipient breaking at each of the 61 longshore cells. The average monthly longshore flux factor for each longshore cell was calculated using the following equation:

$$P_{ls(j)} = \sum^{k=1}_{W} \sum^{i=1}_{M} P_{ls(i,j)} * wt_k \qquad (7)$$

where:

i = offshore cell

j = longshore cell

W = number of waves in a particular record

k = number of a particular deepwater wave in the data set of W waves.

wt = weighting factor, which is the percent occurrence of the deepwater wave divided by 100.

M = total number of offshore cells (68)

This series of calculations was conducted separately for each monthly record of sea, swell and southern swell. Each calculation yielded a set of 61 longshore flux values that represent the average flux value for the month, one value for each longshore cell and each wave type (sea, swell or southern swell). These individual longshore flux factors were then combined for each longshore cell as follows:

$$P_{ls(total)} = P_{ls(sea)}+P_{ls(swell)}+P_{ls(southern\ swell)} \qquad (8)$$

Figures A-1 through A-12 show the $P_{ls(total)}$ values with respect to longshore cell for each month of the record. Because

of the boundary effects of the RCPWAVE grid and the extreme curvature of Estero Bay in the far reaches of the grid, the best results are at least several longshore cells inward from the lateral boundaries. Thus, the figures show the longshore flux factors for cells 5 through 36 only. Additionally, cells 15 through 20 have been removed because they cover the harbor area. The remaining cells model approximately six miles of shoreline.

29. Strong longshore variations and high magnitudes of the longshore flux factors are evident in Figures A-1 through A-12. The cause of the magnitudes and variations seem to be the breaking wave angles. These high breaking wave angles can be attributed to the curving shoreline and the divergence of the wave rays as they propagate into Estero Bay. Analysis of individual results indicated that these waves tend to break before their direction becomes normal to the shore, resulting in a high breaking wave angle. Because the shoreline is curved, the shoreline angle is different for each cell, resulting in significant differences in breaking wave angles between neighboring cells. This accounts for the high P_{ls} values and the longshore variation of their magnitude.

30. It can also be seen from Figures A-1 through A-12 that the primary directional trend for longshore flux factor is southward. An additional analysis was done, in which all waves which broke toward the harbor were saved. This would allow calculation of the gross transport rate toward the entrance channel.

PART IV: WAVE ACTION AND WAVE BREAKING IN THE ENTRANCE CHANNEL AND THE OUTER HARBOR

Hazardous Conditions

31. The City of Morro Bay Harbor Patrol has compiled a record of the occurrence of hazardous conditions at the entrance, and has concluded that these conditions occur approximately 28 days per year (SPL, personal communication 1989). Table 1 shows a breakdown into seasons. This section of the report addresses depth-limited wave breaking at the entrance and in the outer harbor, and current-induced breaking at the entrance.

Table 1. Morro Bay Harbor Patrol Observations

Days of Breaking - Harbor Patrol Observations

Season	Number of Days of Breaking/Year
Spring	1.0
Summer	0.0
Fall	9.5
Winter	17.9
Total	28.4

Wave Breaking at the Entrance and in the Channel

32. It is evident that enlarging and deepening the channel at the entrance would reduce the number of breaking events near the structures. The effect of this channel enlargement on the wave

action inside the outer harbor is not readily apparent. Waves which would have broken and dissipated at the entrance under existing conditions would propagate and break inside the outer harbor after channel enlargement. These propagating waves would tend to be larger than those presently entering the outer harbor.

Numerical Model

33. The numerical model HARBD (Chen and Houston 1987) was used to model the harbor wave climate at Morro Bay Harbor, California. HARBD is a steady state hybrid finite element model which calculates linear wave oscillations in harbors of arbitrary configuration and variable water depth. The model is advantageous over other numerical harbor models since bottom friction and boundary absorption are included. The bottom friction is assumed to be proportional to flow velocity with a phase difference. The boundary absorption is based on a formulation similar to that in the impedance condition in acoustics and is expressed in terms of wave number and reflection coefficient of the boundary. The result is that HARBD predicts wave amplitudes which are more realistic than those from previous models (Chen and Houston 1987). HARBD was originally developed for harbor oscillations (long period waves), but the general formulation was adapted for wind waves (short period waves) by Houston (1981).

34. The model has been tested for a number of cases for which analytic solutions are known with excellent results (Chen 1984 and Chen and Houston 1987). It was applied in analyzing proposed designs of Agat Harbor, Guam (Farrar and Chen 1987) and

developing design improvements at Barbers Point Harbor, Hawaii. The model was used to plan wave protection at Fisherman's Wharf, San Francisco, California (Bottin, Sargent, and Mize 1985), Green Harbor, Massachusetts (Weishar and Aubrey 1986), and Los Angeles-Long Beach Harbor (Houston 1976), and to estimate the wave conditions in Indiana Harbor, Indiana during a study of sediment disposal alternatives (Clausner and Abel 1986). HARBD was compared to laboratory data collected from the physical model study of Barcelona Harbor, Buffalo, New York (Crawford and Chen 1988) with encouraging results.

35. In the HARBD solution formulation, the water domain is divided into near and far regions. The near region is bounded by an artificial semicircular ring outside the harbor and includes the harbor and all marine structures and bathymetry of interest. The far region is an infinite semicircular ring bounded by the near region and extends to infinity in all horizontal directions. The infinite far region is assumed to have a constant water depth and no bottom friction. The finite near region, which contains the area of interest, is subdivided into a mesh of triangular shaped finite elements. The length of the sides of each element is determined from the desired grid resolution and design wavelength. The water depth and bottom friction coefficient are specified for each element, and a reflection coefficient is assigned to every boundary element. The model requires a wave period and direction as input. The solution consists of an amplification factor (the ratio of the wave height to the incident wave height) and a corresponding phase for the entire near region. The phase is of little importance to the present study.

36. The model solves the following governing equation:

$$CC_g\lambda(\partial^2\phi/\partial x^2) + CC_g\lambda(\partial^2\phi/\partial y^2) + (\sigma^2 C_g/C)\phi = 0 \qquad (9)$$

where

C = wave phase velocity, ft/sec

C_g = wave group velocity, ft/sec

ϕ = spatial flow potential, ft^2/sec

k = wave number, dimensionless

The complex bottom friction factor λ is assumed proportional to the maximum velocity at the bottom of the flow field and is defined as:

$$\lambda = 1/(1+(i\beta a_o/h \sinh kh)e^{i\gamma}) \qquad (10)$$

where

β = dimensionless bottom friction coefficient

a_o= incident wave amplitude, ft

h = water depth, ft

γ = phase difference from flow velocity, dimensionless

An absorbing boundary condition is applied along the solid boundaries inside the harbor and is expressed as:

$$\partial\phi/\partial n - \alpha\phi = 0 \qquad (11)$$

and

$$\alpha = ik\ (1-K_r/1+K_r) \qquad (12)$$

where

n = the unit-normal vector outward from the water regions

K_r = the reflection coefficient of the boundary.

37. A conventional finite element approximation is used in the near region, and an analytical solution with unknown coefficients is used to describe the far region. The conditions in the near and far regions must be matched along the artificial semicircle boundary. This requirement is met by HARBD routines which automatically match the solutions (using the stationarity of a functional) to a series of Hankel functions which give the solution for the infinite region (Farrar and Chen 1987). The hybrid element numerical techniques used in the formulation are discussed in greater detail in Chen and Mei (1974).

38. The HARBD model is intended to simulate waves which can be adequately described by the mild slope equation (Equation 9). Model accuracy decreases as wave conditions approach those outside the validity of this governing equation. The model does not simulate such nonlinear transformation processes as wave breaking. However, techniques for accounting for these processes while using HARBD results have been developed. One such technique is described in a later section of this report.

Finite Element Grid for Existing and Proposed Channel Modifications

39. Figure 6 depicts the finite element grid used to model the harbor configuration of this study. The grid consisted of 22,293 triangular elements, 11,487 nodes (triangular corners), and 493 boundary elements. The size of each element was sufficient to obtain a resolution of 6 elements per wavelength.

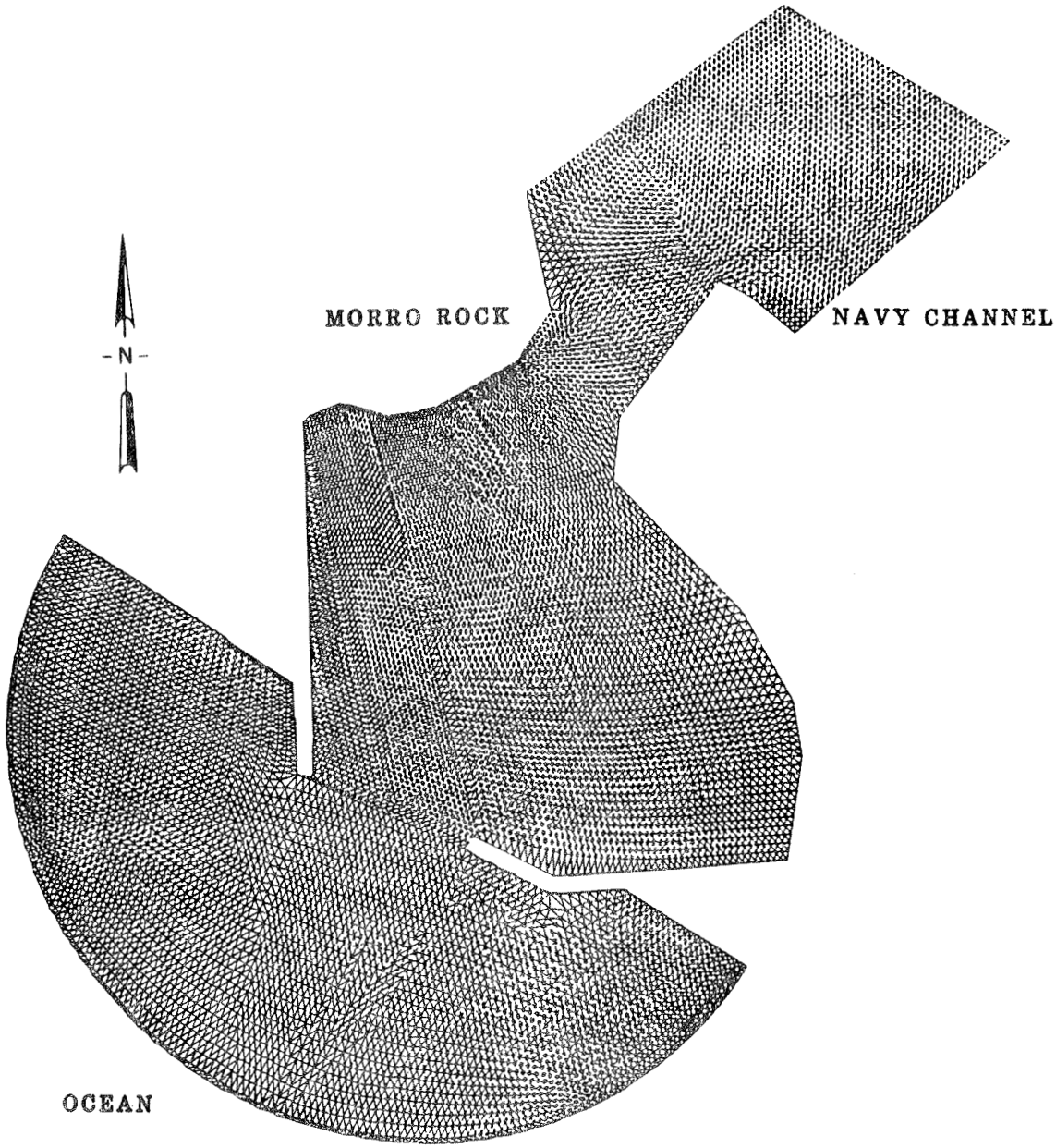

Figure 6. Finite Element Grid for Morro Bay

The wavelength was determined by a design period of 10 seconds and a water depth of 15 feet.

40. The grid extended from the artificial semicircular boundary outside the breakwaters, through the outer harbor to the wave absorbing back bay area. The semicircular boundary enclosed the entrance channel and a large enough area to adequately model the incident wave climate from the pertinent directions of approach. This resulted in a 3,968 ft diameter semicircle oriented approximately 300 ft inside the midpoint of the breakwater tips. It was unnecessary to envelop the entire seaward side of the breakwaters inside the grid since these were not the primary areas of interest.

41. One grid was used since the proposed entrance channel modifications only required increasing the depth values of the elements. However, this bathymetry must be complete, as the model results are sensitive to water depth. The bathymetry for the existing conditions was obtained from District surveys. The reflection coefficients were calculated using the method in the Shore Protection Manual (SPM 1984). The assigned reflection coefficients were 0.39 for the 5/2 sloped North Breakwater and revetments in the back bay, 0.51 for the 3/2 sloped South Breakwater, 0.31 for the transitional area between the north breakwater and Morro Rock, and 0.09 for the beaches. Because short sea and swell waves were to be modeled, it was felt that the choice of reflection coefficients would only have a local effect on results. The bottom friction factor was set to 0.05 for all elements since the entire bottom was sandy.

42. The grid for this study was generated using a finite element grid generation program. This was the initial

application of the computer program to a field study at CERC. Generating the grid manually would have been unmanageable due to the large number of nodes and elements necessary to meet the resolution requirements.

43. In finite element modeling, the computational time required for one inversion of the solution matrix is proportional to the cube of the grid bandwidth, the maximum difference in nodal numbering of two adjacent nodes. Even though the bandwidth was minimized, the large size of the grid necessitated the use of super computing facilities. This induced the requirement that the number of input wave conditions be kept to a minimum. Forty-two representative waves were selected and refracted (via RCPWAVE) to the semi-circular boundary of the HARBD grid. The refracted values were then used as the incident wave conditions to HARBD. The 42 input wave conditions and their refracted angles are listed in Table 2.

44. The resulting wave information at individual nodes was not useful due to the strong variations in results between adjacent nodes. These variations were present because of the lack of sufficient grid resolution in areas of extremely shallow water. To remedy this, several "basins" were defined throughout the harbor. A basin is an area comprised of several adjacent elements which are grouped together and the individual results averaged. The assigned basins and their locations are shown in Figure 7. These basins, their distance from the grid origin and average depth are listed in Table 3. Results at these basins were saved and tabulated (Tables B-1 through B-42). Wave amplification factors of the basins located through the length of the channel, both inside and outside the harbor, are plotted for each wave condition and shown in Figures

Table 2. HARBD Input Waves

Input Information for HARBD Production Runs

Period (Sec.)	Deep Water Dir. (Deg.)	Refracted Dir. (Deg.)
10.02	202.5	227.1
11.14	202.5	231.1
12.54	202.5	235.0
14.75	202.5	239.3
16.77	202.5	241.9
20.14	202.5	244.8
22.22	202.5	246.1
10.02	225.0	237.3
11.14	225.0	240.1
12.54	225.0	243.0
14.75	225.0	246.1
16.77	225.0	248.0
20.14	225.0	250.1
22.22	225.0	251.0
10.02	247.5	252.2
11.14	247.5	253.4
12.54	247.5	254.6
14.75	247.5	255.8
16.77	247.5	256.5
20.14	247.5	257.0
22.22	247.5	257.2
10.02	270.0	268.4
11.14	270.0	268.0
12.54	270.0	267.4
14.75	270.0	266.5
16.77	270.0	265.7
20.14	270.0	264.6
22.22	270.0	264.1
10.02	292.5	283.6
11.14	292.5	281.3
12.54	292.5	278.4
14.75	292.5	275.9
16.77	292.5	273.9
20.14	292.5	271.3
22.22	292.5	270.0
10.02	315.0	293.0
11.14	315.0	289.3
12.54	315.0	285.8
14.75	315.0	281.8
16.77	315.0	279.1
20.14	315.0	275.6
22.22	315.0	273.9

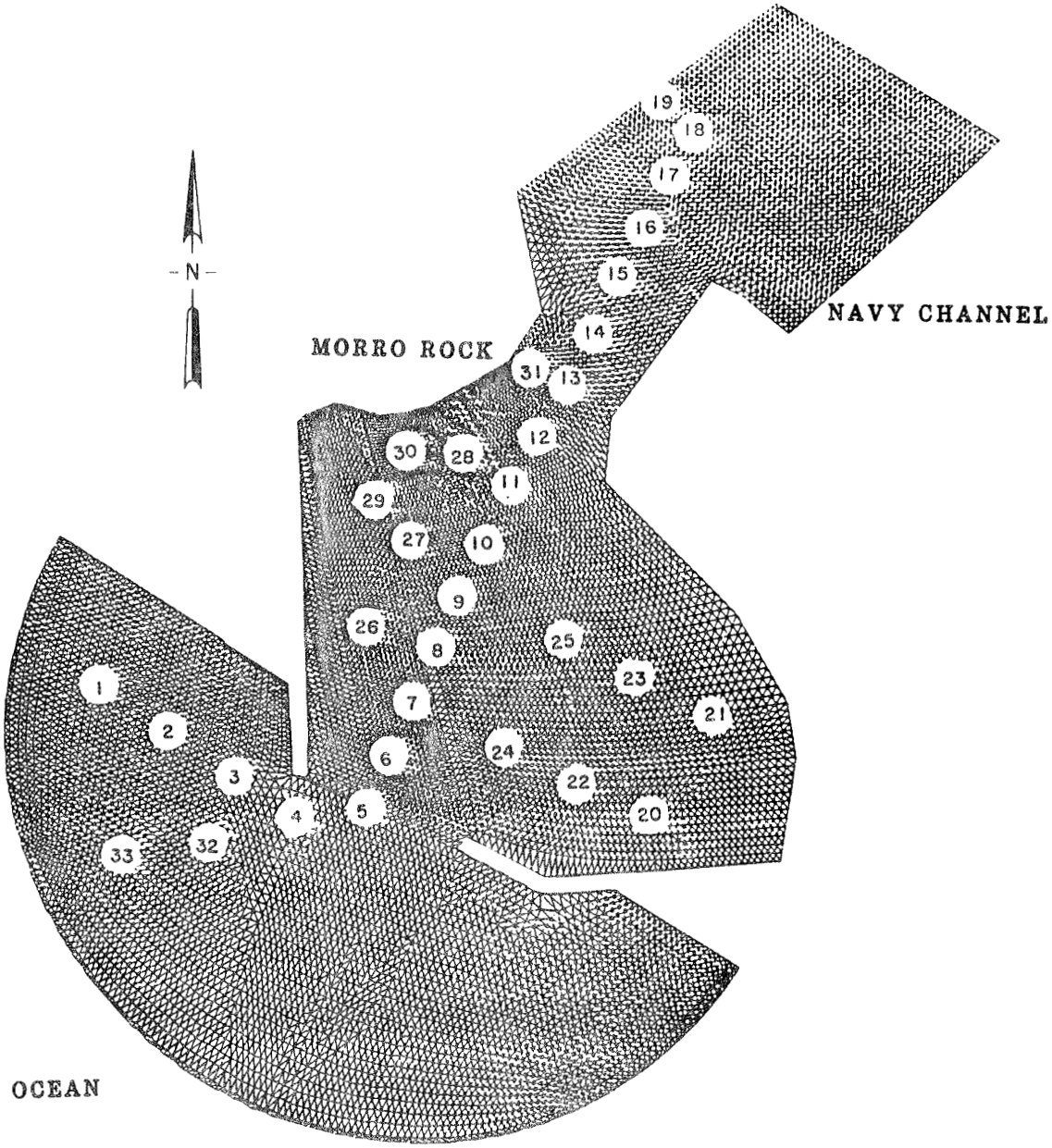

Figure 7. Output Basin Locations for HARBD

Table 3. Basin Locations and Depths

Summary of Basin Locations

X and Y are with respect to finite element grid origin.
Depths are for existing bathymetry.

Basin	Distance from Origin X (ft.)	Y (ft.)	Depth (ft. MLLW)
1	1377.0	1070.0	37.9
2	991.0	960.0	32.5
3	659.0	870.0	30.3
4	288.0	760.0	28.1
5	15.0	550.0	23.9
6	44.2	257.4	21.0
7	50.5	-25.2	17.0
8	32.7	-285.3	15.9
9	65.2	-552.3	14.4
10	95.7	-824.9	14.3
11	91.8	-1119.4	13.1
12	113.2	-1335.0	8.0
13	116.1	-1594.1	3.5
14	125.6	-1855.7	8.2
15	124.5	-2192.4	7.9
16	132.0	-2436.4	15.2
17	163.8	-2662.7	15.3
18	161.6	-2953.0	15.6
19	502.2	-2955.0	20.2
20	-1356.8	-454.6	4.9
21	-1345.7	-977.7	6.6
22	-851.7	-397.6	9.9
23	-192.5	-834.2	9.4
24	-387.9	-343.2	13.7
25	-369.0	-880.1	11.4
26	438.9	-259.7	11.0
27	505.9	-791.1	18.6
28	536.7	-1599.1	16.7
29	778.9	-788.9	3.3
30	813.5	-1289.3	1.6
31	536.7	-1599.1	16.7
32	830.0	1650.0	28.2
33	557.0	1220.0	33.1

B-1 through B-42. These plots reveal the change in amplification factors between existing conditions and the two proposed channel modifications.

45. As noted previously, HARBD contains no provisions for wave breaking. Interpretation of Figures B-1 through B-42 must be done cautiously. The actual wave height at the semi-circular outer boundary of the HARBD grid may be slightly different between the three bathymetry conditions modeled. Since it is these wave heights that are multiplied by the wave amplification factor, it is possible that similar wave amplification factors between the three conditions at any basin would lead to very different wave heights. Thus, direct comparisons between wave amplification factors should be done with care.

46. An alternate procedure for ascertaining the breaking wave climate was used to compensate for the lack of wave breaking inside HARBD. This technique was used for all 42 period-direction combinations run with HARBD.

47. The incipient breaking wave height was calculated for basins 1 through 11 using the method of Weggel (1972). Weggel's criterion is:

$$H_b/h_b = (b)/(1+(ba/gT^2)) \qquad (13)$$

where:

$a = 43.75(1-e^{(-19m)})$

$b = 1.56/(1+e^{(19.5m)})$

m = bottom slope

h_b = depth of incipient breaking, ft

T = wave period, sec

H_b = breaking wave height, ft

The ratio H_b/h_b can vary between 0.78 and 1.56 (Dean and Dalrymple 1984). These incipient breaking wave heights are listed in Table 4.

48. These incipient breaking heights were then back-transformed to the semi-circular outer boundary of the HARBD grid by dividing by the wave amplification factor for the particular basin and the particular wave condition. These heights were "unshoaled" to deep water (using linear theory). Assuming that these incipient breaking heights were $H_{(1/10)}$, or the average of the highest 10 percent of the waves in a given wave climate, the corresponding $H_{(1/3)}$ (significant wave height) may be found by (Wiegel 1964):

$$H_{(1/3)} = 0.78\ H_{(1/10)} \tag{14}$$

assuming a Rayleigh distribution of wave heights.

49. For each basin, the monthly WIS record was then searched for waves with this height or higher. The percent occurrences of these waves were totaled and converted to days of breaking by the following equation:

$$\text{Breaking days}(i) = (\text{number of days in month}) * \sum_{Hb(i)}^{j=Hb(i-1)} \%\ \text{occur. } H_j \tag{15}$$

Table 4. Incipient Breaking Wave Heights Through Channel

Basin No.	Incipient Breaking Wave Heights Exist H_b (ft.)	Alt. 5 H_b (ft.)	Alt. 6 H_b (ft.)
1	29.56	31.20	31.20
2	26.07	31.20	31.20
3	27.59	31.20	31.20
4	22.17	31.20	31.20
5	19.32	31.20	31.20
6	16.93	20.76	20.76
7	13.89	15.36	15.36
8	12.61	13.05	13.05
9	11.50	11.50	11.50
10	11.17	11.17	11.17
11	10.43	10.43	10.43
12	6.74	6.74	6.74
13	2.92	2.92	2.92

provided $H_{b(i-1)} > H > H_{b(i)}$, where i would be the number of the basin under consideration. This equation accounts for wave breaking in basins seaward of the basin considered. If a wave is found to break in a particular basin, it is then left out of summations for higher-numbered (landward) basins.

50. The results of this analysis are shown in Figures B-43 through B-54. They are also listed in Tables B-43 through B-54. A yearly summary of breaking conditions is found in Table B-55. The number of breaking days for basins 4 and 5 (considered the harbor entrance) is 31.4 days per year, which is close to the 28.9 days per year reported by the Morro Bay Harbor Patrol. It is likely that the difference between the reported and predicted numbers could be attributed to quantifying "hazardous conditions" as breaking waves.

51. From these results it can also be deduced that the

breaking conditions present at the entrance (basins 4 and 5) under existing conditions will decrease dramatically. Breaking at these locations will decrease from 33.8 days per year to 1.5 days per year with Alternative 5 and 2.5 days per year with Alternative 6. However, it appears that the frequency of breaking will increase just inside the entrance (basins 6 and 7) after improvement. In the case of basin 6, breaking which occurs 0.34 days per year presently will occur 6.72 days per year with Alternative 5 and 5.03 days per year with Alternative 6. Similar increases would occur for basin 7. In addition, the incipient breaking wave height for basins 6 and 7 under improved conditions (20.76 ft. and 15.36 ft, respectively) is higher than that for existing conditions (16.92 ft. and 13.89 ft.),indicating that higher waves would break more frequently at these locations.

52. There appears to be another sharp increase in breaking wave days at basin 9 after improvements are implemented. Under present conditions it appears that waves break in this basin 0.98 days per year. Implementation of Alternative 5 will increase this number to 3.62 days per year, while Alternative 6 will cause waves to break there 8.76 days per year. Since the depth and the slope at basin 9 does not change with the improvement, the incipient breaking wave height there remains the same (11.17 ft.). Thus waves of the same or similar height will break in basin 9 more frequently after dredging.

53. It appears from the above that the proposed improvements may simply move present entrance conditions further into the channel and the outer harbor. It may also worsen these

conditions. One probable reason for this is the steep 5% slope near the structures. One possible solution for this situation is to carry the 40 ft. depth further into the channel, and use a much gentler slope to connect it to the existing channel. This may not decrease the frequency of wave breaking, but it may serve to lower the breaking wave heights. Other alternatives to alleviate this problem, both structural and non-structural, are also possible.

Current-Induced Breaking Wave Climate Analysis

54. In many entrances and inlets, tidal currents are a major concern. These currents are generated when the tide level in the ocean rises or falls, causing a difference in water level between the ocean and the back bay area. A significant quantity of water flows through the connecting inlet, either toward the bay (during flood tide) or out to sea (during ebb tide). The back bay is often of large areal extent. If the entrance or inlet which connects it to the ocean is narrow or otherwise constricted, the current flowing through this inlet can reach considerable velocities during the 6 hour interval between low and high tide.

55. In navigation, it is often the seaward flow, or ebb current, which is of primary concern. Incoming waves will interact with this seaward flow, causing sudden steepening and breaking of these waves within the inlet. The Morro Bay Harbor Patrol has reported wave breaking at an entrance buoy moored at -50 ft. MLLW (U.S. Army Engineer District, Los Angeles 1989).

This suggests that strong wave/current interaction should be considered as a probable cause of breaking.

56. One task of this study was to determine breaking wave events due to pure wave/current interaction. Ebb tidal currents vary with the tidal wave phase. However, analysis of the interaction of the incoming waves with the maximum current velocity issuing from the harbor mouth gives an adequate qualitative depiction of the relative reduction in current-induced breaking with the implementation of the dredged improvements.

57. Section "A-A" of figure 1 is a representative cross-section of the rear entrance channel. It has an average cross-sectional area of 8953 sq. ft. The tidal prism for the back bay to which it connects is 87,200,000 sq. ft. at high tide. Using methods outlined in the Shore Protection Manual (SPM 1984), a maximum current velocity of 3.63 ft/s or 2.15 knots was calculated at section "A-A". This corresponds closely to the 2 knot maximum current velocity reported by the Navy (U.S. Army Corps of Engineers, Los Angeles District 1988).

58. The existing cross section at the mouth of the entrance channel has an area of 19,440 sq. ft. The relationship used between the current velocity at "A-A" and the current velocity at the entrance channel is:

$$U_{(ent)} = [A_{("A-A")} * U_{("A-A")}]/A_{(ent)} \qquad (16)$$

where:

$U_{(ent)}$ = current velocity at entrance, ft/sec

$A_{("A-A")}$ = cross sectional area at "A-A", ft^2

$U_{("A\text{-}A")}$ = current velocity at "A-A", ft/sec

$A_{(ent)}$ = cross sectional area at entrance, ft^2

This amounts to a simple continuity approach. This approach is valid because:

a. The constricting cross-section is section "A-A", not the entrance. This eliminates any temporary storage behind the structures. Thus, any change in surface area within the outer harbor with the change in tide level is negligible with respect to the entrance current.

b. The water level rises and falls as a nearly horizontal surface, incurring no additional velocities as a result of water level gradients within either the back bay or the outer harbor.

The results of these calculations for both existing and improved conditions are shown in Table 5.

59. The modified dispersion relation for waves on a co-linear current is (Perigrine 1976):

$$\Omega = \sigma + kU \tag{17}$$

where:

Ω = absolute frequency, or the wave frequency measured by a stationary observer, radians/sec

σ = intrinsic frequency, or the wave frequency measured by an observer moving with the current, radians/sec

k = wave number, dimensionless

U = current velocity, ft/sec

The relationship between the height of a wave modified by a current and the height of a wave without current is (Herchenroder 1981):

Maximum Current Velocities at Entrance Mouth

Existing Conditions	1.67 ft/sec
Alternative 5	1.45 ft/sec
Alternative 6	1.46 ft/sec

Table 5. Maximum Ebb Current Velocities at Entrance Mouth

$$H_{\text{with current}}/H_{\text{without current}} = \cosh(2\pi h/L_i)/\cosh(2\pi h/L_a) \quad (18)$$

where:

L_A = absolute wavelength.

L_I = intrinsic wavelength.

60. A program was written based on Equations 17 and 18 which would calculate the modified wave heights and lengths due to interaction with a co-linear current. Although the majority of the waves analyzed approach the harbor from north of west, the co-linear assumption is conservative, representing a worst-case generation/transformation event. To analyze steepness-limited breaking due to wave/current interaction, the following maximum wave steepness criterion was used (Kinsman 1965):

$$H/L_{(max)} = 1/7 \quad (19)$$

Wave heights, periods, directions, and percent occurrences just seaward of the entrance were saved during the RCPWAVE production runs. These unbroken waves, along with the currents in Table 5, were input into the wave/current program and the breaking events

noted. This was done for existing and improved conditions. Figures B-55 through B-57 show the hours/month of maximum current-induced wave breaking on a monthly basis for both existing and improved conditions. The reduction in breaking wave events with project conditions is evident. From these figures it appears that current-induced breaking would be reduced from 25 hours per year under existing conditions to 6 hours per year with Alternative 5 and 6.5 hours per year with Alternative 6.

PART V: LONGSHORE SEDIMENT TRANSPORT RATE

Entrance Shoaling and Maintenance Dredging

61. Because Estero Bay is located in an area with a high energy wave climate, an appreciable amount of sediment transport occurs along the shoreline. Determination of the rate of this sediment transport is important for proper feasibility planning of coastal projects.

TetraTech Study of 1975

62. TetraTech (Noda 1975) performed a study of the sand transport processes present at Morro Bay. They used ship observations compiled by U.S. Naval Oceanography Command in the "Summary of Synoptic Meterological Observations" (SSMO) as their wave climate input. They used a longshore flux formulation similar to Equation 2, and used the following equation for their sediment transport computation:

$$Q = 125\ E_a \tag{20}$$

where:

Q = longshore transport rate in cu. yd/day

E_a = longshore energy flux in millions of ft-lb/day per foot of beach.

They concluded that approximately 237,000 cu. yd. gross potential transport is directed toward the harbor entrance per year. Of

this, 76,965 cu. yd. come from the north beach, and the remaining 160,396 cu. yd. from the south beach. They also concluded that the net trend of sediment movement on the south beach is northward. However, they do not state the extent of the shoreline modeled. It appears that the length of the shoreline modeled could not have been great, as they use only one shoreline angle for their longshore flux calculations. Additionally, they use ship observations which are usually biased toward fair weather samples (Inman, et.al, 1986) and poorly correlated with wave periods and directions from other sources (Thompson and Harris 1972).

Sediment Transport

63. According to the present analysis, sediment transport along the Estero Bay coast tends to be predominantly southward, as seen from the longshore flux bar graphs of Figures A-1 through A-12. This implies that the net transport on the south beach is directed away from the harbor. However, there is a substantial number of breaking waves directed toward the harbor as well. These waves will transport sediment into the dredged entrance. Individual wave breaking events directed toward the harbor occurring in two regions were saved from the RCPWAVE production runs. These regions were:

a. North of the harbor and seaward of Morro Rock.
b. South of the harbor and seaward of the south jetty tip.

64. The presence of Morro Rock and the south jetty acts to trap any material moving along the shore. In the case of the north beach, it seems

unreasonably conservative to account for material shoreward of Morro Rock. This area is a deep embayment, with the distance from Morro Rock to the deepest part of the embayment being approximately 1,500 ft. It seems likely that sediment transport occurring shoreward of Morro Rock would be trapped behind it. Thus only transport seaward of the rock was taken into account. The jetty on the south beach would block northerly transport from migrating toward the harbor for a short time. As mentioned before, the primary direction for sediment transport is southward; thus, it would appear that sediment trapped behind the jetty would remain there for some period of time. In any case, analysis of the individual breaking events in this area indicates that the majority of waves break seaward of the jetty tip. The purpose of this minor adjustment was to account for the impoundment of material behind the south jetty.

65. The longshore flux factors in the two regions of interest were converted to potential sediment transport rate via the following relation:

$$Q_j = 7500 * P_{ls(w)j} \tag{21}$$

where Q is in cubic yards per year , j is the index for the longshore cell and the weighted longshore flux factor $P_{ls(w)}$ is in ft-lb/sec per foot of beach. These longshore flux factors were calculated during the RCPWAVE runs.The individual Q_j values were then arithmetically averaged for a reach of coastline. Q_j values were averaged together for cells 5-13 and 21-36. This was done for the monthly sea, swell and southern swell data sets. The results are tabulated in Tables D-1 and D-2. The result of this analysis is that about 214,343 cu.

yd/year potential transport is expected to move toward the entrance channel. This is divided into 197,669 cu. yd/year from the south beach and 16,674 cu. yd/year from the north beach.

66. There are many assumptions associated with this method for calculating sediment transport. Among them are the following:

> a. Equation 21 is an empirical relation. The actual value of the coefficient is dependent on grain size, porosity and mass density of material.
> b. The method does not account for bathymetric changes due to transport, shoreline changes, and filling of scour holes due to transport.

However, the total rate of potential deposition into the channel agrees very well with that predicted by TetraTech (Noda 1975). The predominant direction and transport rate calculated along the south beach differs significantly from the TetraTech prediction. This could be attributed to:

> a. The greater number of high waves and better representations of wave periods and directions in the WIS hindcasts than in the SSMO data.
>
> b. The representation of the Estero Bay shoreline as a series of straight line segments, rather than as a homogeneous straight shoreline as was done in the TetraTech study.

Additionally, the calculated potential sediment transport rate north of Morro Rock seems quite small compared to what may be expected from the high southerly longshore flux factors calculated in Part III of this report. The fact that this potential transport rate only accounts for material seaward of Morro Rock implies that a considerable amount of sediment is trapped behind the rock. This does not coincide with observations. However, it appears that there is a very limited supply of sediment in this region, with no apparent sediment source. This deviates from the "infinite supply" assumption of potential sediment transport calculation techniques. Therefore it is likely that no material will enter the harbor entrance from the north side.

PART VII : CONCLUSION

68. Based on the results of the study, the following may be concluded:

a. Based on the results of the HARBD analysis, the number of breaking days at the entrance (basins 4 and 5 of Figure 6) will be reduced from 28 days under existing conditions to 1.5 days with Alternative 5 and 2.5 days with Alternative 6.

b. From Table B-55 and Figures B-43 through B-54, it appears that much of the wave breaking has moved inside the outer harbor (basins 6 and 7). The number of breaking days for basin 6, for example, would increase from 0.34 days per year to 6.72 days per year with Alternative 5 and 5.03 days per year with Alternative 6. Additionally, the incipient breaking wave height at these locations is higher for improved conditions than for existing conditions, indicating that higher waves would break more frequently at these locations after channel enlargement.

c. To further reduce the amount of breaking inside the channel, the 40 ft. enlarged channel depth could be carried further inside the channel and a slope less than 0.05 could be used to tie the improvement into the existing channel. Other alternatives are also possible.

d. Enlarging the channel would also serve to reduce the maximum current through the entrance. Current-induced breaking under these maximum conditions would be reduced from 25 hours of breaking per year under existing conditions to approximately 6 hours per year with Alternative 5 and nearly 6.5 hours per year with Alternative 6.

e. The results of the sediment transport study indicate that about 214,000 cu yd of material would move toward the harbor per year. This is divided into 197,000 cu yd from the south beach and 16,000 cu yd from the north beach.

Need for Physical Model Study

69. This numerical model study has been sufficient for determining the increase in wave action inside the outer harbor and the reduction of wave

breaking at the entrance with the dredged improvements. A relative measure of the accuracy of the numerical approach adopted for this study is its ability to compute existing conditions which are close to recorded observations (wave breaking frequency in the harbor entrance, for instance). However, in order to gain a more accurate depiction of the absolute wave heights inside the harbor and the broken wave propagation through several proposed dredged channel configurations, a physical model study is necessary. An important modeling component of any such study should be the combined effects of shoaling and tidal currents on waves.

REFERENCES

Berkhoff, J.C.W. 1972. "Computation of Combined Refraction-Diffraction," Proceedings of the 13th International Conference on Coastal Engineering, American Society of Civil Engineers, Vol. 1, pp 471-490

Berkhoff, J.C.W. 1976. "Mathematical Models for Simple Harmonic Linear Water Waves, Wave Diffraction and Refraction," Publication No. 1963, Delft Hydraulics Laboratory, Delft, The Netherlands.

Berkhoff, J.C.W., Booij, N., and Radder, A.C. 1982. "Verification of Numerical Wave Propagation Models for Simple Harmonic Linear Water Waves," Coastal Engineering, Vol. 6, pp 255-279.

Bottin, R.R., Jr., Sargent, F.E., and Mize, M.G. 1985. "Fisherman's Wharf Area, San Francisco Bay, California, Design for Wave Protection: Physical and Numerical Model Investigation," Technical Report CERC-86-7, US Army Engineer Waterways Experiment Station, Vicksburg, Miss.

Chen, H.S., and Houston, J.R. 1987. "Calculation of Water Oscillation in Coastal Harbors: HARBS and HARBD User's Manual," Instruction Report CERC-87-2, US Army Engineer Waterways Experiment Station, Vicksburg, Miss.

Chen, H.S. and Mei, C.C. 1974. "Oscillations and Wave Forces in an Offshore Harbor," Report No. 190, Department of Civil Engineering, Massachusetts Institute of Technology, Cambridge, MA.

Corson, W.D., Abel, C.E., Brooks, R.M., Farrar, P.D., Groves, B.J., Payne, J.B., McAneny, D.S., and Tracy, B.A. 1987. "Pacific Coast Hindcast Phase II Wave Information,", WIS Report 16, US Army Engineer Waterways Experiment Station, Vicksburg, Miss.

Crawford, P.L., and Chen, H.S. 1988. "Comparison of Numerical and Physical Models of Wave Response in a Harbor," Miscellaneous Paper CERC-88-11, US Army Engineer Waterways Experiment Station, Vicksburg, Miss.

Dally, W.R., Dean, R.G., and Dalrymple, R.A. 1985. "Wave Height Variation Across Beaches of Arbitrary Profile," Journal of Geophysical Research, Vol. 90, No. C6, pp 11917-11927.

Dean, R.G., and Dalrymple, R.A. 1984. Water Wave Mechanics for Scientists and Engineers, Prentice-Hall, Inc., Englewood Cliffs, NJ., 353 p.

Ebersole, B.A., Cialone, M.A., and Prater, M.D. 1986. "Regional Coastal Processes Numerical Modeling System Report 1: RCPWAVE - A Linear Wave Propagation Model for Engineering Use," Technical Report CERC-86-4, US Army Engineer Waterways Experiment Station, Vicksburg, Miss.

Farrar, P.D. and Chen, H.S. 1986. "Wave Response of the Proposed Harbor at Agat, Guam: Numerical Model Investigation," Technical Report CERC-87-4, US Army Engineer Waterways Experiment Station, Vicksburg, Miss.

Herchenroder, B.A. 1981. "Effects of Currents on Waves," Coastal Engineering Technical Aid No. 81-14, U.S. Army Corps of Engineers Coastal Engineering Research Center, Fort Belvoir, Va.

Houston, J.R. 1976. "Long Beach Harbor Numerical Analysis of Harbor Oscillation; Existing Conditions and Proposed Improvements," Miscellaneous Paper H-76-20, Report 1, U.S. Army Engineer Waterways Experiment Station, Vicksburg, Miss.

Houston, J.R. 1981. "Combined Refraction and Diffraction of Short Waves Using the Finite Element Method," Applied Ocean Research, Vol. 3, No. 4, pp. 163-170.

Inman, D.L., Guza, R.T., Skelly, D.W., White, T.E. 1986. "Southern California Coastal Processes Data Summary," Ref. No. CCSTWS 86-1, prepared for US Army Corps of Engineers, Los Angeles District, Planning Division, Los Angeles, Ca.

Kinsman, B. 1965. Wind Waves, Prentice-Hall, Inc., Englewood Cliffs, NJ., 676 p.

Noda, E.K. 1975. "Preliminary Report: Sand Transport Analysis, Morro Bay," TetraTech Report No. TC-467, Pasadena, Ca.

Perigrine, D.H. 1976. "Interaction of Water Waves and Currents," Advances in Applied Mechanics, Vol. 16, Academic Press, New York, pp. 9-117.

Shore Protection Manual 1984. 2 vol. US Army Engineer Waterways Experiment Station, Vicksburg, Miss.

Thompson, E.F. and Harris, D.L. 1972. "A Wave Climatology for U.S. Coastal Waters," Proceedings of the Fourth Annual Offshore Technology Conference, Houston, Texas.

US Army Engineer District, Los Angeles. 1988. "Reconnaissance Report: Morro Bay Harbor, San Luis Obispo County, Ca," Los Angeles, Ca.

US Army Engineer District, Los Angeles. 1989. "Memorandum for Record Concerning Morro Bay Meeting of 19 December 1988," Los Angeles, Ca.

Weggel, J.R. 1972. "Maximum Breaker Height," Journal of the Waterways, Port, Coastal and Ocean Division, Vol. 78, No WW4, pp. 529-548.

Weishar, L.L. and Aubrey, D.G. 1986. "A Study of Inlet Hydraulics at Green Harbor,Marshfield, Mass.," Miscellaneous Report CERC 88-10, U.S. Army Engineer

Waterways Experiment Station, Vicksburg, Miss.

Wiegel, R.L. 1964. Oceanographic Engineering, Prentice-Hall, Inc., Englewood Cliffs, NJ. 532 p.

APPENDIX A: LONGSHORE FLUX FACTOR DISTRIBUTIONS: MONTHLY

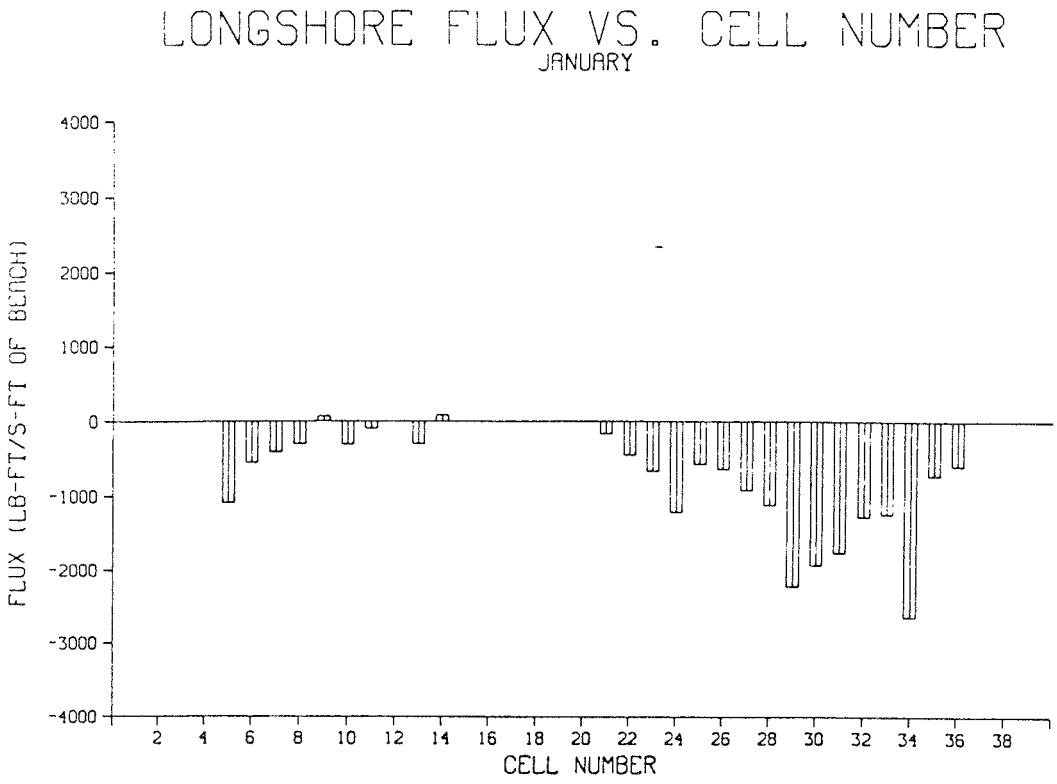

Figure A-1. Longshore Flux Distribution - January

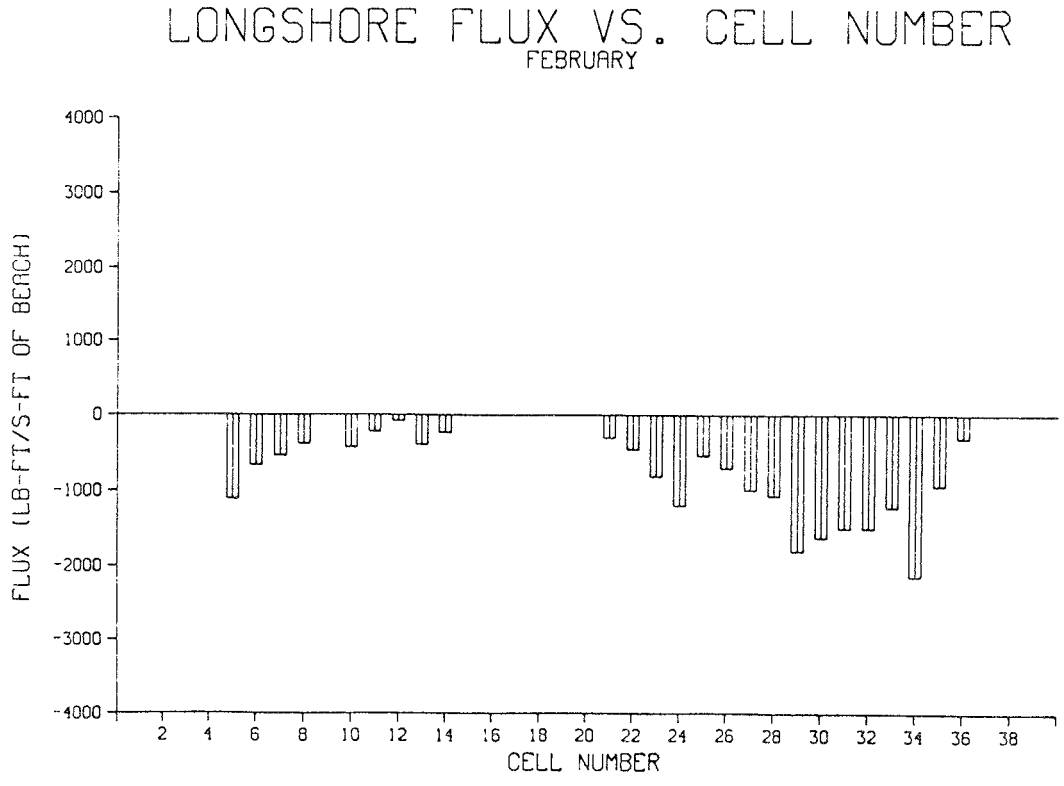

Figure A-2. Longshore Flux Distribution - February

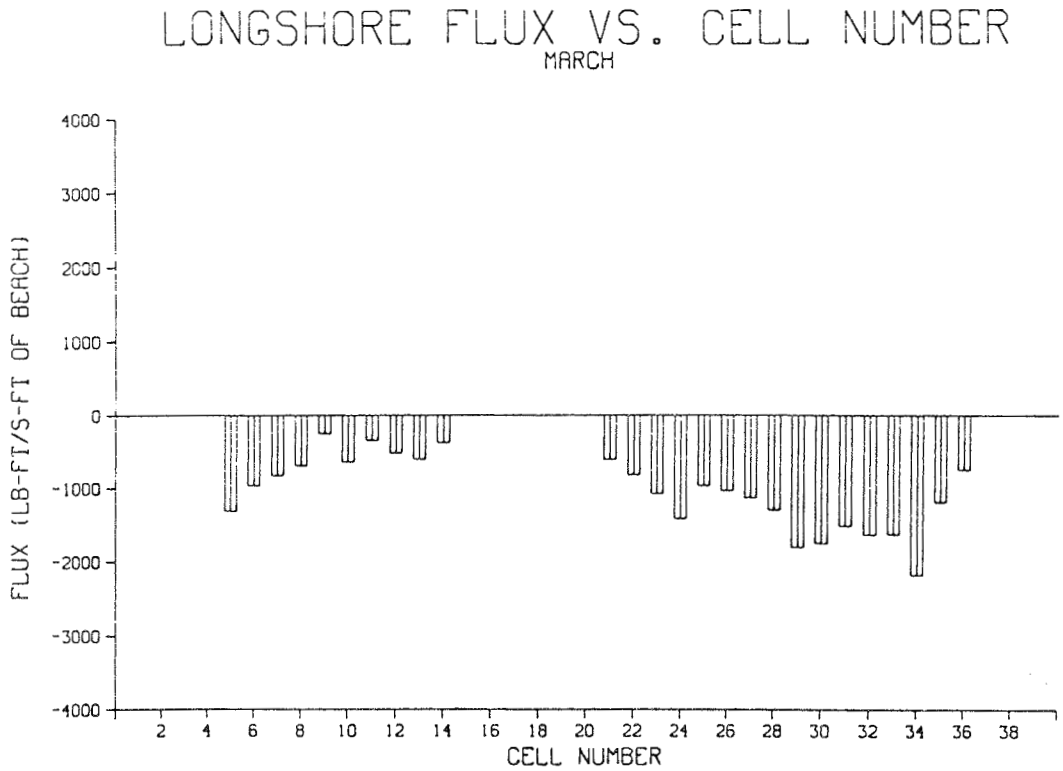

Figure A-3. Longshore Flux Distribution - March

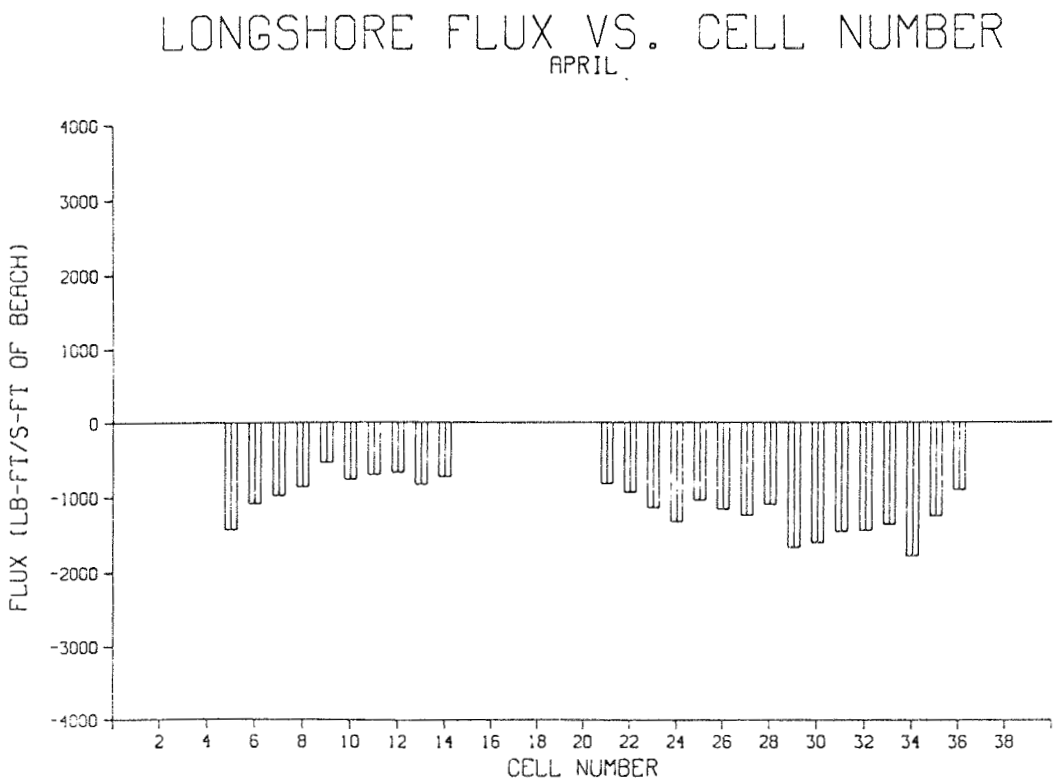

Figure A-4. Longshore Flux Distribution - April

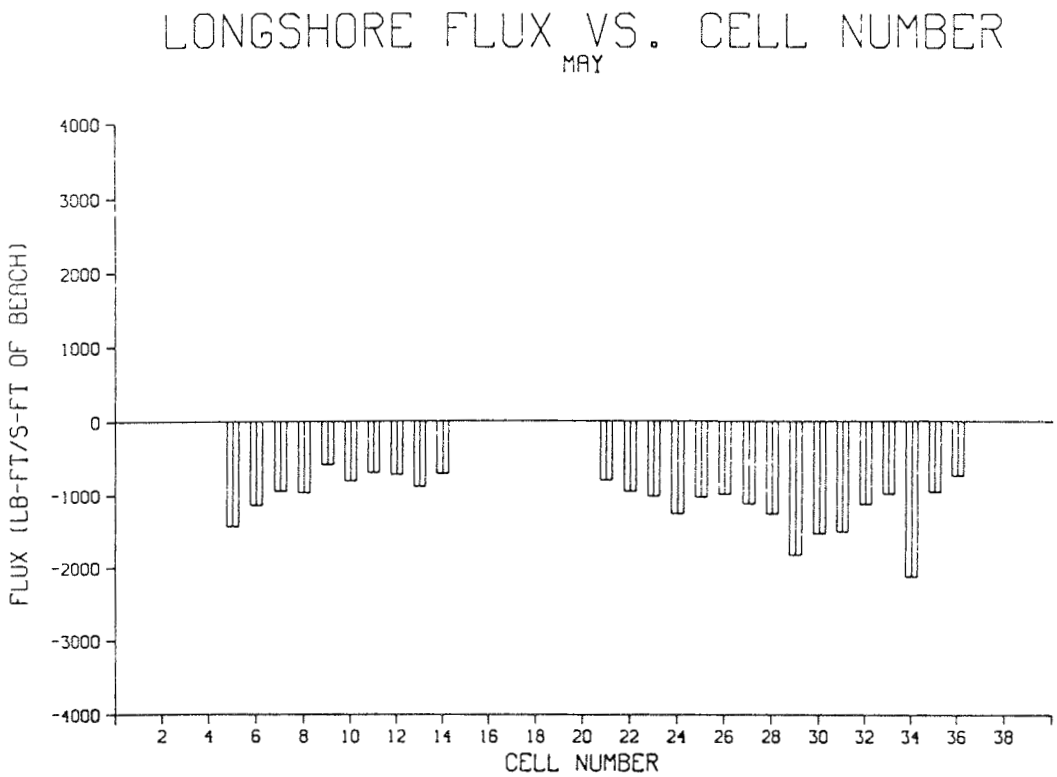

Figure A-5. Longshore Flux Distribution - May

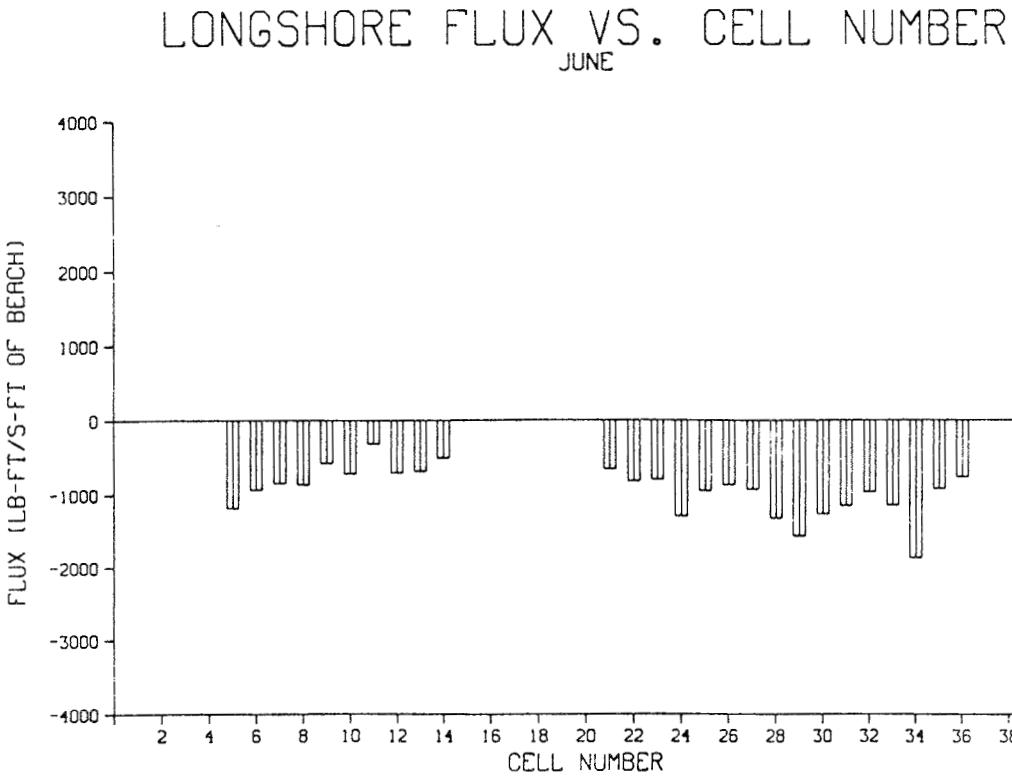

Figure A-6. Longshore Flux Distribution - June

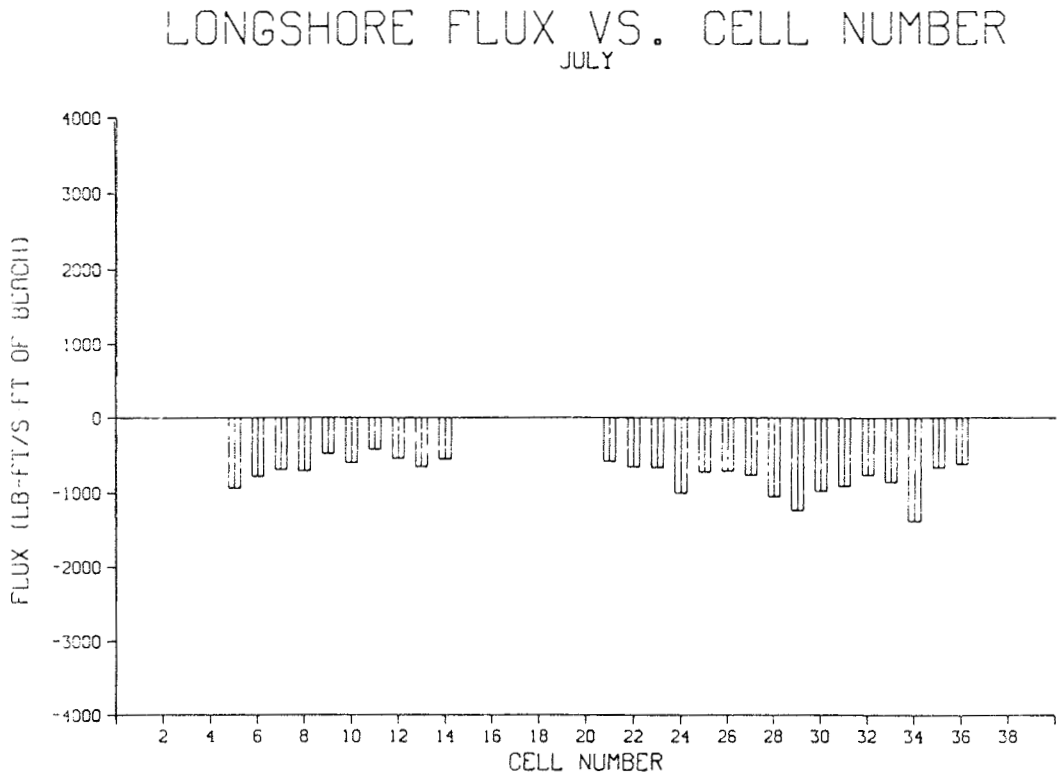

Figure A-7. Longshore Flux Distribution - July

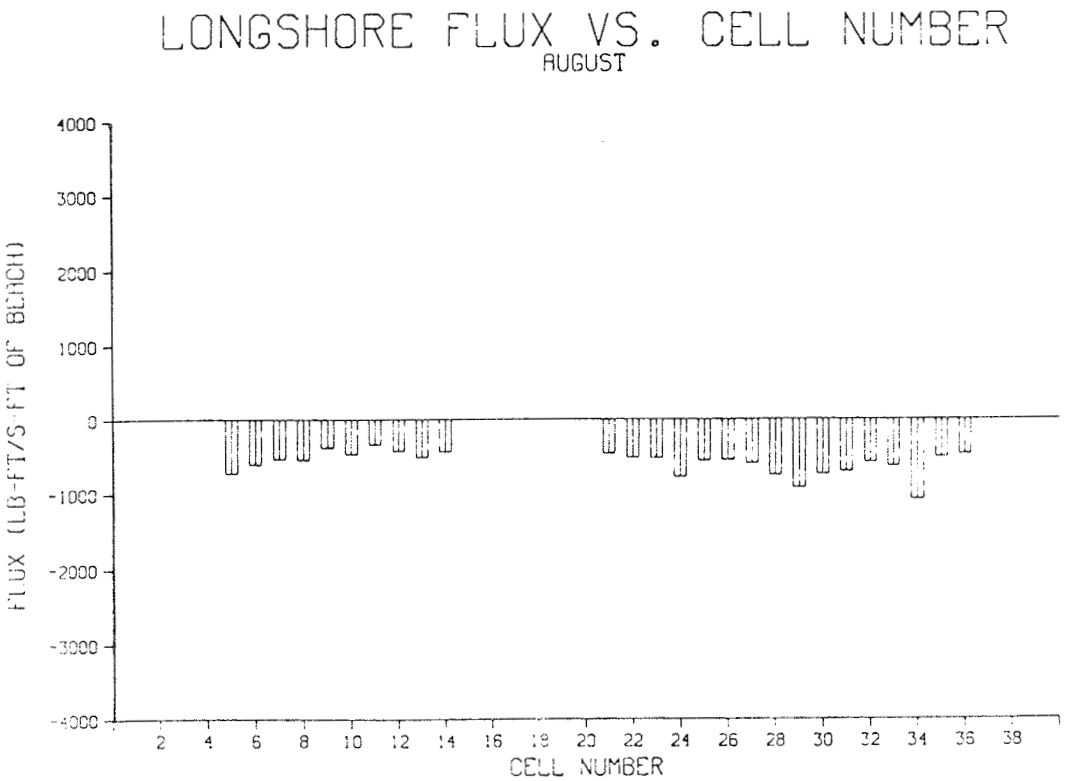

Figure A-8. Longshore Flux Distribution - August

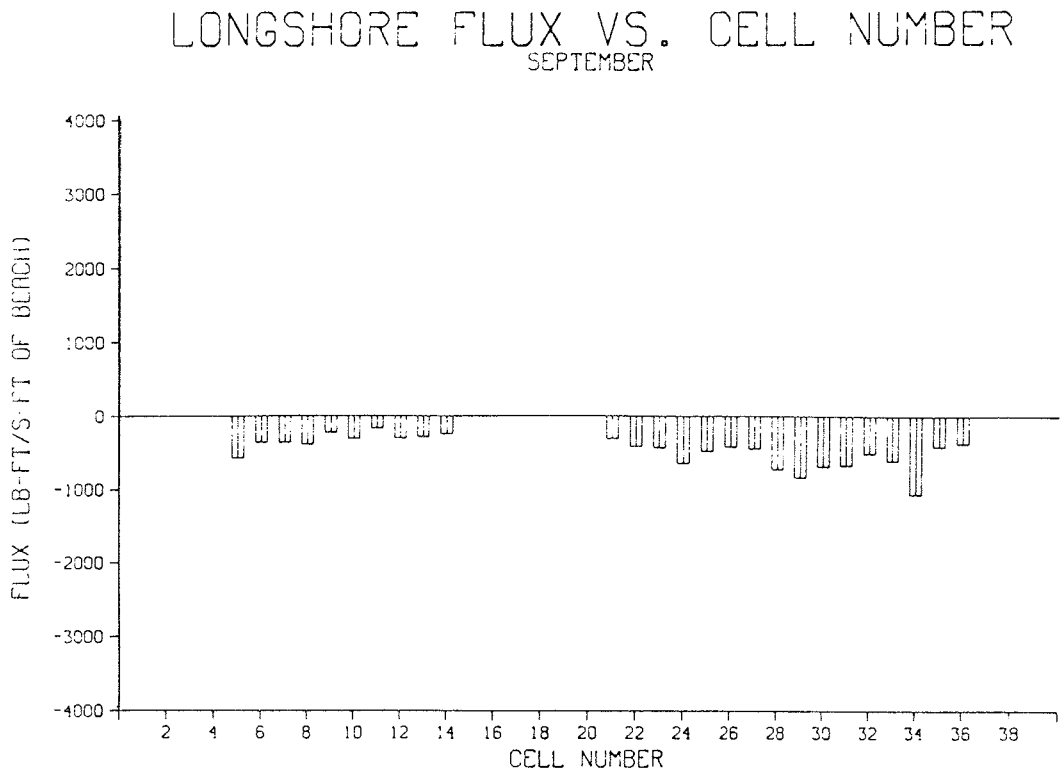

Figure A-9. Longshore Flux Distribution - September

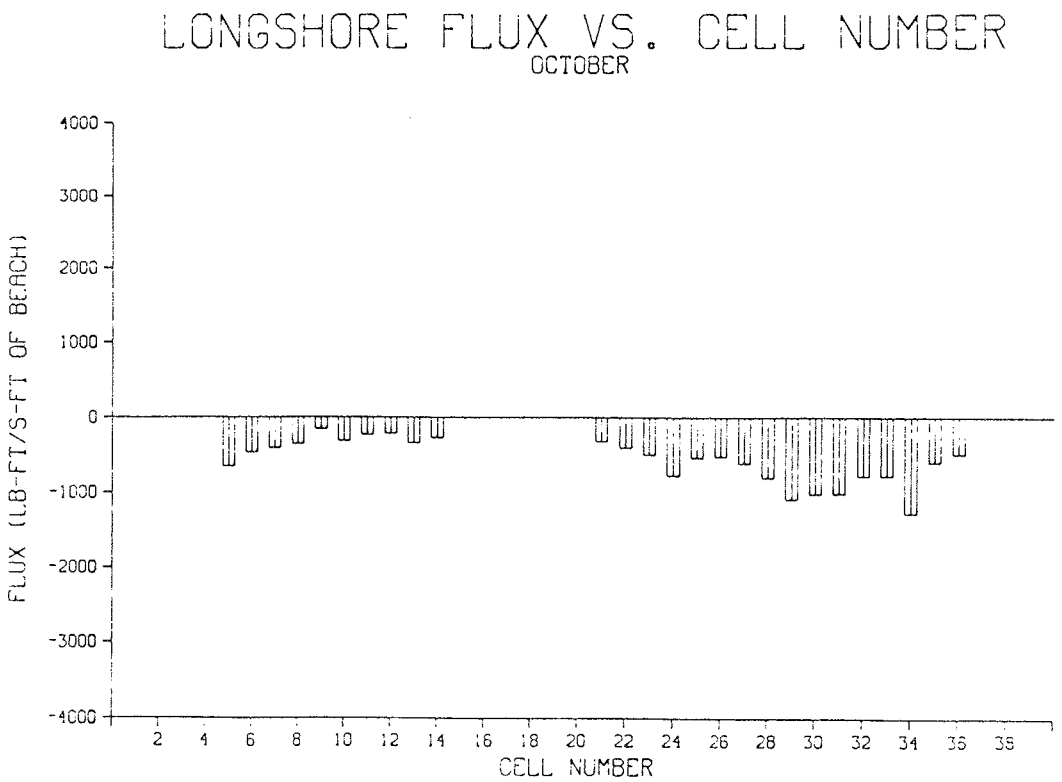

Figure A-10. Longshore Flux Distribution - October

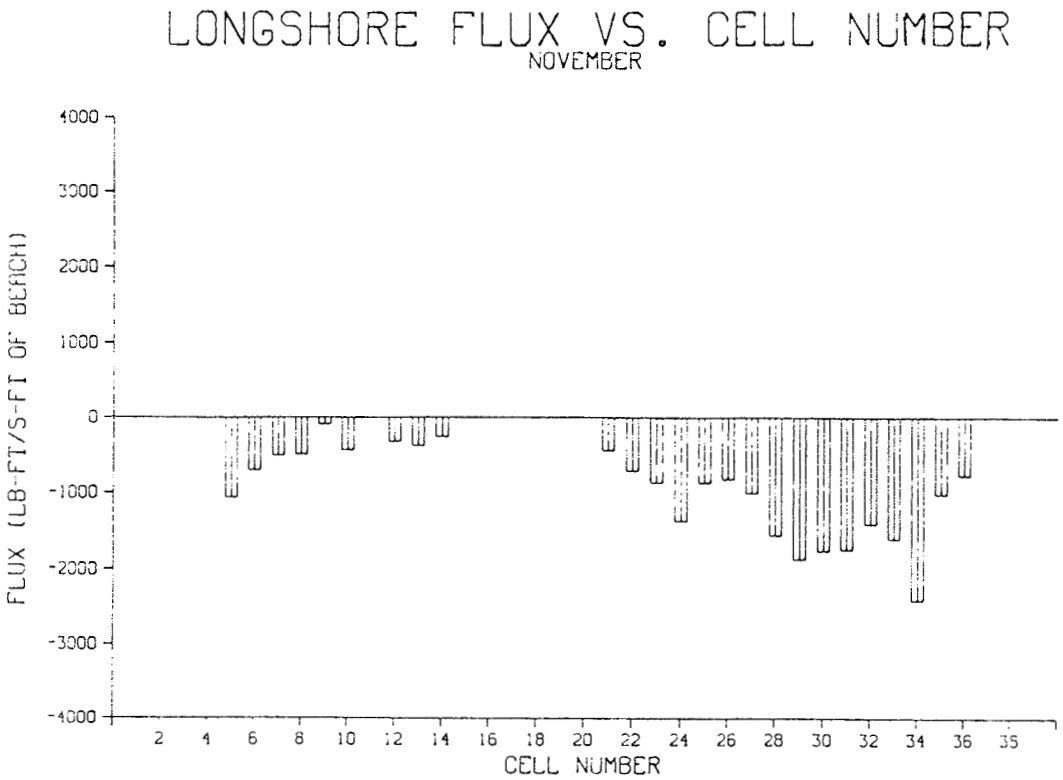

Figure A-11. Longshore Flux Distribution - November

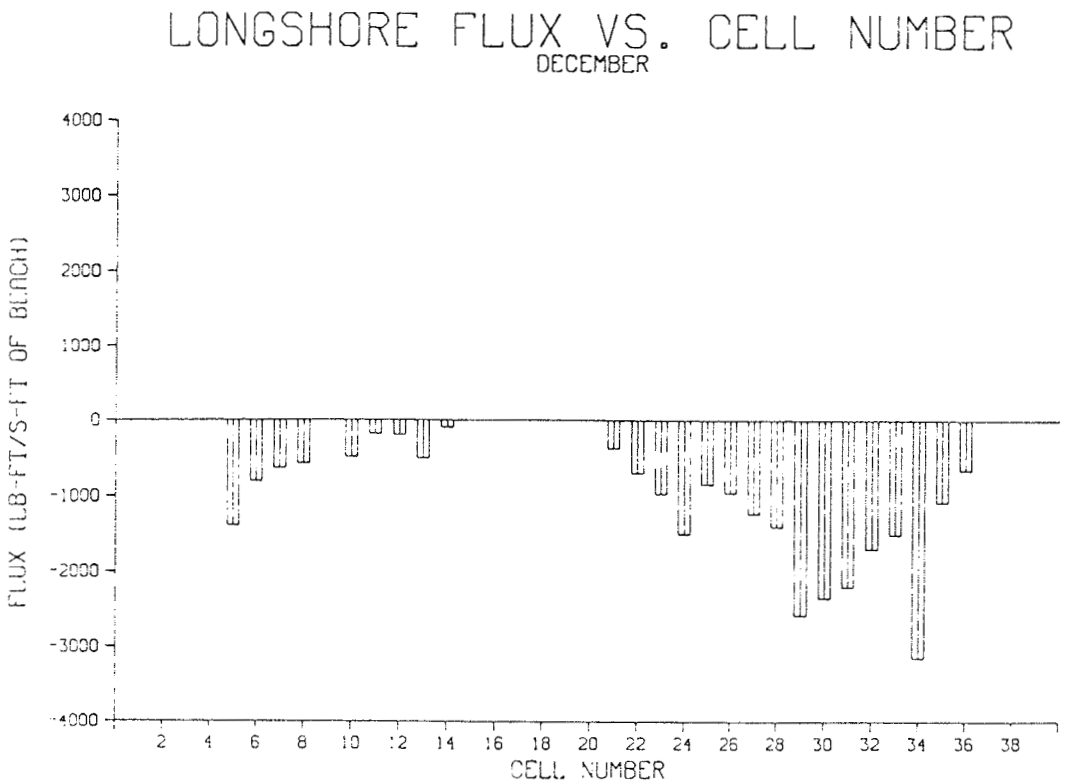

Figure A-12. Longshore Flux Distribution - December

APPENDIX B: BREAKING WAVE CLIMATE ANALYSIS

Table B-1

T = 10.02 seconds Deep Water Direction = 202.5 deg. az.

Basin	Amp. Fac. (Exist.)	Amp. Fac. (Alt.5)	% Change (Ex.& Alt.5)	Amp. Fac. (Alt.6)	% Change (Ex.& Alt.6)
1	1.3244	1.2340	-6.8257	1.3967	5.4591
2	1.3564	1.2572	-7.3135	1.3228	-2.4771
3	1.3008	1.0993	-15.4905	1.2641	-2.8213
4	1.2106	1.0540	-12.9357	1.2428	2.6598
5	1.3080	1.1957	-8.5856	1.3473	3.0046
6	0.9753	1.1087	13.6778	1.1393	16.8153
7	0.7240	0.9727	34.3508	0.9513	31.3950
8	0.6572	0.8668	31.8929	0.8128	23.6762
9	0.6184	0.8565	38.5026	0.8136	31.5653
10	0.4686	0.5928	26.5045	0.5684	21.2975
11	0.4735	0.6024	27.2228	0.5697	20.3168
12	0.4618	0.5795	25.4872	0.5433	17.6483
13	0.4312	0.5513	27.8525	0.5186	20.2690
14	0.0253	0.0513	102.7668	0.1047	313.8340
15	0.0468	0.0883	88.6752	0.1611	244.2308
16	0.0975	0.0253	-74.0513	0.0274	-71.8974
17	0.0319	0.0203	-36.3636	0.0198	-37.9310
18	0.0371	0.0219	-40.9703	0.0144	-61.1860
19	0.0213	0.0213	0.0000	0.0196	-7.9812
20	0.6780	0.7597	12.0502	0.6891	1.6372
21	0.7083	0.7955	12.3112	0.7139	0.7906
22	0.6985	0.7879	12.7989	0.7218	3.3357
23	0.6856	0.8064	17.6196	0.7824	14.1190
24	0.5682	0.7821	37.6452	0.7051	24.0936
25	0.5968	0.7274	21.8834	0.6429	7.7245
26	0.4822	0.6040	25.2592	0.3711	-23.0402
27	0.1881	0.2143	13.9288	0.1758	-6.5391
28	0.4968	0.5575	12.2182	0.4348	-12.4799
29	0.5462	0.7569	38.5756	0.5913	8.2571
30	0.5890	0.4113	-30.1698	0.3623	-38.4890
31	0.0202	0.0231	14.3564	0.0213	5.4455
32	1.7840	1.6253	-8.8957	1.6232	-9.0135
33	1.6871	1.5301	-9.3059	1.6510	-2.1398

Table B-2

T = 11.14 seconds Deep Water Direction = 202.5 deg. az.

Basin	Amp.Fac. (Exist.)	Amp.Fac. (Alt.5)	% Change (Ex.& Alt.5)	Amp.Fac. (Alt.6)	% Change (Ex.& Alt.6)
1	1.4451	1.4821	2.5604	1.5561	7.6811
2	1.4327	1.4668	2.3801	1.5837	10.5395
3	1.4527	1.4691	1.1289	1.6168	11.2962
4	1.3738	1.4443	5.1318	1.5771	14.7984
5	1.4820	1.6187	9.2240	1.7213	16.1471
6	0.9219	1.0046	8.9706	0.8567	-7.0723
7	0.9168	0.9242	0.8072	0.7778	-15.1614
8	0.8447	0.8561	1.3496	0.7279	-13.8274
9	0.8347	0.8156	-2.2882	0.6616	-20.7380
10	0.6985	0.7045	0.8590	0.5940	-14.9606
11	0.6856	0.6932	1.1085	0.6028	-12.0770
12	0.6505	0.6877	5.7187	0.5981	-8.0553
13	0.5373	0.6147	14.4054	0.5520	2.7359
14	0.0571	0.0280	-50.9632	0.0256	-55.1664
15	0.0231	0.0518	124.2424	0.0486	110.3896
16	0.0472	0.0457	-3.1780	0.0384	-18.6441
17	0.0198	0.0160	-19.1919	0.0146	-26.2626
18	0.0282	0.0212	-24.8227	0.0169	-40.0709
19	0.0251	0.0081	-67.7291	0.0051	-79.6813
20	0.6010	0.7506	24.8918	0.7110	18.3028
21	0.6730	0.8421	25.1263	0.7772	15.4829
22	0.6882	0.8353	21.3746	0.7573	10.0407
23	0.7260	0.8765	20.7300	0.7773	7.0661
24	0.7749	0.8840	14.0792	0.7430	-4.1167
25	0.7304	0.8250	12.9518	0.6999	-4.1758
26	0.8299	0.8444	1.7472	0.7813	-5.8561
27	0.3648	0.3970	8.8268	0.3968	8.7719
28	0.4374	0.3505	-19.8674	0.3107	-28.9666
29	0.7936	0.9054	14.0877	0.8517	7.3211
30	0.7671	0.7451	-2.8679	0.5781	-24.6382
31	0.0462	0.0183	-60.3896	0.0113	-75.5411
32	1.5513	1.3533	-12.7635	1.4633	-5.6727
33	1.4677	1.2462	-15.0916	1.3740	-6.3841

Table B-3

T = 12.54 seconds Deep Water Direction = 202.5 deg. az.

Basin	Amp.Fac. (Exist.)	Amp.Fac. (Alt.5)	% Change (Ex.& Alt.5)	Amp.Fac. (Alt.6)	% Change (Ex.& Alt.6)
1	1.5286	1.5128	-1.0336	1.5839	3.6177
2	1.5588	1.4639	-6.0880	1.5178	-2.6302
3	1.6266	1.4956	-8.0536	1.5786	-2.9509
4	1.6514	1.4843	-10.1187	1.5778	-4.4568
5	1.8113	1.5779	-12.8858	1.7349	-4.2180
6	1.1513	0.9745	-15.3565	1.1843	2.8663
7	1.1043	0.9942	-9.9701	1.1224	1.6390
8	0.9883	0.9197	-6.9412	1.0132	2.5195
9	1.0530	0.9791	-7.0180	1.0549	0.1804
10	0.9612	0.8827	-8.1669	0.8857	-7.8548
11	0.9131	0.8521	-6.6805	0.8427	-7.7100
12	0.8577	0.8131	-5.2000	0.8012	-6.5874
13	0.7166	0.7032	-1.8699	0.6938	-3.1817
14	0.0819	0.0800	-2.3199	0.0822	0.3663
15	0.1054	0.0746	-29.2220	0.0712	-32.4478
16	0.0839	0.0766	-8.7008	0.0716	-14.6603
17	0.0458	0.0461	0.6550	0.0426	-6.9869
18	0.0126	0.0136	7.9365	0.0124	-1.5873
19	0.0314	0.0312	-0.6369	0.0301	-4.1401
20	1.0217	1.0354	1.3409	0.9870	-3.3963
21	1.1263	1.1053	-1.8645	1.0263	-8.8786
22	1.1623	1.1144	-4.1211	1.0241	-11.8902
23	1.2372	1.1840	-4.3000	1.0818	-12.5606
24	1.2404	1.1203	-9.6824	0.9550	-23.0087
25	1.1650	1.0600	-9.0129	0.9092	-21.9571
26	1.1917	1.3150	10.3466	1.1456	-3.8684
27	0.6077	0.6403	5.3645	0.6156	1.3000
28	0.7963	0.8057	1.1805	0.7478	-6.0907
29	1.4565	1.3826	-5.0738	1.1786	-19.0800
30	0.4823	0.7357	52.5399	0.7359	52.5814
31	0.0136	0.0218	60.2941	0.0196	44.1176
32	1.2095	1.4912	23.2906	1.3899	14.9153
33	1.0587	1.3095	23.6894	1.2213	15.3585

Table B-4

T = 14.75 seconds Deep Water Direction = 202.5 deg. az.

Basin	Amp.Fac. (Exist.)	Amp.Fac. (Alt.5)	% Change (Ex.& Alt.5)	Amp.Fac. (Alt.6)	% Change (Ex.& Alt.)
1	1.4875	1.4091	-5.2706	1.3709	-7.8387
2	1.5599	1.4933	-4.2695	1.4170	-9.1608
3	1.6127	1.5877	-1.5502	1.4685	-8.9415
4	1.7112	1.7282	0.9935	1.5678	-8.3801
5	1.9751	1.9948	0.9974	1.7964	-9.0476
6	1.5490	1.6629	7.3531	1.4545	-6.1007
7	1.1671	1.1768	0.8311	1.0242	-12.2440
8	0.9666	0.9348	-3.2899	0.8128	-15.9114
9	0.9365	0.8215	-12.2798	0.7084	-24.3566
10	0.7063	0.5740	-18.7314	0.5205	-26.3061
11	0.6189	0.5244	-15.2690	0.4903	-20.7788
12	0.5335	0.4849	-9.1097	0.4520	-15.2765
13	0.3923	0.3830	-2.3706	0.3664	-6.6021
14	0.0196	0.0273	39.2857	0.0168	-14.2857
15	0.0650	0.0750	15.3846	0.0626	-3.6923
16	0.0250	0.0274	9.6000	0.0228	-8.8000
17	0.0228	0.0254	11.4035	0.0209	-8.3333
18	0.0069	0.0066	-4.3478	0.0054	-21.7391
19	0.0291	0.0329	13.0584	0.0272	-6.5292
20	0.8260	0.7533	-8.8014	0.6811	-17.5424
21	0.9609	0.8224	-14.4136	0.7866	-18.1392
22	1.0007	0.8233	-17.7276	0.8121	-18.8468
23	1.0820	0.8866	-18.0591	0.8828	-18.4104
24	1.1215	0.8637	-22.9871	0.9438	-15.8449
25	1.0635	0.7852	-26.1683	0.8846	-16.8218
26	1.1776	1.0698	-9.1542	1.1849	0.6199
27	0.6092	0.6439	5.6960	0.6708	10.1116
28	0.3546	0.4744	33.7845	0.4318	21.7710
29	1.2848	1.2478	-2.8798	1.3239	3.0433
30	0.4383	0.4074	-7.0500	0.3981	-9.1718
31	0.0465	0.0477	2.5806	0.0407	-12.4731
32	1.0871	1.1123	2.3181	1.2007	10.4498
33	0.9673	0.9301	-3.8458	1.0183	5.2724

Table B-5

T = 16.77 seconds Deep Water Direction = 202.5 deg. az.

Basin	Amp.Fac. (Exist.)	Amp.Fac. (Alt.5)	% Change (Ex.& Alt.5)	Amp.Fac. (Alt.6)	% Change (Ex.& Alt.6)
1	1.2943	1.4751	13.9689	1.3711	5.9337
2	1.2674	1.4338	13.1292	1.3062	3.0614
3	1.2978	1.4455	11.3808	1.3106	0.9863
4	1.4052	1.6543	17.7270	1.5257	8.5753
5	1.5323	1.9382	26.4896	1.7932	17.0267
6	1.3658	1.9341	41.6093	1.8239	33.5408
7	1.1438	1.5340	34.1144	1.4255	24.6284
8	0.9604	1.2539	30.5602	1.1555	20.3145
9	0.9591	1.1669	21.6661	1.0600	10.5203
10	0.7676	0.7932	3.3351	0.7018	-8.5722
11	0.6722	0.6491	-3.4365	0.5767	-14.2071
12	0.5801	0.5230	-9.8431	0.4653	-19.7897
13	0.4222	0.3900	-7.6267	0.3487	-17.4088
14	0.0780	0.0438	-43.8462	0.0267	-65.7692
15	0.1466	0.0980	-33.1514	0.0796	-45.7026
16	0.0757	0.0537	-29.0621	0.0435	-42.5363
17	0.0613	0.0441	-28.0587	0.0361	-41.1093
18	0.0433	0.0311	-28.1755	0.0254	-41.3395
19	0.0655	0.0477	-27.1756	0.0389	-40.6107
20	0.5837	0.5347	-8.3947	0.4104	-29.6899
21	0.7838	0.5734	-26.8436	0.4979	-36.4761
22	0.8653	0.5640	-34.8203	0.5018	-42.0086
23	0.9393	0.5855	-37.6663	0.5320	-43.3621
24	1.0557	0.5715	-45.8653	0.5783	-45.2212
25	1.0518	0.4966	-52.7857	0.5524	-47.4805
26	1.1359	0.7369	-35.1263	0.8808	-22.4580
27	0.6587	0.4043	-38.6215	0.3424	-48.0188
28	0.3749	0.2272	-39.3972	0.1960	-47.7194
29	1.2057	0.8996	-25.3877	0.8790	-27.0963
30	0.3964	0.3089	-22.0737	0.3128	-21.0898
31	0.1049	0.0790	-24.6902	0.0646	-38.4175
32	0.9720	1.0517	8.1996	0.9616	-1.0700
33	0.9147	1.0357	13.2284	0.9746	6.5486

Table B-6

T = 20.14 seconds Deep Water Direction = 202.5 deg. az.

Basin	Amp.Fac. (Exist.)	Amp.Fac. (Alt.5)	% Change (Ex.& Alt.5)	Amp.Fac. (Alt.6)	% Change (Ex.& Alt.6)
1	1.1510	1.0092	-12.3197	1.1981	4.0921
2	1.2126	1.0232	-15.6193	1.1741	-3.1750
3	1.2084	1.0447	-13.5468	1.1791	-2.4247
4	1.3099	1.0054	-23.2461	1.1909	-9.0847
5	1.4527	1.1294	-22.2551	1.3998	-3.6415
6	1.4044	1.3506	-3.8308	1.6102	14.6539
7	1.1033	1.1970	8.4927	1.3733	24.4720
8	0.9044	1.0676	18.0451	1.2015	32.8505
9	0.9072	1.0928	20.4586	1.1991	32.1759
10	0.7513	0.8788	16.9706	0.9162	21.9486
11	0.6789	0.7617	12.1962	0.7789	14.7297
12	0.5954	0.6320	6.1471	0.6350	6.6510
13	0.4526	0.4623	2.1432	0.4469	-1.2594
14	0.0352	0.0458	30.1136	0.0470	33.5227
15	0.0079	0.0095	20.2532	0.0099	25.3165
16	0.0009	0.0022	144.4444	0.0028	211.1111
17	0.0045	0.0031	-31.1111	0.0025	-44.4444
18	0.0037	0.0027	-27.0270	0.0024	-35.1351
19	0.0057	0.0044	-22.8070	0.0039	-31.5789
20	0.5228	0.4517	-13.5999	0.2575	-50.7460
21	0.6613	0.5764	-12.8384	0.3922	-40.6926
22	0.6921	0.6142	-11.2556	0.4427	-36.0353
23	0.7507	0.6345	-15.4789	0.4730	-36.9921
24	0.8178	0.7089	-13.3162	0.5708	-30.2030
25	0.7972	0.7485	-6.1089	0.6020	-24.4857
26	1.3704	1.0411	-24.0295	0.8802	-35.7706
27	0.7788	0.6424	-17.5141	0.5791	-25.6420
28	0.4732	0.4188	-11.4962	0.3966	-16.1877
29	1.4035	1.1523	-17.8981	1.0195	-27.3602
30	0.3072	0.2933	-4.5247	0.2715	-11.6211
31	0.0180	0.0162	-10.0000	0.0156	-13.3333
32	1.1232	1.2670	12.8027	1.2617	12.3308
33	0.8788	1.0397	18.3091	0.9563	8.8188

Table B-7

T = 22.22 seconds Deep Water Direction = 202.5 deg. az.

Basin	Amp.Fac. (Exist.)	Amp.Fac. (Alt.5)	% Change (Ex.& Alt.5)	Amp.Fac. (Alt.6)	% Change (Ex.& Alt.6)
1	1.3280	1.0901	-17.9141	1.1461	-13.6973
2	1.3120	1.1014	-16.0518	1.1495	-12.3857
3	1.3196	1.0564	-19.9454	1.0579	-19.8318
4	1.3999	1.0891	-22.2016	1.1213	-19.9014
5	1.6180	1.1815	-26.9778	1.3368	-17.3795
6	1.5059	1.3081	-13.1350	1.4979	-0.5312
7	1.0825	1.0998	1.5982	1.2454	15.0485
8	0.8340	0.9448	13.2854	1.0641	27.5899
9	0.8223	0.9753	18.6063	1.0856	32.0199
10	0.6602	0.7912	19.8425	0.8501	28.7640
11	0.5810	0.6848	17.8658	0.7208	24.0620
12	0.5053	0.5642	11.6564	0.5845	15.6739
13	0.3815	0.4254	11.5072	0.4229	10.8519
14	0.0101	0.0172	70.2970	0.0180	78.2178
15	0.0037	0.0060	62.1622	0.0063	70.2703
16	0.0064	0.0080	25.0000	0.0084	31.2500
17	0.0079	0.0082	3.7975	0.0085	7.5949
18	0.0053	0.0053	0.0000	0.0054	1.8868
19	0.0066	0.0062	-6.0606	0.0062	-6.0606
20	0.5599	0.3789	-32.3272	0.3099	-44.6508
21	0.7362	0.5606	-23.8522	0.4996	-32.1380
22	0.7533	0.5908	-21.5718	0.5368	-28.7402
23	0.8318	0.6198	-25.4869	0.5775	-30.5723
24	0.8624	0.6987	-18.9819	0.6771	-21.4865
25	0.8161	0.7506	-8.0260	0.7056	-13.5400
26	1.5720	1.4147	-10.0064	1.3297	-15.4135
27	0.6274	0.5943	-5.2757	0.6058	-3.4428
28	0.3308	0.2845	-13.9964	0.3002	-9.2503
29	1.2671	1.1617	-8.3182	1.1376	-10.2202
30	0.2834	0.2686	-5.2223	0.2830	-0.1411
31	0.0227	0.0193	-14.9780	0.0200	-11.8943
32	1.0572	1.1025	4.2849	1.0733	1.5229
33	0.6355	0.7162	12.6987	0.6582	3.5720

Table B-8

T = 10.02 seconds Deep Water Direction = 225 deg. az.

Basin	Amp.Fac. (Exist.)	Amp.Fac. (Alt.5)	% Change (Ex.& Alt.5)	Amp.Fac. (Alt.6)	% Change (Ex.& Alt.6)
1	1.4897	1.4826	-0.4766	1.4423	-3.1818
2	1.5443	1.5551	0.6993	1.5031	-2.6679
3	1.5666	1.6362	4.4427	1.5711	0.2872
4	1.5967	1.6706	4.6283	1.5908	-0.3695
5	1.6447	1.7284	5.0891	1.6403	-0.2675
6	0.6108	0.6102	-0.0982	0.5459	-10.6254
7	0.7140	0.7224	1.1765	0.6675	-6.5126
8	0.6661	0.6660	-0.0150	0.6336	-4.8792
9	0.7372	0.7324	-0.6511	0.6872	-6.7824
10	0.6722	0.6663	-0.8777	0.6006	-10.6516
11	0.6558	0.6442	-1.7688	0.5851	-10.7807
12	0.6226	0.6171	-0.8834	0.5645	-9.3318
13	0.5567	0.5415	-2.7304	0.5113	-8.1552
14	0.0637	0.0871	36.7347	0.0811	27.3155
15	0.0826	0.0506	-38.7409	0.0434	-47.4576
16	0.0437	0.0758	73.4554	0.0854	95.4233
17	0.0196	0.0385	96.4286	0.0400	104.0816
18	0.0253	0.0494	95.2569	0.0513	102.7668
19	0.0217	0.0254	17.0507	0.0248	14.2857
20	0.4136	0.4081	-1.3298	0.4172	0.8704
21	0.4961	0.5248	5.7851	0.5170	4.2129
22	0.5064	0.5513	8.8665	0.5386	6.3586
23	0.5081	0.5776	13.6784	0.5639	10.9821
24	0.5178	0.6105	17.9027	0.5826	12.5145
25	0.5522	0.6309	14.2521	0.5960	7.9319
26	0.9563	1.0656	11.4295	1.0789	12.8202
27	0.4012	0.3511	-12.4875	0.3667	-8.5992
28	0.4086	0.6540	60.0587	0.6147	50.4405
29	0.6029	0.7110	17.9300	0.7584	25.7920
30	0.5868	0.6349	8.1970	0.6244	6.4076
31	0.0132	0.0318	140.9091	0.0301	128.0303
32	1.6189	1.6405	1.3342	1.6021	-1.0377
33	1.1071	1.0751	-2.8904	1.0425	-5.8351

Table B-9

T = 11.14 seconds Deep Water Direction = 225 deg. az.

Basin	Amp.Fac. (Exist.)	Amp.Fac. (Alt.5)	% Change (Ex.& Alt.5)	Amp.Fac. (Alt.6)	% Change (Ex.& Alt.6)
1	1.5658	1.5578	-0.5109	1.4321	-8.5388
2	1.6161	1.6361	1.2376	1.5064	-6.7879
3	1.7002	1.7113	0.6529	1.5435	-9.2166
4	1.7994	1.7686	-1.7117	1.5366	-14.6049
5	1.9107	1.7443	-8.7088	1.5043	-21.2697
6	1.2603	1.0940	-13.1953	1.1396	-9.5771
7	1.0437	1.0583	1.3989	1.2127	16.1924
8	0.9098	1.0122	11.2552	1.1891	30.6991
9	0.9012	1.0800	19.8402	1.2624	40.0799
10	0.8413	1.0364	23.1903	1.1398	35.4808
11	0.8229	1.0594	28.7398	1.1422	38.8018
12	0.7909	1.0527	33.1015	1.1297	42.8373
13	0.6826	0.9522	39.4960	1.0124	48.3153
14	0.0719	0.0531	-26.1474	0.0453	-36.9958
15	0.0540	0.0564	4.4444	0.0538	-0.3704
16	0.1208	0.1139	-5.7119	0.0999	-17.3013
17	0.0399	0.0353	-11.5288	0.0317	-20.5514
18	0.0626	0.0567	-9.4249	0.0506	-19.1693
19	0.0614	0.0384	-37.4593	0.0320	-47.8827
20	1.0344	1.1816	14.2305	1.2061	16.5990
21	1.1689	1.2691	8.5722	1.2968	10.9419
22	1.2329	1.2637	2.4982	1.2977	5.2559
23	1.3197	1.3059	-1.0457	1.3568	2.8112
24	1.3060	1.1800	-9.6478	1.3468	3.1240
25	1.2582	1.2005	-4.5859	1.2607	0.1987
26	1.3705	1.2296	-10.2809	0.9948	-27.4134
27	0.7167	0.8704	21.4455	0.8443	17.8038
28	0.9201	0.8826	-4.0756	0.8316	-9.6185
29	0.8114	1.0046	23.8107	0.8411	3.6603
30	0.9455	0.8020	-15.1772	0.7398	-21.7557
31	0.0899	0.0685	-23.8042	0.0616	-31.4794
32	1.3164	1.5352	16.6211	1.5396	16.9553
33	1.0265	1.3225	28.8359	1.2479	21.5684

Table B-10

T = 12.54 seconds Deep Water Direction = 225 deg. az.

Basin	Amp.Fac. (Exist.)	Amp.Fac. (Alt.5)	% Change (Ex.& Alt.5)	Amp.Fac. (Alt.6)	% Change (Ex.& Alt.6)
1	1.3060	1.5415	18.0322	1.4572	11.5773
2	1.2749	1.4755	15.7346	1.4653	14.9345
3	1.2808	1.4043	9.6424	1.4501	13.2183
4	1.3122	1.5296	16.5676	1.5598	18.8691
5	1.4166	1.7822	25.8083	1.7952	26.7260
6	1.4546	1.7796	22.3429	1.7662	21.4217
7	1.3073	1.4652	12.0783	1.3968	6.8462
8	1.1853	1.2192	2.8600	1.1599	-2.1429
9	1.2083	1.1706	-3.1201	1.0854	-10.1713
10	1.0142	0.8882	-12.4236	0.8169	-19.4538
11	0.9493	0.8122	-14.4422	0.7582	-20.1306
12	0.8867	0.7570	-14.6273	0.7088	-20.0632
13	0.7256	0.6397	-11.8385	0.6158	-15.1323
14	0.0742	0.0567	-23.5849	0.0501	-32.4798
15	0.0828	0.0720	-13.0435	0.0710	-14.2512
16	0.0873	0.0666	-23.7113	0.0620	-28.9805
17	0.0508	0.0386	-24.0157	0.0366	-27.9528
18	0.0173	0.0119	-31.2139	0.0112	-35.2601
19	0.0248	0.0250	0.8065	0.0268	8.0645
20	0.4661	0.6625	42.1369	0.4854	4.1407
21	0.6577	0.8093	23.0500	0.6371	-3.1321
22	0.7289	0.8726	19.7146	0.6966	-4.4313
23	0.7587	0.9365	23.4348	0.7394	-2.5438
24	0.7991	0.9977	24.8530	0.8128	1.7144
25	0.8555	0.9862	15.2776	0.8353	-2.3612
26	1.3586	1.1389	-16.1711	1.2370	-8.9504
27	0.4470	0.6068	35.7494	0.6025	34.7875
28	0.9593	0.6396	-33.3264	0.6033	-37.1104
29	0.7160	0.9201	28.5056	0.9597	34.0363
30	0.5463	0.5922	8.4020	0.5473	0.1830
31	0.0288	0.0166	-42.3611	0.0174	-39.5833
32	1.2179	1.2905	5.9611	1.2282	0.8457
33	0.9332	1.0823	15.9773	0.9970	6.8367

Table B-11

T = 14.75 seconds Deep Water Direction = 225 deg. az.

Basin	Amp.Fac. (Exist.)	Amp.Fac. (Alt.5)	% Change (Ex.& Alt.5)	Amp.Fac. (Alt.6)	% Change (Ex.& Alt.6)
1	1.4710	1.0875	-26.0707	1.0638	-27.6818
2	1.4522	1.0766	-25.8642	1.0310	-29.0043
3	1.4244	1.1157	-21.6723	1.0282	-27.8152
4	1.5514	1.1930	-23.1017	1.0615	-31.5779
5	1.7420	1.2741	-26.8599	1.1494	-34.0184
6	1.5575	1.3705	-12.0064	1.3825	-11.2360
7	1.2186	1.1830	-2.9214	1.2238	0.4267
8	0.9273	1.0233	10.3526	1.0841	16.9093
9	0.8780	1.0280	17.0843	1.0972	24.9658
10	0.7019	0.8572	22.1257	0.8887	26.6135
11	0.6517	0.7868	20.7304	0.7983	22.4950
12	0.5961	0.6954	16.6583	0.7017	17.7151
13	0.4484	0.5156	14.9866	0.5195	15.8564
14	0.0570	0.0532	-6.6667	0.0572	0.3509
15	0.1074	0.0868	-19.1806	0.0938	-12.6629
16	0.0364	0.0300	-17.5824	0.0327	-10.1648
17	0.0307	0.0247	-19.5440	0.0276	-10.0977
18	0.0101	0.0083	-17.8218	0.0091	-9.9010
19	0.0390	0.0314	-19.4872	0.0348	-10.7692
20	0.5330	0.4246	-20.3377	0.4208	-21.0507
21	0.7095	0.5186	-26.9063	0.5107	-28.0197
22	0.7694	0.5723	-25.6174	0.5579	-27.4890
23	0.8231	0.5852	-28.9029	0.5710	-30.6281
24	0.9124	0.6419	-29.6471	0.6268	-31.3021
25	0.9426	0.7069	-25.0053	0.6649	-29.4611
26	1.1978	0.7849	-34.4715	0.7408	-38.1533
27	0.8665	0.6769	-21.8811	0.5999	-30.7675
28	0.3601	0.3289	-8.6643	0.3159	-12.2744
29	1.0955	0.8534	-22.0995	0.7070	-35.4633
30	0.6364	0.5130	-19.3903	0.5181	-18.5889
31	0.0506	0.0454	-10.2767	0.0489	-3.3597
32	1.2230	1.1527	-5.7482	1.2074	-1.2756
33	0.7509	0.8567	14.0898	0.8321	10.8137

Table B-12

T = 16.77 seconds Deep Water Direction = 225 deg. az.

Basin	Amp.Fac. (Exist.)	Amp.Fac. (Alt.5)	% Change (Ex.& Alt.5)	Amp.Fac. (Alt.6)	% Change (Ex.& Alt.6)
1	1.4073	1.3460	-4.3559	1.1859	-15.7323
2	1.3857	1.3101	-5.4557	1.1407	-17.6806
3	1.4459	1.3481	-6.7640	1.1873	-17.8851
4	1.5457	1.4322	-7.3430	1.1819	-23.5363
5	1.7989	1.6691	-7.2155	1.3599	-24.4038
6	1.8415	1.8253	-0.8797	1.5788	-14.2655
7	1.5146	1.5053	-0.6140	1.4060	-7.1702
8	1.2390	1.3147	6.1098	1.2580	1.5335
9	1.1986	1.2804	6.8246	1.2501	4.2967
10	0.9491	1.0008	5.4473	1.0113	6.5536
11	0.8417	0.8834	4.9543	0.9029	7.2710
12	0.7325	0.7470	1.9795	0.7710	5.2560
13	0.5171	0.5334	3.1522	0.5447	5.3375
14	0.1004	0.0659	-34.3626	0.0743	-25.9960
15	0.1450	0.1055	-27.2414	0.1082	-25.3793
16	0.0732	0.0521	-28.8251	0.0534	-27.0492
17	0.0591	0.0411	-30.4569	0.0412	-30.2876
18	0.0419	0.0292	-30.3103	0.0293	-30.0716
19	0.0631	0.0438	-30.5864	0.0440	-30.2694
20	0.4897	0.4202	-14.1924	0.3832	-21.7480
21	0.6221	0.5469	-12.0881	0.5133	-17.4891
22	0.6701	0.5908	-11.8341	0.5545	-17.2512
23	0.7154	0.6347	-11.2804	0.6111	-14.5793
24	0.7677	0.7280	-5.1713	0.6907	-10.0300
25	0.8045	0.7278	-9.5339	0.6799	-15.4879
26	1.0469	0.8145	-22.1989	0.8651	-17.3656
27	0.6441	0.5117	-20.5558	0.5573	-13.4762
28	0.3456	0.2538	-26.5625	0.2537	-26.5914
29	1.2612	1.0122	-19.7431	1.0116	-19.7907
30	0.2984	0.3405	14.1086	0.3444	15.4155
31	0.1028	0.0724	-29.5720	0.0730	-28.9883
32	1.3323	1.3768	3.3401	1.3039	-2.1316
33	0.9718	1.0161	4.5586	0.9220	-5.1245

Table B-13

T = 20.14 seconds Deep Water Direction = 225 deg. az.

Basin	Amp.Fac. (Exist.)	Amp.Fac. (Alt.5)	% Change (Ex.& Alt.5)	Amp.Fac. (Alt.6)	% Change (Ex.& Alt.6)
1	1.0979	1.0404	-5.2373	1.0773	-1.8763
2	1.0415	1.0079	-3.2261	1.0806	3.7542
3	1.0917	1.0223	-6.3571	1.1338	3.8564
4	1.1566	1.1729	1.4093	1.3199	14.1190
5	1.2506	1.3511	8.0361	1.4858	18.8070
6	1.1579	1.5557	34.3553	1.7685	52.7334
7	1.0198	1.3377	31.1728	1.4757	44.7049
8	0.8906	1.1652	30.8331	1.2717	42.7914
9	0.9268	1.1767	26.9637	1.2600	35.9517
10	0.7842	0.9183	17.1002	0.9414	20.0459
11	0.7194	0.7984	10.9814	0.8051	11.9127
12	0.6393	0.6657	4.1295	0.6606	3.3318
13	0.4927	0.4958	0.6292	0.4706	-4.4855
14	0.0331	0.0404	22.0544	0.0410	23.8671
15	0.0058	0.0060	3.4483	0.0066	13.7931
16	0.0018	0.0012	-33.3333	0.0015	-16.6667
17	0.0054	0.0041	-24.0741	0.0034	-37.0370
18	0.0042	0.0032	-23.8095	0.0027	-35.7143
19	0.0065	0.0048	-26.1538	0.0039	-40.0000
20	0.6551	0.4632	-29.2932	0.3447	-47.3821
21	0.7331	0.5556	-24.2122	0.4601	-37.2391
22	0.7464	0.5949	-20.2974	0.5166	-30.7878
23	0.8090	0.6065	-25.0309	0.5532	-31.6193
24	0.7903	0.6506	-17.6768	0.6281	-20.5239
25	0.6887	0.7014	1.8440	0.6456	-6.2582
26	1.1477	0.8610	-24.9804	0.7525	-34.4341
27	0.7246	0.5506	-24.0133	0.4829	-33.3563
28	0.4760	0.3863	-18.8445	0.3616	-24.0336
29	1.1740	0.9165	-21.9336	0.8170	-30.4089
30	0.2983	0.2564	-14.0463	0.2254	-24.4385
31	0.0185	0.0158	-14.5946	0.0144	-22.1622
32	1.0299	0.9483	-7.9231	0.9560	-7.1755
33	0.7579	0.7434	-1.9132	0.7403	-2.3222

Table B-14

T = 22.22 seconds Deep Water Direction = 225 deg. az.

Basin	Amp.Fac. (Exist.)	Amp.Fac. (Alt.5)	% Change (Ex.& Alt.5)	Amp.Fac. (Alt.6)	% Change (Ex.& Alt.6)
1	1.1480	1.0830	-5.6620	1.1384	-0.8362
2	1.1612	1.0132	-12.7454	1.0665	-8.1554
3	1.1507	1.0152	-11.7754	1.1107	-3.4761
4	1.2261	1.0313	-15.8878	1.1760	-4.0861
5	1.3135	1.1617	-11.5569	1.3391	1.9490
6	1.1600	1.2677	9.2845	1.4813	27.6983
7	0.9256	1.1138	20.3328	1.2491	34.9503
8	0.7533	0.9606	27.5189	1.0621	40.9930
9	0.7631	0.9980	30.7823	1.0831	41.9342
10	0.6285	0.8161	29.8489	0.8542	35.9109
11	0.5711	0.7166	25.4771	0.7367	28.9967
12	0.5146	0.6136	19.2383	0.6234	21.1426
13	0.3972	0.4701	18.3535	0.4534	14.1490
14	0.0102	0.0117	14.7059	0.0116	13.7255
15	0.0027	0.0042	55.5555	0.0044	62.9630
16	0.0057	0.0071	24.5614	0.0074	29.8246
17	0.0079	0.0085	7.5949	0.0089	12.6582
18	0.0054	0.0058	7.4074	0.0059	9.2593
19	0.0071	0.0072	1.4084	0.0073	2.8169
20	0.6028	0.4345	-27.9197	0.2970	-50.7299
21	0.7385	0.5678	-23.1144	0.4660	-36.8991
22	0.7467	0.5979	-19.9277	0.5136	-31.2174
23	0.8178	0.6065	-25.8376	0.5512	-32.5997
24	0.7954	0.6676	-16.0674	0.6423	-19.2482
25	0.7290	0.7120	-2.3320	0.6651	-8.7654
26	1.4098	1.1776	-16.4704	1.0769	-23.6133
27	0.6319	0.5874	-7.0423	0.5849	-7.4379
28	0.3388	0.3291	-2.8630	0.3455	1.9776
29	1.1695	1.0434	-10.7824	1.0018	-14.3395
30	0.2905	0.3005	3.4423	0.3084	6.1618
31	0.0244	0.0237	-2.8688	0.0244	0.0000
32	1.1697	1.1923	1.9321	1.2240	4.6422
33	1.0772	1.0870	0.9098	1.0704	-0.6313

Table B-15

T = 10.02 seconds Deep Water Direction = 247.5 deg. az.

Basin	Amp.Fac. (Exist.)	Amp.Fac. (Alt.5)	% Change (Ex.& Alt.5)	Amp.Fac. (Alt.6)	%Change (Ex.& Alt.6)
1	1.4862	1.4324	-3.6200	1.3592	-8.5453
2	1.4741	1.4451	-1.9673	1.4118	-4.2263
3	1.4991	1.4541	-3.0018	1.4388	-4.0224
4	1.5144	1.5363	1.4461	1.5027	-0.7726
5	1.5436	1.5291	-0.9394	1.5600	1.0625
6	1.3091	1.3049	-0.3208	1.4053	7.3486
7	1.1447	1.2028	5.0756	1.3110	14.5278
8	0.9309	1.0083	8.3145	1.1015	18.3264
9	0.9101	1.0198	12.0536	1.1111	22.0855
10	0.7461	0.8743	17.1827	0.9502	27.3556
11	0.7011	0.8457	20.6247	0.9119	30.0670
12	0.6899	0.8199	18.8433	0.8743	26.7285
13	0.6237	0.7117	14.1093	0.7533	20.7792
14	0.0866	0.0750	-13.3949	0.0869	0.3464
15	0.1332	0.1687	26.6516	0.1812	36.0360
16	0.1376	0.1158	-15.8430	0.1291	-6.1773
17	0.0837	0.0695	-16.9654	0.0711	-15.0538
18	0.0904	0.0847	-6.3053	0.0889	-1.6593
19	0.0411	0.0431	4.8662	0.0436	6.0827
20	0.6457	0.6107	-5.4205	0.5864	-9.1838
21	0.8182	0.7462	-8.7998	0.7040	-13.9575
22	0.9048	0.7807	-13.7157	0.7224	-20.1592
23	0.9602	0.7858	-18.1629	0.7162	-25.4114
24	1.1999	0.9907	-17.4348	0.9028	-24.7604
25	1.2686	1.0627	-16.2305	0.9569	-24.5704
26	0.9956	0.9528	-4.2989	0.9544	-4.1382
27	0.6662	0.3864	-41.9994	0.4427	-33.5485
28	0.9001	0.7058	-21.5865	0.7155	-20.5088
29	2.1923	1.8376	-16.1794	1.7245	-21.3383
30	1.1804	0.8937	-24.2884	0.8289	-29.7780
31	0.0452	0.0435	-3.7611	0.0476	5.3097
32	1.6618	1.6981	2.1844	1.6714	0.5777
33	1.3710	1.5122	10.2990	1.3947	1.7287

Table B-16

T = 11.14 seconds Deep Water Direction = 247.5 deg. az.

Basin	Amp.Fac. (Exist.)	Amp.Fac. (Alt.5)	% Change (Ex.& Alt.5)	Amp.Fac. (Alt.6)	% Change (Ex.& Alt.6)
1	1.2188	1.2078	-0.9025	1.1851	-2.7650
2	1.1829	1.2142	2.6460	1.1995	1.4033
3	1.1884	1.2321	3.6772	1.2187	2.5496
4	1.3230	1.3675	3.3636	1.3864	4.7921
5	1.3730	1.5114	10.0801	1.5400	12.1631
6	1.3428	1.6455	22.5424	1.7191	28.0235
7	1.2091	1.5411	27.4584	1.5986	32.2140
8	1.0154	1.3797	35.8775	1.4129	39.1471
9	0.9519	1.3512	41.9477	1.3560	42.4519
10	0.7798	1.0644	36.4965	1.0452	34.0344
11	0.7267	0.9973	37.2368	0.9785	34.6498
12	0.6827	0.9452	38.4503	0.9194	34.6712
13	0.5584	0.7510	34.4914	0.7354	31.6977
14	0.1296	0.1464	12.9630	0.1480	14.1975
15	0.0792	0.0672	-15.1515	0.0608	-23.2323
16	0.1315	0.1130	-14.0684	0.1227	-6.6920
17	0.0405	0.0343	-15.3086	0.0366	-9.6296
18	0.0464	0.0409	-11.8534	0.0480	3.4483
19	0.0518	0.0452	-12.7413	0.0488	-5.7915
20	0.7033	0.6708	-4.6211	0.6050	-13.9770
21	0.8098	0.8267	2.0869	0.7564	-6.5942
22	0.8703	0.9014	3.5735	0.8501	-2.3210
23	0.9288	0.9338	0.5383	0.8966	-3.4668
24	1.0588	0.9924	-6.2712	0.9766	-7.7635
25	1.0354	1.0542	1.8157	1.0201	-1.4777
26	1.1673	1.2542	7.4445	1.1724	0.4369
27	0.8219	0.7616	-7.3367	0.7399	-9.9769
28	0.9680	0.8598	-11.1777	0.9038	-6.6322
29	1.8938	1.1644	-38.5152	1.1476	-39.4023
30	0.7276	0.6774	-6.8994	0.7318	0.5772
31	0.0766	0.0621	-18.9295	0.0695	-9.2689
32	1.4963	1.4572	-2.6131	1.5106	0.9557
33	1.2024	1.1697	-2.7196	1.2348	2.6946

Table B-17

T = 12.54 seconds Deep Water Direction = 247.5 deg. az.

Basin	Amp.Fac. (Exist.)	Amp.Fac. (Alt.5)	% Change (Ex.& Alt.5)	Amp.Fac. (Alt.6)	% Change (Ex.& Alt.6)
1	1.4519	1.4599	0.5510	1.4094	-2.9272
2	1.4830	1.3421	-9.5010	1.2765	-13.9245
3	1.5099	1.2842	-14.9480	1.2556	-16.8422
4	1.6427	1.3893	-15.4258	1.3143	-19.9915
5	1.7502	1.4369	-17.9008	1.3150	-24.8657
6	1.5193	1.5286	0.6121	1.4802	-2.5735
7	1.4010	1.4600	4.2113	1.4532	3.7259
8	1.1753	1.3711	16.6596	1.3736	16.8723
9	1.1439	1.4105	23.3062	1.4187	24.0231
10	0.9882	1.2071	22.1514	1.2372	25.1973
11	0.9373	1.0945	16.7716	1.1197	19.4601
12	0.8850	0.9799	10.7232	1.0134	14.5085
13	0.7207	0.7816	8.4501	0.7994	10.9199
14	0.0754	0.0595	-21.0875	0.0557	-26.1273
15	0.0529	0.0505	-4.5369	0.0414	-21.7391
16	0.0779	0.0460	-40.9499	0.0494	-36.5854
17	0.0446	0.0247	-44.6188	0.0265	-40.5830
18	0.0138	0.0106	-23.1884	0.0120	-13.0435
19	0.0217	0.0119	-45.1613	0.0092	-57.6037
20	0.8214	0.5426	-33.9421	0.5472	-33.3820
21	0.9872	0.7136	-27.7148	0.7278	-26.2763
22	1.0808	0.7557	-30.0796	0.7870	-27.1836
23	1.1616	0.7955	-31.5169	0.8360	-28.0303
24	1.2935	0.8104	-37.3483	0.8715	-32.6247
25	1.2518	0.8604	-31.2670	0.9118	-27.1609
26	1.0172	1.2115	19.1015	1.2015	18.1184
27	0.5927	0.4026	-32.0736	0.4027	-32.0567
28	1.1059	0.6629	-40.0579	0.6894	-37.6616
29	1.0791	0.5685	-47.3172	0.5203	-51.7839
30	1.1340	0.7393	-34.8060	0.8134	-28.2716
31	0.0201	0.0248	23.3831	0.0296	47.2637
32	1.2068	1.3487	11.7584	1.2819	6.2231
33	0.8593	1.0517	22.3903	0.9386	9.2284

Table B-18

T = 14.75 seconds Deep Water Direction = 247.5 deg. az.

Basin	Amp.Fac. (Exist.)	Amp.Fac. (Alt.5)	% Change (Ex.& Alt.5)	Amp.Fac. (Alt.6)	% Change (Ex.& Alt.6)
1	1.1486	1.2796	11.4052	1.1432	-0.4701
2	1.1666	1.2641	8.3576	1.1324	-2.9316
3	1.1673	1.2771	9.4063	1.1582	-0.7796
4	1.2367	1.3770	11.3447	1.2937	4.6090
5	1.3807	1.4940	8.2060	1.4943	8.2277
6	1.6312	1.8867	15.6633	1.9715	20.8619
7	1.5614	1.7706	13.3982	1.8420	17.9710
8	1.4356	1.6375	14.0638	1.6847	17.3516
9	1.4831	1.6688	12.5211	1.6883	13.8359
10	1.2445	1.3614	9.3933	1.3400	7.6738
11	1.1271	1.2275	8.9078	1.1995	6.4236
12	0.9737	1.0699	9.8798	1.0392	6.7269
13	0.7588	0.8559	12.7965	0.8121	7.0242
14	0.0858	0.1124	31.0023	0.0973	13.4033
15	0.1199	0.1359	13.3445	0.1209	0.8340
16	0.0417	0.0459	10.0719	0.0413	-0.9592
17	0.0373	0.0399	6.9705	0.0364	-2.4129
18	0.0121	0.0125	3.3058	0.0116	-4.1322
19	0.0453	0.0492	8.6093	0.0446	-1.5453
20	0.7294	0.7303	0.1234	0.5791	-20.6060
21	0.8474	0.8495	0.2478	0.7167	-15.4236
22	0.8761	0.8532	-2.6139	0.7305	-16.6191
23	0.9039	0.9230	2.1131	0.8046	-10.9857
24	0.8425	0.9593	13.8635	0.8219	-2.4451
25	0.8730	0.8300	-4.9255	0.7434	-14.8454
26	1.2068	1.3594	12.6450	1.3433	11.3109
27	0.6068	0.6090	0.3626	0.6691	10.2670
28	0.2405	0.3279	36.3410	0.3069	27.6091
29	0.6076	0.8065	32.7354	0.8781	44.5194
30	0.6129	0.5600	-8.6311	0.5803	-5.3190
31	0.0543	0.0562	3.4991	0.0524	-3.4991
32	1.1893	1.2095	1.6985	1.2033	1.1772
33	0.9932	1.1075	11.5083	1.0115	1.8425

Table B-19

T = 16.77 seconds Deep Water Direction = 247.5 deg. az.

Basin	Amp.Fac. (Exist.)	Amp.Fac. (Alt.5)	% Change (Ex.& Alt.5)	Amp.Fac. (Alt.6)	% Change (Ex.& Alt.6)
1	1.3681	1.2224	-10.6498	1.1444	-16.3511
2	1.3666	1.1698	-14.4007	1.0859	-20.5400
3	1.4242	1.1909	-16.3811	1.1163	-21.6192
4	1.5394	1.2590	-18.2149	1.2217	-20.6379
5	1.6684	1.2465	-25.2877	1.3500	-19.0842
6	1.3458	1.3495	0.2749	1.4958	11.1458
7	1.1330	1.2178	7.4846	1.3082	15.4634
8	0.9493	1.1118	17.1179	1.1675	22.9854
9	0.9493	1.1621	22.4165	1.2008	26.4932
10	0.7704	0.9503	23.3515	0.9752	26.5836
11	0.7047	0.8419	19.4693	0.8561	21.4843
12	0.6280	0.7207	14.7611	0.7265	15.6847
13	0.4884	0.5395	10.4627	0.5081	4.0336
14	0.1086	0.0937	-13.7201	0.0920	-15.2854
15	0.1597	0.1171	-26.6750	0.1175	-26.4245
16	0.0782	0.0580	-25.8312	0.0598	-23.5294
17	0.0631	0.0463	-26.6244	0.0487	-22.8209
18	0.0447	0.0328	-26.6219	0.0344	-23.0425
19	0.0665	0.0490	-26.3158	0.0518	-22.1053
20	0.6758	0.5491	-18.7482	0.4745	-29.7869
21	0.7472	0.6160	-17.5589	0.5554	-25.6692
22	0.7698	0.6414	-16.6797	0.5751	-25.2923
23	0.8045	0.6922	-13.9590	0.6306	-21.6159
24	0.6916	0.7477	8.1116	0.6340	-8.3285
25	0.7172	0.6548	-8.7005	0.5620	-21.6397
26	0.9022	0.9405	4.2452	0.8597	-4.7107
27	0.5574	0.4419	-20.7212	0.4274	-23.3226
28	0.4346	0.2685	-38.2191	0.2595	-40.2899
29	0.5927	0.7473	26.0840	0.7278	22.7940
30	0.3504	0.2637	-24.7431	0.2617	-25.3139
31	0.1039	0.0791	-23.8691	0.0845	-18.6718
32	1.0183	0.9311	-8.5633	0.9769	-4.0656
33	0.9749	0.9284	-4.7697	0.9445	-3.1183

Table B-20

T = 20.14 seconds Deep Water Direction = 247.5 deg. az.

Basin	Amp.Fac. (Exist.)	Amp.Fac. (Alt.5)	% Change (Ex.& Alt.5)	Amp.Fac. (Alt.6)	% Change (Ex.& Alt.6)
1	1.3001	1.2342	-5.0688	1.2417	-4.4920
2	1.2081	1.2258	1.4651	1.2404	2.6736
3	1.2242	1.2772	4.3294	1.2778	4.3784
4	1.3068	1.4179	8.5017	1.4280	9.2746
5	1.2833	1.5650	21.9512	1.6252	26.6422
6	1.1692	1.6341	39.7622	1.6495	41.0794
7	0.8809	1.2908	46.5319	1.3524	53.5248
8	0.7090	1.0561	48.9563	1.1176	57.6305
9	0.7150	0.9995	39.7902	1.0513	47.0350
10	0.5994	0.7210	20.2870	0.7413	23.6737
11	0.5518	0.6229	12.8851	0.6357	15.2048
12	0.5004	0.5284	5.5955	0.5374	7.3941
13	0.3973	0.4063	2.2653	0.3954	-0.4782
14	0.0219	0.0281	28.3105	0.0295	34.7032
15	0.0061	0.0061	0.0000	0.0067	9.8361
16	0.0018	0.0009	-50.0000	0.0010	-44.4444
17	0.0049	0.0039	-20.4082	0.0037	-24.4898
18	0.0040	0.0031	-22.5000	0.0029	-27.5000
19	0.0062	0.0046	-25.8065	0.0042	-32.2581
20	0.5560	0.3915	-29.5863	0.3341	-39.9101
21	0.6556	0.5218	-20.4088	0.5030	-23.2764
22	0.6783	0.5664	-16.4971	0.5540	-18.3252
23	0.7296	0.5919	-18.8734	0.6003	-17.7220
24	0.6980	0.6592	-5.5587	0.6873	-1.5329
25	0.6640	0.6906	4.0060	0.6993	5.3163
26	1.1280	1.0504	-6.8794	1.0683	-5.2926
27	0.6854	0.5477	-20.0905	0.5491	-19.8862
28	0.4401	0.3852	-12.4744	0.3957	-10.0886
29	0.9457	0.9446	-0.1163	0.9622	1.7447
30	0.2917	0.2310	-20.8090	0.2242	-23.1402
31	0.0173	0.0144	-16.7630	0.0138	-20.2312
32	0.9365	1.0762	14.9172	1.0490	12.0128
33	1.0329	1.1767	13.9220	1.1264	9.0522

Table B-21

T = 22.22 seconds Deep Water Direction = 247.5 deg. az.

Basin	Amp.Fac. (Exist.)	Amp.Fac. (Alt.5)	% Change (Ex.& Alt.5)	Amp.Fac. (Alt.6)	% Change (Ex.& Alt.6)
1	1.0523	1.0539	0.1521	1.0280	-2.3092
2	1.0867	1.1013	1.3435	1.0651	-1.9877
3	1.1426	1.1611	1.6191	1.1060	-3.2032
4	1.2426	1.3234	6.5025	1.3135	5.7058
5	1.3350	1.5282	14.4719	1.5202	13.8727
6	0.9182	1.4895	62.2196	1.6019	74.4609
7	0.6955	1.1672	67.8217	1.2775	83.6808
8	0.5470	0.9337	70.6947	1.0203	86.5265
9	0.5662	0.9185	62.2218	0.9855	74.0551
10	0.4901	0.7003	42.8892	0.7254	48.0106
11	0.4603	0.6061	31.6750	0.6175	34.1516
12	0.4279	0.5289	23.6037	0.5337	24.7254
13	0.3470	0.4114	18.5591	0.4062	17.0605
14	0.0072	0.0057	-20.8333	0.0072	0.0000
15	0.0014	0.0027	92.8572	0.0030	114.2857
16	0.0042	0.0060	42.8572	0.0063	50.0000
17	0.0067	0.0080	19.4030	0.0083	23.8806
18	0.0047	0.0054	14.8936	0.0055	17.0213
19	0.0063	0.0069	9.5238	0.0069	9.5238
20	0.5282	0.3453	-34.6270	0.3224	-38.9625
21	0.6421	0.4813	-25.0428	0.4768	-25.7437
22	0.6484	0.5231	-19.3245	0.5342	-17.6126
23	0.7017	0.5470	-22.0465	0.5756	-17.9706
24	0.6801	0.6286	-7.5724	0.6651	-2.2056
25	0.6380	0.6639	4.0596	0.6952	8.9655
26	1.2128	0.9894	-18.4202	0.9511	-21.5782
27	0.6337	0.5672	-10.4939	0.5819	-8.1742
28	0.3101	0.3347	7.9329	0.3506	13.0603
29	1.0255	0.9287	-9.4393	0.9076	-11.4968
30	0.2813	0.2929	4.1237	0.3023	7.4653
31	0.0228	0.0239	4.8246	0.0244	7.0175
32	0.7425	0.8361	12.6061	0.7436	0.1481
33	0.8702	1.0548	21.2135	0.9235	6.1250

Table B-22

T = 10.02 seconds Deep Water Direction = 270 deg. az.

Basin	Amp.Fac. (Exist.)	Amp.Fac. (Alt.5)	% Change (Ex.& Alt.5)	Amp.Fac. (Alt.6)	% Change (Ex.& Alt.6)
1	1.4177	1.5348	8.2599	1.5304	7.9495
2	1.3433	1.4965	11.4048	1.4914	11.0251
3	1.3162	1.4389	9.3223	1.4467	9.9149
4	1.2689	1.4273	12.4832	1.4456	13.9254
5	1.3389	1.4246	6.4008	1.5226	13.7202
6	1.2521	1.2491	-0.2396	1.3334	6.4931
7	1.1005	1.2215	10.9950	1.2554	14.0754
8	1.0037	1.1272	12.3045	1.1491	14.4864
9	1.0408	1.1903	14.3640	1.1869	14.0373
10	0.8904	1.0588	18.9128	1.0071	13.1065
11	0.8973	1.0342	15.2569	0.9667	7.7343
12	0.8422	0.9937	17.9886	0.8967	6.4712
13	0.7772	0.9059	16.5594	0.8138	4.7092
14	0.1377	0.0747	-45.7516	0.1300	-5.5919
15	0.2714	0.2280	-15.9912	0.2770	2.0634
16	0.1843	0.1164	-36.8421	0.1288	-30.1139
17	0.0883	0.0587	-33.5221	0.0600	-32.0498
18	0.0841	0.0520	-38.1688	0.0561	-33.2937
19	0.0205	0.0202	-1.4634	0.0138	-32.6829
20	0.9405	0.9157	-2.6369	0.6977	-25.8161
21	1.0327	0.9695	-6.1199	0.8165	-20.9354
22	1.0253	0.9581	-6.5542	0.8369	-18.3751
23	1.0835	0.9913	-8.5095	0.8684	-19.8523
24	1.0746	0.9929	-7.6028	0.9564	-10.9994
25	0.9148	0.8096	-11.4998	0.9055	-1.0166
26	1.0499	0.9666	-7.9341	1.1602	10.5058
27	0.4919	0.6296	27.9935	0.5334	8.4367
28	0.6203	0.3110	-49.8630	0.3007	-51.5235
29	0.7984	0.9515	19.1759	0.9383	17.5226
30	0.8797	0.7008	-20.3365	0.7931	-9.8443
31	0.0474	0.0436	-8.0169	0.0376	-20.6751
32	1.3105	1.4437	10.1641	1.3706	4.5860
33	1.2351	1.3487	9.1976	1.3050	5.6595

Table B-23

T = 11.14 seconds Deep Water Direction = 270 deg. az.

Basin	Amp.Fac. (Exist.)	Amp.Fac. (Alt.5)	% Change (Ex.& Alt.5)	Amp.Fac. (Alt.6)	% Change (Ex.& Alt.6)
1	1.2392	1.3073	5.4955	1.2783	3.1553
2	1.2442	1.2804	2.9095	1.2433	-0.0723
3	1.2330	1.2706	3.0495	1.2115	-1.7437
4	1.3187	1.3234	0.3564	1.2886	-2.2826
5	1.3963	1.2887	-7.7061	1.3489	-3.3947
6	1.2232	1.3337	9.0337	1.3702	12.0177
7	0.9751	1.1639	19.3621	1.1634	19.3108
8	0.8430	1.0407	23.4520	1.0148	20.3796
9	0.8464	1.1013	30.1158	1.0672	26.0869
10	0.7520	0.9182	22.1011	0.8811	17.1676
11	0.7311	0.8300	13.5276	0.7894	7.9743
12	0.6891	0.7454	8.1701	0.6948	0.8272
13	0.5896	0.5706	-3.2225	0.5125	-13.0767
14	0.1068	0.0572	-46.4419	0.0700	-34.4569
15	0.0395	0.0239	-39.4937	0.0270	-31.6456
16	0.0558	0.0573	2.6882	0.0494	-11.4695
17	0.0223	0.0167	-25.1121	0.0148	-33.6323
18	0.0282	0.0228	-19.1489	0.0186	-34.0426
19	0.0299	0.0256	-14.3813	0.0226	-24.4147
20	0.9307	0.7674	-17.5459	0.6928	-25.5614
21	1.0138	0.8532	-15.8414	0.8138	-19.7278
22	1.0163	0.8393	-17.4161	0.8551	-15.8615
23	1.1037	0.8722	-20.9749	0.9260	-16.1004
24	1.0144	0.9859	-2.8095	1.0337	1.9026
25	0.9069	0.9321	2.7787	0.9984	10.0893
26	1.0055	1.1488	14.2516	1.1651	15.8727
27	0.3381	0.6581	94.6466	0.6497	92.1621
28	0.4939	0.3884	-21.3606	0.3487	-29.3987
29	1.5354	1.8382	19.7212	1.7538	14.2243
30	0.4845	0.4065	-16.0991	0.4739	-2.1878
31	0.0451	0.0315	-30.1552	0.0273	-39.4678
32	1.4962	1.4975	0.0869	1.5142	1.2030
33	1.3381	1.3520	1.0388	1.2845	-4.0057

Table B-24

T = 12.54 seconds Deep Water Direction = 270 deg. az.

Basin	Amp.Fac. (Exist.)	Amp.Fac. (Alt.5)	% Change (Ex.& Alt.5)	Amp.Fac. (Alt.6)	% Change (Ex.& Alt.6)
1	1.3650	1.2880	-5.6410	1.2011	-12.0073
2	1.3550	1.1857	-12.4945	1.0575	-21.9557
3	1.4434	1.2489	-13.4751	1.1080	-23.2368
4	1.4650	1.3162	-10.1570	1.2203	-16.7031
5	1.4330	1.2540	-12.4913	1.2655	-11.6888
6	1.0222	1.0367	1.4185	1.0722	4.8914
7	0.7297	0.8133	11.4568	0.8873	21.5979
8	0.5834	0.7102	21.7347	0.7522	28.9338
9	0.5468	0.6346	16.0571	0.6775	23.9027
10	0.4903	0.4940	0.7546	0.5448	11.1156
11	0.4900	0.4282	-12.6122	0.4839	-1.2449
12	0.4677	0.3969	-15.1379	0.4567	-2.3519
13	0.4125	0.3845	-6.7879	0.3967	-3.8303
14	0.0388	0.0153	-60.5670	0.0186	-52.0619
15	0.0334	0.0264	-20.9581	0.0246	-26.3473
16	0.0331	0.0436	31.7221	0.0450	35.9517
17	0.0199	0.0245	23.1156	0.0245	23.1156
18	0.0057	0.0097	70.1754	0.0087	52.6316
19	0.0161	0.0067	-58.3851	0.0086	-46.5839
20	0.8164	0.5732	-29.7893	0.6169	-24.4365
21	0.9169	0.6609	-27.9202	0.7431	-18.9552
22	0.9148	0.6792	-25.7543	0.7826	-14.4512
23	0.9943	0.7069	-28.9048	0.8371	-15.8101
24	0.9793	0.8013	-18.1763	0.9473	-3.2676
25	0.8602	0.8100	-5.8359	0.9458	9.9512
26	1.3589	1.0480	-22.8788	1.0937	-19.5158
27	0.5344	0.4355	-18.5067	0.4802	-10.1422
28	0.5616	0.5874	4.5940	0.6500	15.7407
29	1.3896	1.1824	-14.9108	1.2844	-7.5705
30	0.7650	0.7539	-1.4510	0.8001	4.5882
31	0.0094	0.0253	169.1489	0.0212	125.5319
32	1.2723	1.2606	-0.9196	1.1705	-8.0013
33	1.0624	1.0514	-1.0354	0.9942	-6.4194

Table B-25

T = 14.75 seconds Deep Water Direction = 270 deg. az.

Basin	Amp.Fac. (Exist.)	Amp.Fac. (Alt.5)	% Change (Ex.& Alt.5)	Amp.Fac. (Alt.6)	% Change (Ex.& Alt.6)
1	1.3169	1.2233	-7.1076	1.1655	-11.4967
2	1.3845	1.2653	-8.6096	1.2114	-12.5027
3	1.4565	1.2734	-12.5712	1.2291	-15.6128
4	1.5741	1.3849	-12.0196	1.3667	-13.1758
5	1.7003	1.3787	-18.9143	1.4305	-15.8678
6	1.7269	1.5472	-10.4059	1.6300	-5.6112
7	1.4596	1.3444	-7.8926	1.3985	-4.1861
8	1.3241	1.2454	-5.9437	1.2846	-2.9832
9	1.2948	1.2451	-3.8384	1.2510	-3.3828
10	1.0034	0.9823	-2.1028	0.9457	-5.7504
11	0.8636	0.8901	3.0685	0.8517	-1.3780
12	0.7277	0.7723	6.1289	0.7361	1.1543
13	0.5531	0.6346	14.7351	0.5813	5.0985
14	0.0786	0.0756	-3.8168	0.0731	-6.9975
15	0.1041	0.0960	-7.7810	0.0979	-5.9558
16	0.0351	0.0336	-4.2735	0.0336	-4.2735
17	0.0299	0.0304	1.6722	0.0297	-0.6689
18	0.0099	0.0097	-2.0202	0.0096	-3.0303
19	0.0362	0.0374	3.3149	0.0368	1.6575
20	0.7053	0.5829	-17.3543	0.4999	-29.1224
21	0.8441	0.6705	-20.5663	0.6441	-23.6939
22	0.8358	0.6596	-21.0816	0.6570	-21.3927
23	0.8505	0.7091	-16.6255	0.7169	-15.7084
24	0.8154	0.7244	-11.1602	0.7515	-7.8366
25	0.8279	0.6640	-19.7971	0.7312	-11.6802
26	1.4164	1.2251	-13.5061	1.2765	-9.8772
27	0.5804	0.6723	15.8339	0.7335	26.3784
28	0.2457	0.3003	22.2222	0.2966	20.7163
29	1.1320	0.8657	-23.5247	0.9963	-11.9876
30	0.5675	0.5618	-1.0044	0.5941	4.6872
31	0.0418	0.0461	10.2871	0.0454	8.6124
32	1.2670	1.2227	-3.4964	1.1225	-11.4049
33	1.2133	1.1852	-2.3160	1.0680	-11.9756

Table B-26

T = 16.77 seconds Deep Water Direction = 270 deg. az.

Basin	Amp.Fac. (Exist.)	Amp.Fac. (Alt.5)	% Change (Ex.& Alt.5)	Amp.Fac. (Alt.6)	% Change (Ex.& Alt.6)
1	1.0158	1.0766	5.9854	1.0866	6.9699
2	1.0463	1.0904	4.2148	1.0941	4.5685
3	1.0809	1.1394	5.4122	1.1461	6.0320
4	1.1662	1.2138	4.0816	1.2402	6.3454
5	1.2341	1.3420	8.7432	1.4199	15.0555
6	1.0391	1.2599	21.2491	1.2438	19.6997
7	0.7434	0.9743	31.0600	1.0278	38.2567
8	0.5979	0.7878	31.7612	0.8227	37.5983
9	0.5772	0.7402	28.2398	0.7647	32.4844
10	0.4588	0.5587	21.7742	0.5872	27.9860
11	0.4200	0.4897	16.5952	0.5132	22.1905
12	0.3681	0.4175	13.4203	0.4372	18.7721
13	0.2973	0.3110	4.6081	0.3191	7.3327
14	0.0684	0.0681	-0.4386	0.0706	3.2164
15	0.1094	0.0915	-16.3620	0.0966	-11.7002
16	0.0526	0.0454	-13.6882	0.0487	-7.4144
17	0.0426	0.0368	-13.6150	0.0402	-5.6338
18	0.0301	0.0261	-13.2890	0.0284	-5.6478
19	0.0443	0.0390	-11.9639	0.0425	-4.0632
20	0.6072	0.4683	-22.8755	0.4292	-29.3149
21	0.7330	0.6108	-16.6712	0.5919	-19.2497
22	0.7324	0.6314	-13.7903	0.6093	-16.8078
23	0.7659	0.6952	-9.2310	0.6673	-12.8737
24	0.6348	0.7159	12.7757	0.6717	5.8129
25	0.6586	0.6435	-2.2927	0.6381	-3.1127
26	1.3288	1.2614	-5.0722	1.3096	-1.4449
27	0.4605	0.5106	10.8795	0.4742	2.9750
28	0.3480	0.2668	-23.3333	0.2786	-19.9425
29	0.3860	0.6079	57.4870	0.5370	39.1192
30	0.2751	0.2381	-13.4496	0.2430	-11.6685
31	0.0677	0.0622	-8.1241	0.0679	0.2954
32	0.9760	1.0005	2.5102	0.8595	-11.9365
33	0.8599	0.9174	6.6868	0.7479	-13.0248

Table B-27

T = 20.14 seconds Deep Water Direction = 270 deg. az.

Basin	Amp.Fac. (Exist.)	Amp.Fac. (Alt.5)	% Change (Ex.& Alt.5)	Amp.Fac. (Alt.6)	% Change (Ex.& Alt.6)
1	1.0178	0.9141	-10.1886	0.8840	-13.1460
2	1.0674	0.9573	-10.3148	0.9028	-15.4206
3	1.1234	0.9773	-13.0052	0.9313	-17.0999
4	1.2758	1.1081	-13.1447	1.1027	-13.5680
5	1.4256	1.1792	-17.2839	1.2364	-13.2716
6	1.2653	1.0945	-13.4988	1.1879	-6.1171
7	0.9912	0.9425	-4.9132	1.0156	2.4617
8	0.7788	0.8165	4.8408	0.8828	13.3539
9	0.7291	0.7728	5.9937	0.8197	12.4263
10	0.5568	0.5483	-1.5266	0.5493	-1.3470
11	0.4813	0.4782	-0.6441	0.4729	-1.7453
12	0.4151	0.4097	-1.3009	0.4045	-2.5536
13	0.3266	0.3306	1.2247	0.3241	-0.7655
14	0.0130	0.0230	76.9231	0.0263	102.3077
15	0.0048	0.0043	-10.4167	0.0041	-14.5833
16	0.0013	0.0013	0.0000	0.0018	38.4615
17	0.0035	0.0037	5.7143	0.0041	17.1429
18	0.0028	0.0027	-3.5714	0.0029	3.5714
19	0.0041	0.0039	-4.8781	0.0041	0.0000
20	0.5744	0.3804	-33.7744	0.4203	-26.8280
21	0.6616	0.5333	-19.3924	0.6178	-6.6203
22	0.6553	0.5671	-13.4595	0.6633	1.2208
23	0.6877	0.6132	-10.8332	0.7244	5.3366
24	0.5649	0.6894	22.0393	0.8097	43.3351
25	0.5356	0.6841	27.7259	0.8144	52.0538
26	1.0907	1.1521	5.6294	1.3097	20.0788
27	0.4208	0.5257	24.9287	0.5962	41.6825
28	0.3153	0.3189	1.1418	0.3291	4.3768
29	0.5144	0.8996	74.8834	1.0297	100.1750
30	0.1934	0.1917	-0.8790	0.2148	11.0652
31	0.0121	0.0100	-17.3554	0.0098	-19.0083
32	0.9346	0.9973	6.7088	0.9661	3.3704
33	0.9096	1.0671	17.3153	1.0118	11.2357

Table B-28

T = 22.22 seconds Deep Water Direction = 270 deg. az.

Basin	Amp.Fac. (Exist.)	Amp.Fac. (Alt.5)	% Change (Ex.& Alt.5)	Amp.Fac. (Alt.6)	% Change (Ex.& Alt.6)
1	1.3474	1.3006	-3.4733	1.3567	0.6902
2	1.2823	1.1997	-6.4415	1.2746	-0.6005
3	1.2712	1.1844	-6.8282	1.2934	1.7464
4	1.3025	1.2832	-1.4818	1.4026	7.6852
5	1.2030	1.2507	3.9651	1.4672	21.9618
6	1.1043	1.3115	18.7630	1.3959	26.4059
7	0.8623	1.1198	29.8620	1.2078	40.0673
8	0.6770	0.9285	37.1492	1.0084	48.9513
9	0.6821	0.8837	29.5558	0.9457	38.6454
10	0.5494	0.6036	9.8653	0.6184	12.5592
11	0.4958	0.5029	1.4320	0.5035	1.5530
12	0.4448	0.4246	-4.5414	0.4167	-6.3174
13	0.3671	0.3340	-9.0166	0.3132	-14.6826
14	0.0029	0.0102	251.7242	0.0133	358.6207
15	0.0013	0.0032	146.1538	0.0039	200.0000
16	0.0043	0.0053	23.2558	0.0057	32.5581
17	0.0065	0.0063	-3.0769	0.0063	-3.0769
18	0.0045	0.0043	-4.4444	0.0042	-6.6667
19	0.0058	0.0053	-8.6207	0.0052	-10.3448
20	0.5736	0.3229	-43.7064	0.3493	-39.1039
21	0.6069	0.4448	-26.7095	0.5026	-17.1857
22	0.6047	0.4840	-19.9603	0.5417	-10.4184
23	0.6273	0.5165	-17.6630	0.5889	-6.1215
24	0.5462	0.5742	5.1263	0.6396	17.1000
25	0.4774	0.6033	26.3720	0.6632	38.9191
26	0.6666	0.8657	29.8680	0.9693	45.4095
27	0.5264	0.3798	-27.8495	0.3704	-29.6353
28	0.2889	0.2387	-17.3762	0.2295	-20.5607
29	0.5823	0.6309	8.3462	0.6533	12.1930
30	0.2665	0.2002	-24.8780	0.1907	-28.4428
31	0.0210	0.0169	-19.5238	0.0157	-25.2381
32	1.3118	1.3148	0.2287	1.3262	1.0977
33	1.2732	1.2050	-5.3566	1.1930	-6.2991

Table B-29

T = 10.02 seconds Deep Water Direction = 292.5 deg. az.

Basin	Amp.Fac. (Exist.)	Amp.Fac. (Alt.5)	% Change (Ex.& Alt.5)	Amp.Fac. (Alt.6)	% Change (Ex.& Alt.6)
1	1.4775	1.6599	12.3452	1.4399	-2.5448
2	1.4846	1.6494	11.1006	1.4399	-3.0109
3	1.4860	1.6432	10.5787	1.4181	-4.5693
4	1.2975	1.4618	12.6628	1.2005	-7.4759
5	1.2497	1.3166	5.3533	1.0355	-17.1401
6	0.6726	0.5724	-14.8974	0.6776	0.7434
7	0.4603	0.5968	29.6546	0.6093	32.3702
8	0.4058	0.5462	34.5983	0.5223	28.7087
9	0.3925	0.5968	52.0510	0.5418	38.0382
10	0.3304	0.5400	63.4383	0.4524	36.9249
11	0.3311	0.5231	57.9885	0.4290	29.5681
12	0.3044	0.5077	66.7871	0.4111	35.0526
13	0.4757	0.4952	4.0992	0.3941	-17.1537
14	0.0704	0.0330	-53.1250	0.0632	-10.2273
15	0.1104	0.0671	-39.2210	0.0548	-50.3623
16	0.0538	0.0804	49.4424	0.0668	24.1636
17	0.0175	0.0292	66.8571	0.0231	32.0000
18	0.0186	0.0293	57.5269	0.0266	43.0107
19	0.0145	0.0132	-8.9655	0.0111	-23.4483
20	0.8311	0.5727	-31.0913	0.6214	-25.2316
21	0.7270	0.5760	-20.7703	0.6575	-9.5598
22	0.6508	0.5078	-21.9730	0.6225	-4.3485
23	0.5369	0.4069	-24.2131	0.5708	6.3140
24	0.5407	0.4360	-19.3638	0.5719	5.7703
25	0.4082	0.4471	9.5296	0.5755	40.9848
26	0.3733	0.6573	76.0782	0.4137	10.8224
27	0.3738	0.1267	-66.1049	0.2171	-41.9208
28	0.2570	0.2289	-10.9339	0.2239	-12.8794
29	0.3739	0.5730	53.2495	0.5948	59.0800
30	0.2413	0.2553	5.8019	0.3029	25.5284
31	0.0170	0.0120	-29.4118	0.0120	-29.4118
32	1.5014	1.6535	10.1305	1.6712	11.3094
33	1.4546	1.6926	16.3619	1.6098	10.6696

Table B-30

T = 11.14 seconds Deep Water Direction = 292.5 deg. az.

Basin	Amp.Fac. (Exist.)	Amp.Fac. (Alt.5)	% Change (Ex.& Alt.5)	Amp.Fac. (Alt.6)	% Change (Ex.& Alt.6)
1	1.4192	1.4744	3.8895	1.4461	1.8954
2	1.3505	1.4195	5.1092	1.4261	5.5979
3	1.4024	1.4692	4.7633	1.4289	1.8896
4	1.3523	1.4051	3.9045	1.3579	0.4141
5	1.3184	1.4129	7.1678	1.1916	-9.6177
6	0.9907	0.8910	-10.0636	0.8490	-14.3030
7	0.7675	0.8355	8.8599	0.8190	6.7101
8	0.6431	0.7336	14.0725	0.6897	7.2461
9	0.6695	0.7879	17.6848	0.7269	8.5736
10	0.5930	0.6874	15.9191	0.6523	10.0000
11	0.5698	0.6670	17.0586	0.6282	10.2492
12	0.5223	0.6010	15.0680	0.5725	9.6113
13	0.5832	0.5100	-12.5514	0.4735	-18.8100
14	0.0708	0.0197	-72.1751	0.0211	-70.1977
15	0.0497	0.0668	34.4064	0.0426	-14.2857
16	0.0261	0.0432	65.5172	0.0306	17.2414
17	0.0096	0.0160	66.6667	0.0116	20.8333
18	0.0139	0.0085	-38.8489	0.0056	-59.7122
19	0.0049	0.0145	195.9184	0.0125	155.1020
20	1.0763	0.6505	-39.5615	0.6849	-36.3653
21	1.0345	0.6671	-35.5147	0.7440	-28.0812
22	0.8416	0.6282	-25.3565	0.7395	-12.1317
23	0.6849	0.6431	-6.1031	0.7615	11.1841
24	0.6389	0.6638	3.8973	0.7760	21.4588
25	0.5506	0.6171	12.0777	0.7631	38.5943
26	0.2377	0.5538	132.9828	0.4730	98.9903
27	0.3785	0.5406	42.8269	0.4720	24.7028
28	0.3074	0.3140	2.1470	0.2503	-18.5751
29	1.0295	1.1133	8.1399	1.0314	0.1846
30	0.3244	0.2228	-31.3194	0.3381	4.2232
31	0.0105	0.0146	39.0476	0.0128	21.9048
32	1.7493	1.8753	7.2029	1.6941	-3.1555
33	1.8493	1.8781	1.5573	1.7708	-4.2449

Table B-31

T = 12.54 seconds Deep Water Direction = 292.5 deg. az.

Basin	Amp.Fac. (Exist.)	Amp.Fac. (Alt.5)	% Change (Ex.& Alt.5)	Amp.Fac. (Alt.6)	% Change (Ex.& Alt.6)
1	1.2424	1.2194	-1.8513	1.2468	0.3541
2	1.2556	1.2163	-3.1300	1.2448	-0.8601
3	1.1477	1.1405	-0.6273	1.1026	-3.9296
4	1.1994	1.2037	0.3585	1.1347	-5.3944
5	1.2022	1.1491	-4.4169	1.2367	2.8697
6	0.8306	0.7896	-4.9362	0.7534	-9.2945
7	0.6606	0.6673	1.0142	0.6604	-0.0303
8	0.5610	0.5929	5.6863	0.5584	-0.4635
9	0.5092	0.5663	11.2137	0.5249	3.0833
10	0.4853	0.4606	-5.0896	0.4397	-9.3962
11	0.4969	0.4164	-16.2004	0.4236	-14.7515
12	0.4788	0.3951	-17.4812	0.4087	-14.6408
13	0.5123	0.3328	-35.0381	0.3289	-35.7993
14	0.0340	0.0123	-63.8235	0.0194	-42.9412
15	0.0208	0.0227	9.1346	0.0318	52.8846
16	0.0255	0.0431	69.0196	0.0524	105.4902
17	0.0171	0.0253	47.9532	0.0305	78.3626
18	0.0069	0.0088	27.5362	0.0101	46.3768
19	0.0139	0.0065	-53.2374	0.0090	-35.2518
20	0.8280	0.5064	-38.8406	0.5483	-33.7802
21	0.8084	0.5342	-33.9188	0.6219	-23.0703
22	0.7536	0.5538	-26.5127	0.6550	-13.0839
23	0.6682	0.5573	-16.5968	0.6825	2.1401
24	0.6501	0.6280	-3.3995	0.7210	10.9060
25	0.5991	0.6307	5.2746	0.7296	21.7827
26	0.6362	0.4534	-28.7331	0.5372	-15.5611
27	0.3935	0.6238	58.5260	0.5037	28.0051
28	0.3277	0.5501	67.8670	0.6787	107.1102
29	0.9982	1.2598	26.2072	1.1182	12.0216
30	0.6605	0.5936	-10.1287	0.5332	-19.2733
31	0.0179	0.0172	-3.9106	0.0182	1.6760
32	1.4501	1.4971	3.2412	1.5037	3.6963
33	1.6877	1.6504	-2.2101	1.6663	-1.2680

Table B-32

T = 14.75 seconds Deep Water Direction = 292.5 deg. az.

Basin	Amp.Fac. (Exist.)	Amp.Fac. (Alt.5)	% Change (Ex.& Alt.5)	Amp.Fac. (Alt.6)	% Change (Ex.& Alt.6)
1	1.2506	1.1759	-5.9731	1.1679	-6.6128
2	1.3154	1.2370	-5.9602	1.2330	-6.2643
3	1.2679	1.1636	-8.2262	1.2069	-4.8111
4	1.1733	1.0843	-7.5854	1.1190	-4.6280
5	1.1600	1.1737	1.1810	1.0621	-8.4396
6	0.7909	0.9512	20.2681	0.8748	10.6082
7	0.6145	0.8266	34.5159	0.7280	18.4703
8	0.4480	0.7210	60.9375	0.6453	44.0402
9	0.4337	0.6695	54.3694	0.6177	42.4256
10	0.4004	0.5227	30.5445	0.5053	26.1988
11	0.3980	0.4664	17.1859	0.4641	16.6080
12	0.3998	0.4212	5.3527	0.4241	6.0780
13	0.4042	0.3718	-8.0158	0.3552	-12.1227
14	0.0534	0.0419	-21.5356	0.0376	-29.5880
15	0.0939	0.0763	-18.7433	0.0734	-21.8317
16	0.0326	0.0281	-13.8037	0.0277	-15.0307
17	0.0292	0.0260	-10.9589	0.0261	-10.6164
18	0.0082	0.0080	-2.4390	0.0079	-3.6585
19	0.0370	0.0316	-14.5946	0.0320	-13.5135
20	0.7093	0.4328	-38.9821	0.4367	-38.4323
21	0.7201	0.5012	-30.3986	0.5459	-24.1911
22	0.6912	0.5095	-26.2876	0.5564	-19.5023
23	0.6763	0.5233	-22.6231	0.5808	-14.1210
24	0.6151	0.5256	-14.5505	0.5848	-4.9260
25	0.5973	0.5407	-9.4760	0.5934	-0.6529
26	0.7258	0.9382	29.2643	1.0255	41.2924
27	0.6205	0.3967	-36.0677	0.3750	-39.5649
28	0.4225	0.2923	-30.8166	0.2891	-31.5740
29	1.0475	0.6452	-38.4057	0.5772	-44.8974
30	0.4407	0.5047	14.5224	0.4545	3.1314
31	0.0478	0.0411	-14.0167	0.0429	-10.2510
32	1.2835	1.3258	3.2957	1.3356	4.0592
33	1.3060	1.3478	3.2006	1.3649	4.5100

Table B-33

T = 16.77 seconds Deep Water Direction = 292.5 deg. az.

Basin	Amp.Fac. (Exist.)	Amp.Fac. (Alt.5)	% Change (Ex.& Alt.5)	Amp.Fac. (Alt.6)	% Change (Ex.& Alt.6)
1	1.2803	1.1732	-8.3652	1.0892	-14.9262
2	1.2033	1.0993	-8.6429	1.0072	-16.2969
3	1.2721	1.1654	-8.3877	1.0480	-17.6165
4	1.3651	1.2611	-7.6185	1.2057	-11.6768
5	1.4786	1.2162	-17.7465	1.2902	-12.7418
6	1.2552	1.1368	-9.4328	1.2764	1.6890
7	1.0053	1.0255	2.0094	1.1426	13.6576
8	0.8899	0.9324	4.7758	1.0305	15.7995
9	0.8846	0.9120	3.0974	0.9846	11.3045
10	0.6861	0.6882	0.3061	0.7195	4.8681
11	0.6054	0.6110	0.9250	0.6256	3.3366
12	0.5078	0.5148	1.3785	0.5164	1.6936
13	0.4269	0.3770	-11.6889	0.3776	-11.5484
14	0.0744	0.0838	12.6344	0.0782	5.1075
15	0.1179	0.1082	-8.2273	0.0999	-15.2672
16	0.0572	0.0532	-6.9930	0.0491	-14.1608
17	0.0472	0.0439	-6.9915	0.0411	-12.9237
18	0.0331	0.0311	-6.0423	0.0291	-12.0846
19	0.0486	0.0462	-4.9383	0.0433	-10.9054
20	0.7678	0.4679	-39.0596	0.6009	-21.7374
21	0.8227	0.5363	-34.8122	0.6492	-21.0891
22	0.8193	0.5419	-33.8582	0.6414	-21.7137
23	0.8146	0.5857	-28.0997	0.6816	-16.3270
24	0.6628	0.5385	-18.7538	0.5938	-10.4104
25	0.6706	0.4791	-28.5565	0.5012	-25.2610
26	1.0514	0.8877	-15.5697	0.8472	-19.4217
27	0.4335	0.5293	22.0992	0.5203	20.0231
28	0.3766	0.3279	-12.9315	0.3109	-17.4456
29	0.3113	0.4888	57.0189	0.5513	77.0960
30	0.2748	0.2826	2.8384	0.2633	-4.1849
31	0.0744	0.0721	-3.0914	0.0680	-8.6021
32	1.2965	1.2173	-6.1087	1.2236	-5.6228
33	1.1745	1.1591	-1.3112	1.0888	-7.2967

Table B-34

T = 20.14 seconds Deep Water Direction = 292.5 deg. az.

Basin	Amp.Fac. (Exist.)	Amp.Fac. (Alt.5)	% Change (Ex.& Alt.5)	Amp.Fac. (Alt.6)	% Change (Ex.& Alt.6)
1	1.2790	1.1044	-13.6513	1.2417	-2.9163
2	1.2085	0.9928	-17.8486	1.1747	-2.7969
3	1.1719	0.9252	-21.0513	1.1098	-5.2991
4	1.1297	0.8893	-21.2800	1.0822	-4.2046
5	1.1253	0.8516	-24.3224	0.9761	-13.2587
6	0.9957	0.8225	-17.3948	0.8502	-14.6128
7	0.7496	0.7109	-5.1628	0.7177	-4.2556
8	0.5778	0.6226	7.7536	0.6319	9.3631
9	0.5228	0.6314	20.7728	0.6211	18.8026
10	0.3882	0.5176	33.3333	0.4803	23.7249
11	0.3382	0.4774	41.1591	0.4429	30.9580
12	0.2935	0.4301	46.5417	0.4006	36.4906
13	0.2748	0.3554	29.3304	0.3233	17.6492
14	0.0119	0.0203	70.5882	0.0235	97.4790
15	0.0047	0.0055	17.0213	0.0048	2.1277
16	0.0018	0.0016	-11.1111	0.0018	0.0000
17	0.0032	0.0041	28.1250	0.0044	37.5000
18	0.0024	0.0032	33.3333	0.0033	37.5000
19	0.0036	0.0049	36.1111	0.0050	38.8889
20	0.6111	0.3848	-37.0316	0.3661	-40.0916
21	0.6597	0.4713	-28.5584	0.5057	-23.3439
22	0.6409	0.5087	-20.6272	0.5584	-12.8725
23	0.6482	0.5504	-15.0879	0.6090	-6.0475
24	0.5066	0.6031	19.0486	0.6763	33.4978
25	0.4790	0.5737	19.7704	0.6750	40.9186
26	0.9182	0.8561	-6.7632	0.9459	3.0168
27	0.4350	0.5521	26.9195	0.5996	37.8391
28	0.2631	0.3772	43.3675	0.3667	39.3767
29	0.5226	0.6860	31.2667	0.7830	49.8278
30	0.1663	0.2231	34.1551	0.2361	41.9723
31	0.0093	0.0133	43.0107	0.0126	35.4839
32	1.4118	1.3228	-6.3040	1.3124	-7.0407
33	1.2612	1.0642	-15.6200	1.0525	-16.5477

Table B-35

T = 22.22 seconds Deep Water Dirction = 292.5 deg. az.

Basin	Amp.Fac (Exist.)	Amp.Fac. (ALt.5)	% Change (Ex.& Alt.5)	Amp.Fac. (Alt.6)	% Change (Ex.& Alt.6)
1	0.9139	0.8637	-5.4929	0.8566	-6.2698
2	0.8288	0.7866	-5.0917	0.7569	-8.6752
3	0.8198	0.7859	-4.1352	0.7507	-8.4289
4	0.9276	0.8810	-5.0237	0.9045	-2.4903
5	1.0087	0.9224	-8.5556	0.9772	-3.1228
6	0.9069	0.8028	-11.4787	0.9700	6.9578
7	0.7304	0.6858	-6.1062	0.8207	12.3631
8	0.5945	0.5996	0.8579	0.7051	18.6039
9	0.5780	0.5766	-0.2422	0.6542	13.1834
10	0.4329	0.4033	-6.8376	0.4137	-4.4352
11	0.3803	0.3537	-6.9945	0.3429	-9.8343
12	0.3344	0.3147	-5.8911	0.2912	-12.9187
13	0.3071	0.2868	-6.6102	0.2484	-19.1143
14	0.0040	0.0106	165.0000	0.0131	227.5000
15	0.0018	0.0027	50.0000	0.0034	88.8889
16	0.0036	0.0035	-2.7778	0.0039	8.3333
17	0.0047	0.0046	-2.1277	0.0043	-8.5106
18	0.0032	0.0034	6.2500	0.0031	-3.1250
19	0.0042	0.0046	9.5238	0.0042	0.0000
20	0.5055	0.3803	-24.7676	0.3908	-22.6904
21	0.5051	0.4298	-14.9079	0.4940	-2.1976
22	0.4880	0.4492	-7.9508	0.5202	6.5984
23	0.4716	0.4758	0.8906	0.5619	19.1476
24	0.3691	0.5055	36.9548	0.5954	61.3113
25	0.3364	0.4832	43.6385	0.5933	76.3674
26	0.5548	0.7108	28.1182	0.8344	50.3965
27	0.3149	0.3654	16.0368	0.3253	3.3026
28	0.1815	0.1940	6.8871	0.1597	-12.0110
29	0.3674	0.5569	51.5787	0.5864	59.6081
30	0.1661	0.1614	-2.8296	0.1306	-21.3727
31	0.0137	0.0146	6.5693	0.0121	-11.6788
32	0.7923	0.8800	11.0690	0.8560	8.0399
33	0.8069	0.9991	23.8196	0.9501	17.7469

Table B-36

T = 10.02 seconds Deep Water Direction = 315 deg. az.

Basin	Amp.Fac. (Exist.)	Amp.Fac. (Alt.5)	% Change (Ex.& Alt.5)	Amp.Fac. (Alt.6)	% Change (Ex.& Alt.6)
1	1.3828	1.2613	-8.7865	1.2134	-12.2505
2	1.4056	1.3142	-6.5026	1.2588	-10.4439
3	1.3013	1.2357	-5.0411	1.1431	-12.1571
4	1.1269	1.1113	-1.3843	0.8968	-20.4188
5	0.7773	0.7676	-1.2479	0.7304	-6.0337
6	0.5096	0.7000	37.3626	0.6459	26.7465
7	0.3971	0.5124	29.0355	0.4742	19.4158
8	0.3035	0.4487	47.8419	0.4018	32.3888
9	0.2714	0.4036	48.7104	0.3966	46.1312
10	0.2396	0.3210	33.9733	0.3053	27.4207
11	0.2453	0.3072	25.2344	0.2488	1.4268
12	0.2323	0.3010	29.5738	0.2440	5.0366
13	0.2569	0.2845	10.7435	0.2913	13.3904
14	0.0645	0.0428	-33.6434	0.0223	-65.4264
15	0.1047	0.0971	-7.2588	0.0518	-50.5253
16	0.0409	0.0391	-4.4010	0.0441	7.8240
17	0.0204	0.0389	90.6863	0.0319	56.3725
18	0.0142	0.0403	183.8028	0.0331	133.0986
19	0.0039	0.0170	335.8975	0.0135	246.1539
20	0.3548	0.3894	9.7520	0.5615	58.2582
21	0.3542	0.4429	25.0423	0.5673	60.1638
22	0.3709	0.4783	28.9566	0.5625	51.6581
23	0.3690	0.4985	35.0949	0.5260	42.5474
24	0.4243	0.5520	30.0966	0.5437	28.1405
25	0.4451	0.5694	27.9263	0.5398	21.2761
26	0.2622	0.4635	76.7735	0.2679	2.1739
27	0.3593	0.3046	-15.2240	0.2544	-29.1957
28	0.3204	0.5304	65.5431	0.3834	19.6629
29	0.8333	0.6657	-20.1128	0.5949	-28.6091
30	0.3662	0.5399	47.4331	0.4182	14.1999
31	0.0115	0.0336	192.1739	0.0228	98.2609
32	1.3636	1.2935	-5.1408	1.3859	1.6354
33	1.3751	1.2879	-6.3414	1.4527	5.6432

Table B-37

T = 11.14 seconds Deep Water Direction = 315 deg. az.

Basin	Amp.Fac. (Exist.)	Amp.Fac. (Alt.5)	% Change (Ex.& Alt.5)	Amp.Fac. (Alt.6)	% Change (Ex.& Alt.6)
1	1.3329	1.2455	-6.5571	1.2825	-3.7812
2	1.3408	1.2905	-3.7515	1.3473	0.4848
3	1.2515	1.2305	-1.6780	1.2856	2.7247
4	1.0708	1.0787	0.7378	0.9426	-11.9724
5	0.8855	0.8827	-0.3162	0.9807	10.7510
6	0.5377	0.5654	5.1516	0.6722	25.0140
7	0.4411	0.4817	9.2043	0.4639	5.1689
8	0.3703	0.3785	2.2144	0.3487	-5.8331
9	0.3688	0.3568	-3.2538	0.3269	-11.3612
10	0.3071	0.3057	-0.4559	0.2282	-25.6920
11	0.3049	0.3023	-0.8527	0.1921	-36.9957
12	0.2725	0.2913	6.8991	0.1721	-36.8440
13	0.3132	0.2913	-6.9923	0.2336	-25.4151
14	0.0296	0.0473	59.7973	0.0298	0.6757
15	0.0455	0.0339	-25.4945	0.0485	6.5934
16	0.0419	0.0537	28.1623	0.0651	55.3699
17	0.0143	0.0168	17.4825	0.0192	34.2657
18	0.0119	0.0207	73.9496	0.0208	74.7899
19	0.0191	0.0230	20.4189	0.0224	17.2775
20	0.4777	0.3493	-26.8788	0.6675	39.7321
21	0.4439	0.3378	-23.9018	0.6856	54.4492
22	0.3846	0.3333	-13.3385	0.6222	61.7785
23	0.3387	0.3260	-3.7496	0.6103	80.1890
24	0.3873	0.3705	-4.3377	0.6355	64.0847
25	0.3955	0.3686	-6.8015	0.5848	47.8635
26	0.2573	0.2802	8.9001	0.2895	12.5146
27	0.2372	0.2622	10.5396	0.3429	44.5616
28	0.3145	0.4039	28.4261	0.4143	31.7329
29	0.7295	0.6658	-8.7320	0.8567	17.4366
30	0.2747	0.2691	-2.0386	0.2281	-16.9640
31	0.0242	0.0333	37.6033	0.0311	28.5124
32	1.4487	1.4834	2.3953	1.4873	2.6645
33	1.2856	1.3523	5.1882	1.5204	18.2639

Table B-38

T = 12.54 seconds Deep Water Direction = 315 deg. az.

Basin	Amp.Fac. (Exist.)	Amp.Fac. (Alt.5)	% Change (Ex.& Alt.5)	Amp.Fac. (Alt.6)	% Change (Ex.& Alt.6)
1	1.4125	1.3591	-3.7805	1.3795	-2.3363
2	1.3968	1.3095	-6.2500	1.2725	-8.8989
3	1.2105	1.1892	-1.7596	1.1201	-7.4680
4	1.1754	1.2217	3.9391	1.0750	-8.5418
5	0.9965	0.9325	-6.4225	1.1052	10.9082
6	0.5273	0.3825	-27.4606	0.5934	12.5356
7	0.2955	0.2941	-0.4738	0.4594	55.4653
8	0.2400	0.2165	-9.7917	0.3230	34.5833
9	0.2229	0.1702	-23.6429	0.2830	26.9628
10	0.2030	0.1585	-21.9212	0.2333	14.9261
11	0.1841	0.1625	-11.7328	0.2290	24.3889
12	0.1864	0.1556	-16.5236	0.2104	12.8755
13	0.3550	0.1614	-54.5352	0.2010	-43.3803
14	0.0048	0.0243	406.2500	0.0288	500.0000
15	0.0124	0.0252	103.2258	0.0334	169.3548
16	0.0200	0.0194	-3.0000	0.0250	25.0000
17	0.0105	0.0100	-4.7619	0.0131	24.7619
18	0.0044	0.0026	-40.9091	0.0035	-20.4545
19	0.0041	0.0068	65.8537	0.0077	87.8049
20	0.5914	0.2898	-50.9976	0.4633	-21.6605
21	0.4920	0.3063	-37.7439	0.5354	8.8211
22	0.4547	0.3174	-30.1957	0.5611	23.4000
23	0.3579	0.3114	-12.9925	0.5721	59.8491
24	0.3838	0.3381	-11.9072	0.5907	53.9083
25	0.3416	0.3462	1.3466	0.6216	81.9672
26	0.2459	0.3630	47.6210	0.3959	61.0004
27	0.2455	0.3628	47.7800	0.4556	85.5804
28	0.2592	0.3132	20.8333	0.3869	49.2670
29	0.6967	0.6435	-7.6360	0.7685	10.3057
30	0.1989	0.3135	57.6169	0.3719	86.9784
31	0.0127	0.0028	-77.9528	0.0041	-67.7165
32	1.6388	1.6796	2.4896	1.7523	6.9258
33	1.5344	1.5324	-0.1303	1.6115	5.0248

Table B-39

T = 14.75 seconds Deep Water Direction = 315 deg. az.

Basin	Amp.Fac. (Exist.)	Amp.Fac. (Alt.5)	% Change (Ex.& Alt.5)	Amp.Fac. (Alt.6)	% Change (Ex.& Alt.6)
1	1.1392	1.1883	4.3100	1.1534	1.2465
2	1.1665	1.2093	3.6691	1.1694	0.2486
3	1.1887	1.2421	4.4923	1.1952	0.5468
4	1.0641	1.0744	0.9679	1.1473	7.8188
5	0.7782	0.6592	-15.2917	0.8781	12.8373
6	0.5985	0.5983	-0.0334	0.6156	2.8571
7	0.4629	0.5113	10.4558	0.5603	21.0413
8	0.3961	0.4313	8.8866	0.4762	20.2222
9	0.4036	0.4538	12.4381	0.4922	21.9524
10	0.3336	0.3871	16.0372	0.4067	21.9125
11	0.3132	0.3523	12.4840	0.3755	19.8914
12	0.2813	0.3017	7.2520	0.3235	15.0018
13	0.3185	0.2362	-25.8399	0.2489	-21.8524
14	0.0286	0.0063	-77.9720	0.0195	-31.8182
15	0.0406	0.0102	-74.8769	0.0129	-68.2266
16	0.0129	0.0033	-74.4186	0.0053	-58.9147
17	0.0099	0.0025	-74.7475	0.0054	-45.4545
18	0.0035	0.0006	-82.8571	0.0016	-54.2857
19	0.0124	0.0033	-73.3871	0.0063	-49.1936
20	0.5917	0.2949	-50.1606	0.2886	-51.2253
21	0.5793	0.3049	-47.3675	0.3473	-40.0483
22	0.5232	0.3106	-40.6346	0.3487	-33.3524
23	0.4678	0.3217	-31.2313	0.3693	-21.0560
24	0.3961	0.3305	-16.5615	0.3828	-3.3577
25	0.3665	0.3185	-13.0969	0.3721	1.5280
26	0.6493	0.3457	-46.7580	0.5817	-10.4112
27	0.1006	0.3627	260.5368	0.2735	171.8688
28	0.0502	0.1144	127.8884	0.0609	21.3147
29	0.2309	0.6404	177.3495	0.5339	131.2256
30	0.1416	0.2133	50.6356	0.1778	25.5650
31	0.0130	0.0054	-58.4615	0.0069	-46.9231
32	1.3424	1.3744	2.3838	1.3456	0.2384
33	1.1116	1.2338	10.9932	1.1639	4.7049

Table B-40

T = 16.77 seconds Deep Water Direction = 315 deg. az.

Basin	Amp.Fac. (Exist.)	Amp.Fac (Alt.5)	% Change (Ex.& Alt.5)	Amp.Fac. (Alt.6)	% Change (Ex.& Alt.6)
1	1.3859	1.2101	-12.6849	1.3884	0.1804
2	1.4559	1.2582	-13.5792	1.4643	0.5770
3	1.3463	1.0920	-18.8888	1.3726	1.9535
4	1.1794	0.9370	-20.5528	1.1927	1.1277
5	1.1018	0.8327	-24.4237	0.9263	-15.9285
6	0.7680	0.5683	-26.0026	0.6083	-20.7943
7	0.4927	0.4521	-8.2403	0.4334	-12.0357
8	0.4471	0.3920	-12.3239	0.3856	-13.7553
9	0.4786	0.4068	-15.0021	0.3919	-18.1153
10	0.3801	0.3143	-17.3112	0.3194	-15.9695
11	0.3256	0.2896	-11.0565	0.2908	-10.6880
12	0.2595	0.2633	1.4644	0.2569	-1.0019
13	0.3336	0.2539	-23.8909	0.2246	-32.6739
14	0.0108	0.0611	465.7407	0.0549	408.3333
15	0.0031	0.0796	2467.7417	0.0717	2212.9033
16	0.0026	0.0388	1392.3077	0.0350	1246.1538
17	0.0034	0.0308	805.8824	0.0280	723.5294
18	0.0023	0.0218	847.8261	0.0199	765.2173
19	0.0036	0.0325	802.7778	0.0297	725.0000
20	0.6646	0.4202	-36.7740	0.4736	-28.7391
21	0.6116	0.4180	-31.6547	0.4953	-19.0157
22	0.5700	0.4244	-25.5439	0.5042	-11.5439
23	0.5146	0.4385	-14.7882	0.5322	3.4201
24	0.4118	0.3969	-3.6183	0.4970	20.6897
25	0.3215	0.3834	19.2535	0.4523	40.6843
26	0.4455	0.1864	-58.1594	0.1041	-76.6330
27	0.2446	0.3655	49.4276	0.3522	43.9902
28	0.0609	0.2445	301.4778	0.2249	269.2939
29	0.4484	0.6215	38.6039	0.6605	47.3015
30	0.0468	0.1710	265.3846	0.1609	243.8034
31	0.0070	0.0491	601.4285	0.0450	542.8572
32	1.4733	1.4456	-1.8801	1.4496	-1.6086
33	1.7231	1.6432	-4.6370	1.6165	-6.1865

Table B-41

T = 20.14 seconds Deep Water Direction = 315 deg. az.

Basin	Amp.Fac. (Exist.)	Amp.Fac. (Alt.5)	% Change (Ex.& Alt.5)	Amp.Fac. (Alt.6)	% Change (Ex.& Alt.6)
1	1.0735	1.0910	1.6302	1.0168	-5.2818
2	0.9260	1.0051	8.5421	0.9237	-0.2484
3	0.9378	1.0494	11.9002	0.9533	1.6528
4	1.0171	1.0890	7.0691	1.0342	1.6812
5	1.0768	1.0560	-1.9316	1.0950	1.6902
6	0.8989	0.9020	0.3449	0.9536	6.0852
7	0.7530	0.7204	-4.3294	0.7200	-4.3825
8	0.6338	0.6590	3.9760	0.6557	3.4553
9	0.6024	0.6792	12.7490	0.6729	11.7032
10	0.4615	0.5432	17.7031	0.5321	15.2979
11	0.4014	0.4807	19.7558	0.4801	19.6064
12	0.3446	0.4116	19.4428	0.4189	21.5612
13	0.3180	0.3275	2.9874	0.3437	8.0818
14	0.0125	0.0190	52.0000	0.0245	96.0000
15	0.0042	0.0033	-21.4286	0.0032	-23.8095
16	0.0016	0.0012	-25.0000	0.0018	12.5000
17	0.0029	0.0032	10.3448	0.0038	31.0345
18	0.0022	0.0024	9.0909	0.0027	22.7273
19	0.0033	0.0034	3.0303	0.0040	21.2121
20	0.5539	0.4023	-27.3696	0.5127	-7.4382
21	0.5503	0.4494	-18.3355	0.5716	3.8706
22	0.5308	0.4587	-13.5833	0.5979	12.6413
23	0.5011	0.5005	-0.1197	0.6435	28.4175
24	0.3667	0.4819	31.4153	0.6457	76.0840
25	0.3721	0.4091	9.9436	0.5797	55.7915
26	0.4146	0.7142	72.2624	0.6005	44.8384
27	0.2906	0.3180	9.4288	0.3968	36.5451
28	0.2484	0.2692	8.3736	0.2938	18.2770
29	0.1696	0.3621	113.5024	0.3873	128.3609
30	0.1384	0.1402	1.3006	0.1698	22.6879
31	0.0093	0.0091	-2.1505	0.0097	4.3011
32	0.9485	1.0463	10.3110	0.9851	3.8587
33	0.9166	1.0812	17.9577	1.0247	11.7936

Table B-42

T = 22.22 seconds Deep Water Direction = 315 deg. az.

Basin	Amp.Fac. (Exist.)	Amp.Fac. (Alt.5)	% Change (Ex.& Alt.5)	Amp.Fac. (Alt.6)	% Change (Ex.& Alt.6)
1	1.0373	1.0660	2.7668	0.9933	-4.2418
2	1.0942	1.1284	3.1256	1.0533	-3.7379
3	1.1057	1.1320	2.3786	1.0630	-3.8618
4	1.0675	1.0468	-1.9391	1.0762	0.8150
5	1.0682	0.9716	-9.0433	1.0922	2.2468
6	0.8463	0.7246	-14.3802	0.8521	0.6853
7	0.6775	0.6469	-4.5166	0.7185	6.0517
8	0.5295	0.5637	6.4589	0.6227	17.6015
9	0.5076	0.5549	9.3184	0.5884	15.9180
10	0.3852	0.4201	9.0602	0.4072	5.7113
11	0.3438	0.3764	9.4823	0.3559	3.5195
12	0.3097	0.3379	9.1056	0.3157	1.9374
13	0.2881	0.2739	-4.9288	0.2642	-8.2957
14	0.0032	0.0074	131.2500	0.0109	240.6250
15	0.0012	0.0018	50.0000	0.0027	125.0000
16	0.0030	0.0036	20.0000	0.0039	30.0000
17	0.0045	0.0051	13.3333	0.0049	8.8889
18	0.0032	0.0036	12.5000	0.0035	9.3750
19	0.0042	0.0048	14.2857	0.0047	11.9048
20	0.4347	0.3039	-30.0897	0.4188	-3.6577
21	0.4482	0.3487	-22.1999	0.4884	8.9692
22	0.4425	0.3662	-17.2429	0.5071	14.5989
23	0.4253	0.3981	-6.3955	0.5462	28.4270
24	0.3697	0.4123	11.5229	0.5561	50.4193
25	0.3735	0.3725	-0.2677	0.5216	39.6519
26	0.5780	0.5800	0.3460	0.6923	19.7751
27	0.3405	0.4009	17.7386	0.3850	13.0690
28	0.1901	0.2211	16.3072	0.1977	3.9979
29	0.4380	0.5137	17.2831	0.5558	26.8950
30	0.1683	0.1912	13.6067	0.1691	0.4753
31	0.0143	0.0161	12.5874	0.0145	1.3986
32	1.2660	1.3600	7.4250	1.3737	8.5071
33	1.2830	1.3191	2.8137	1.3094	2.0577

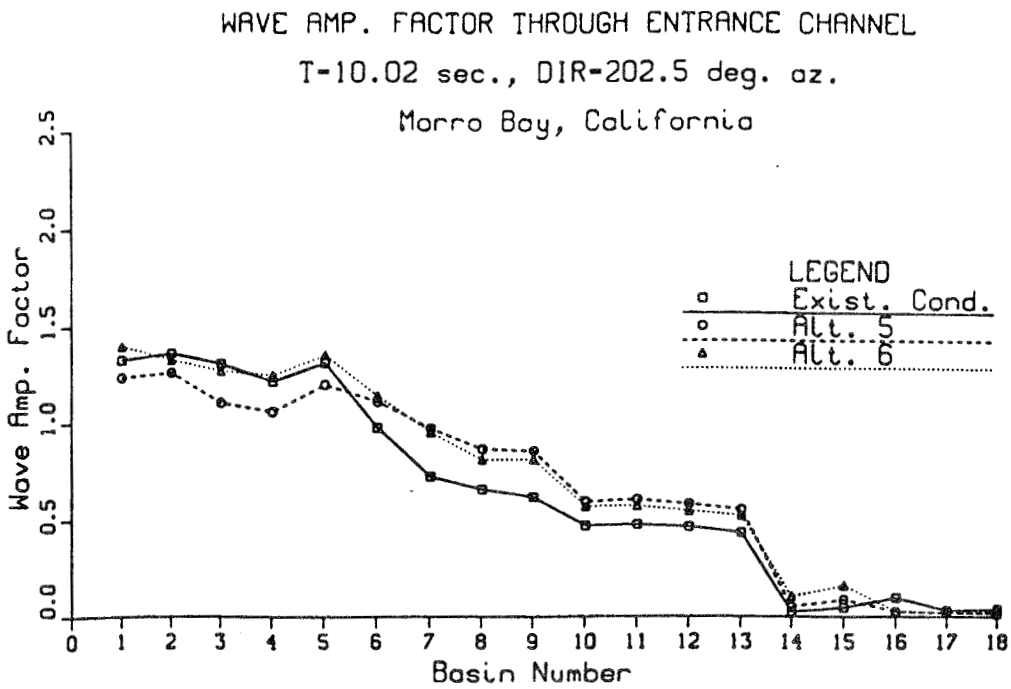

Figure B-1.

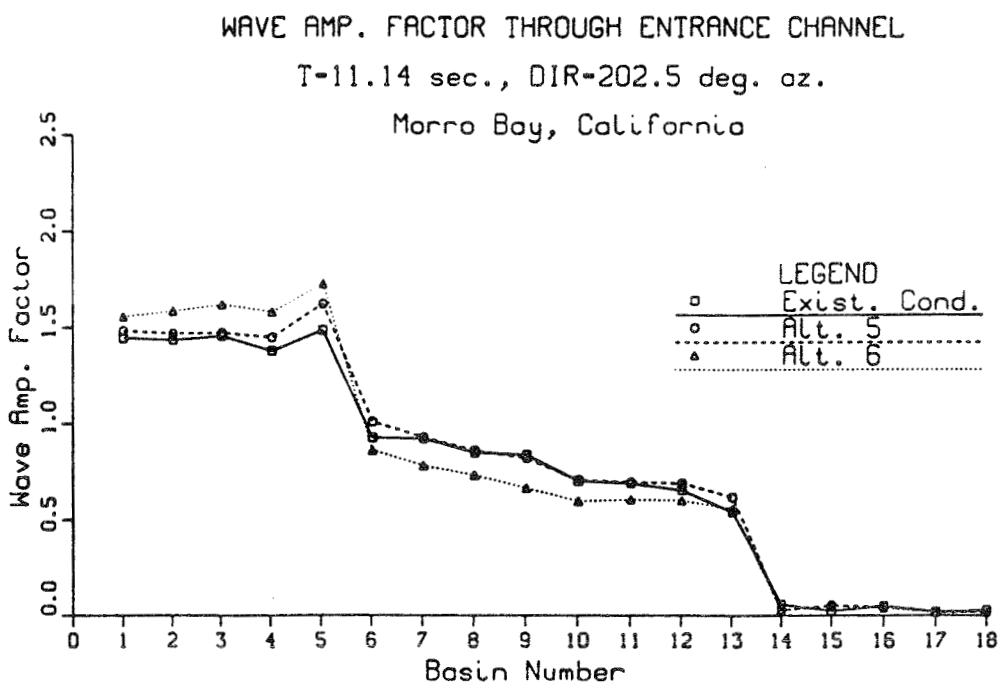

Figure B-2.

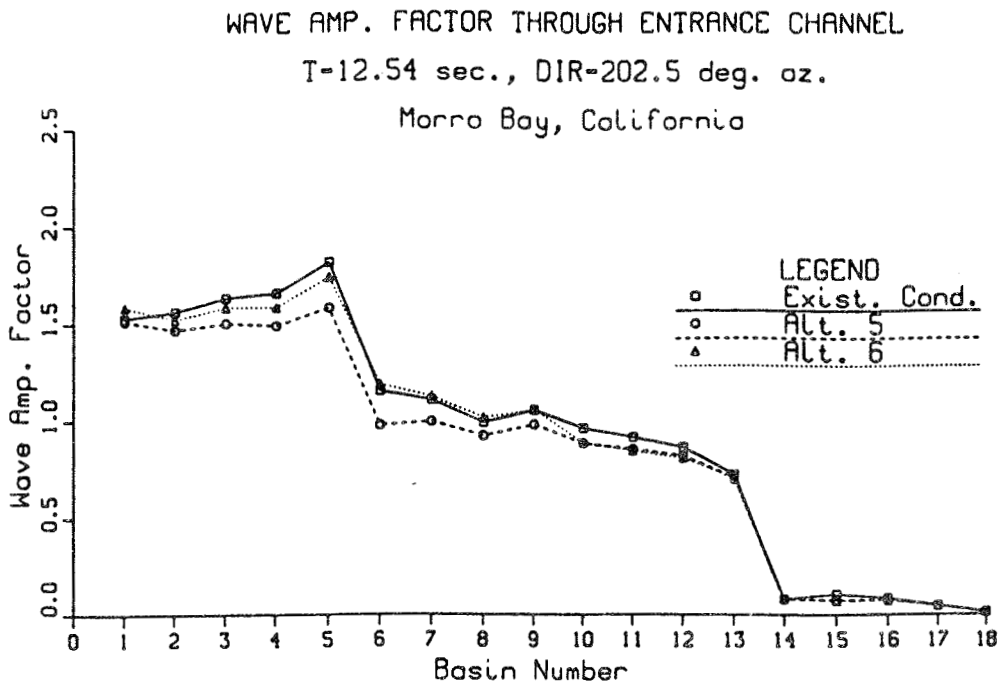

Figure B-3.

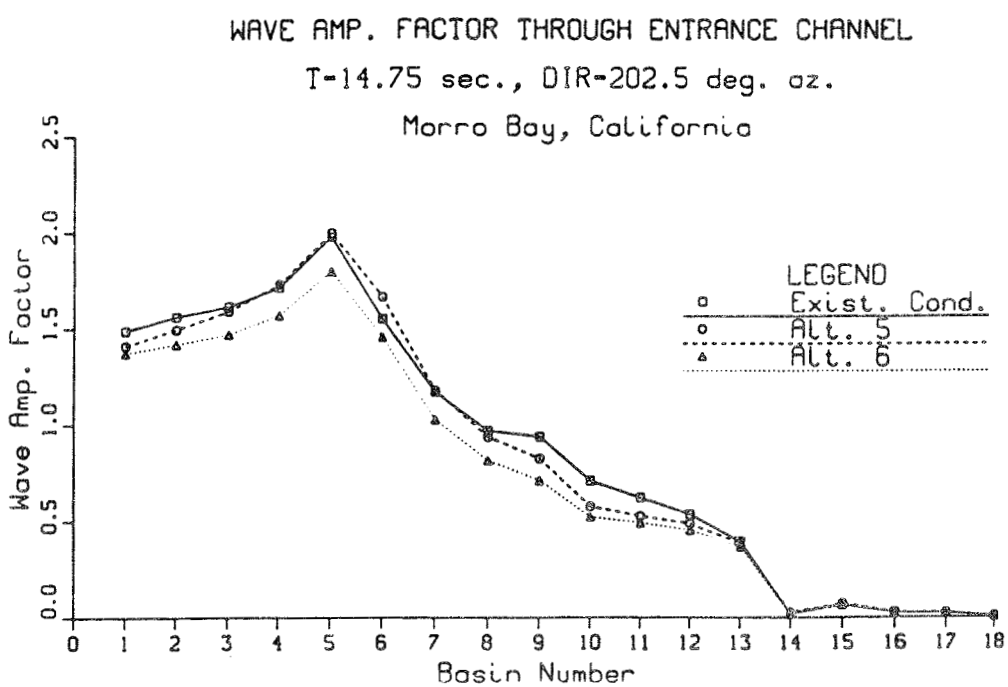

Figure B-4.

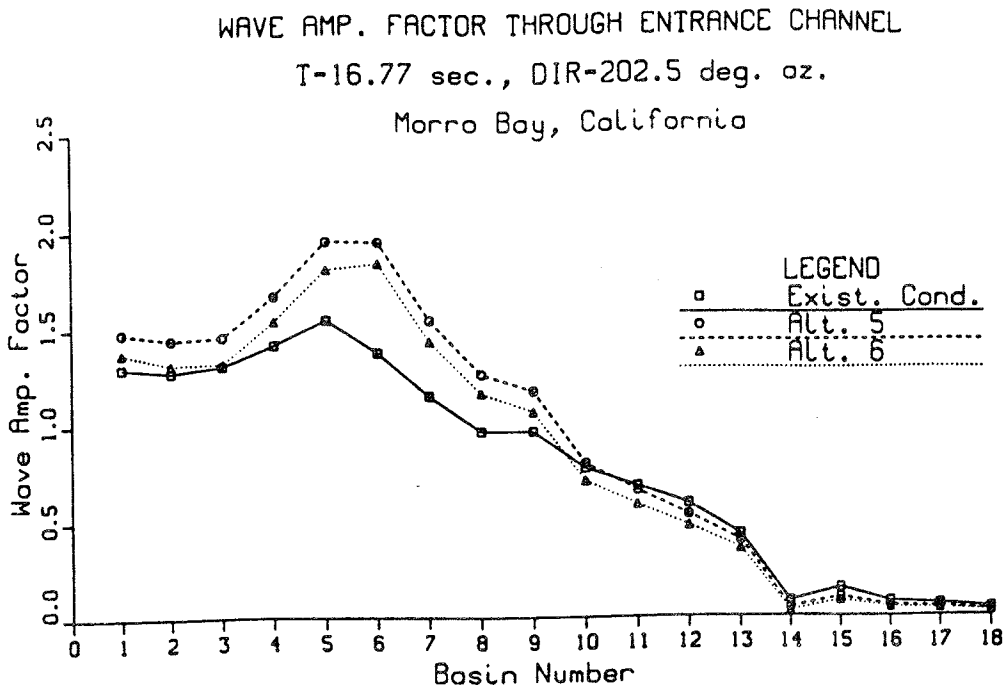

Figure B-5.

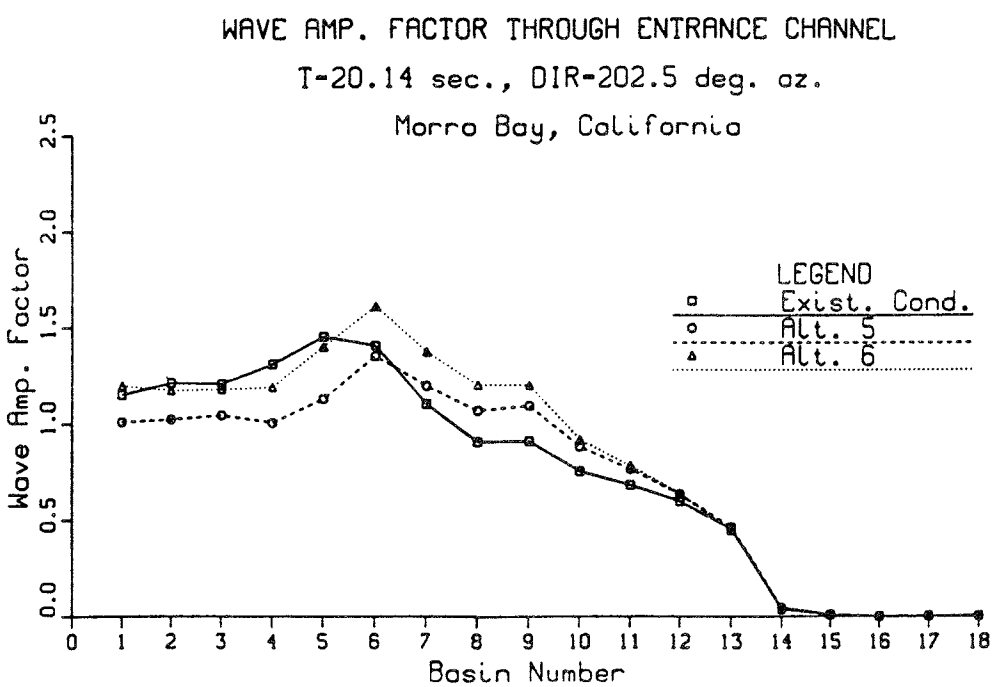

Figure B-6.

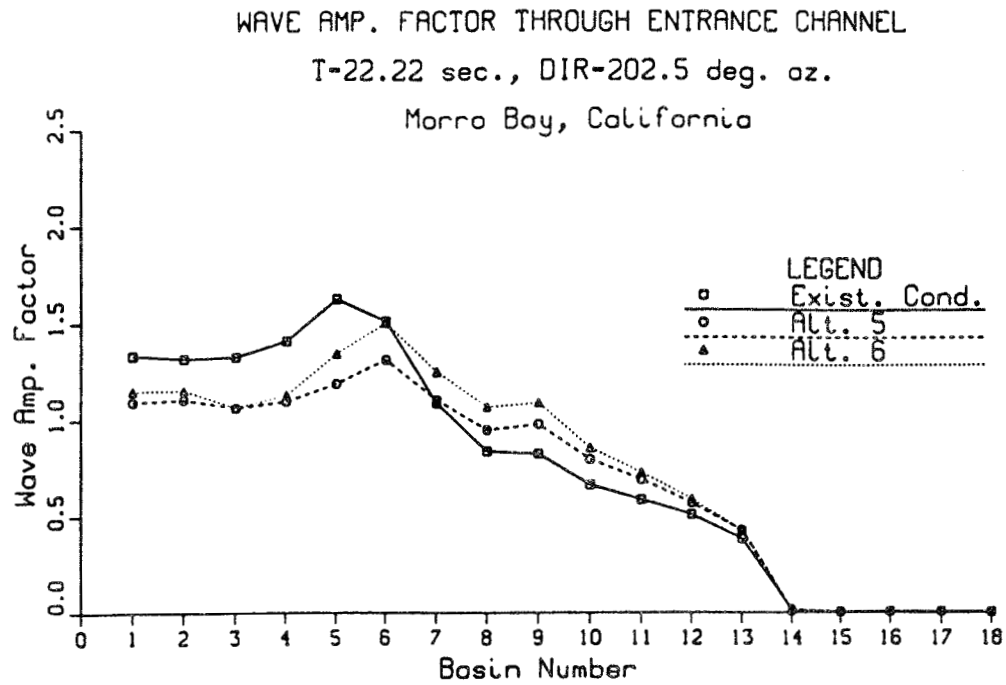

Figure B-7.

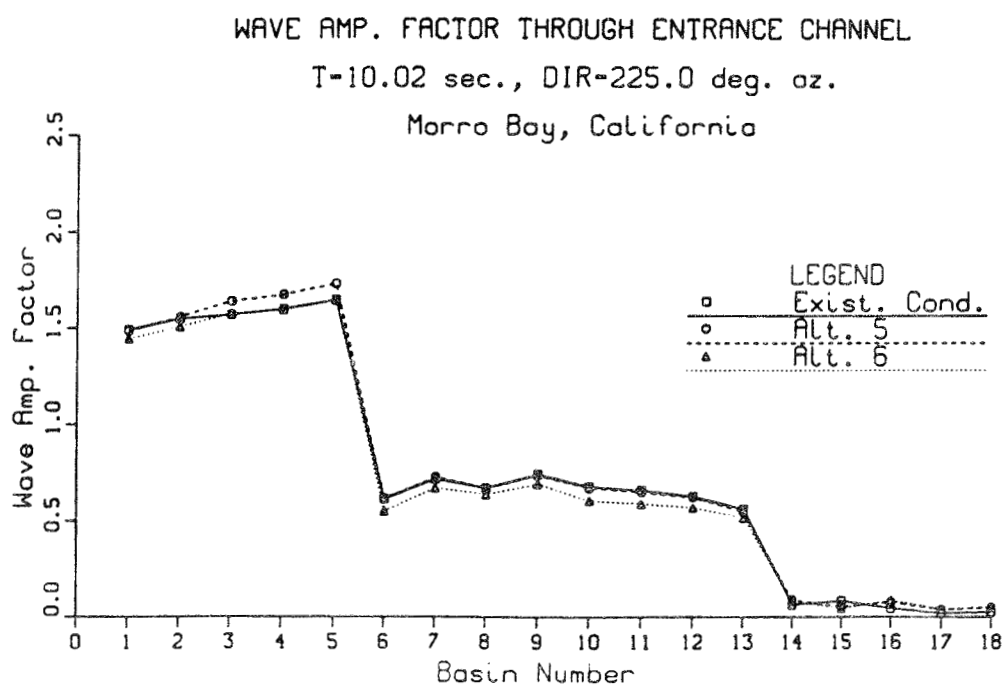

Figure B-8.

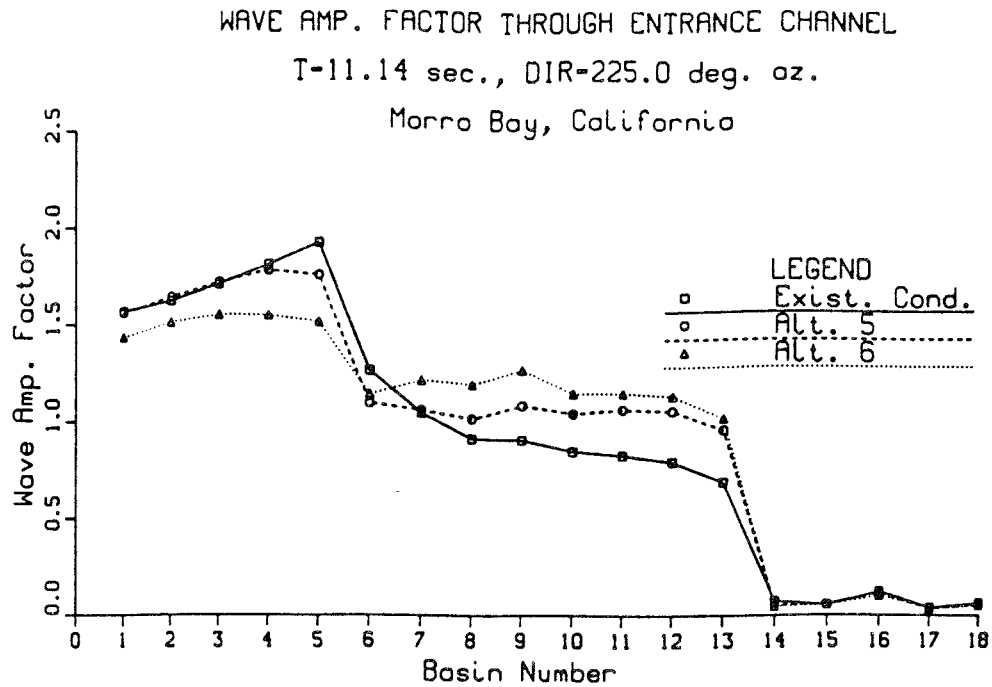

Figure B-9.

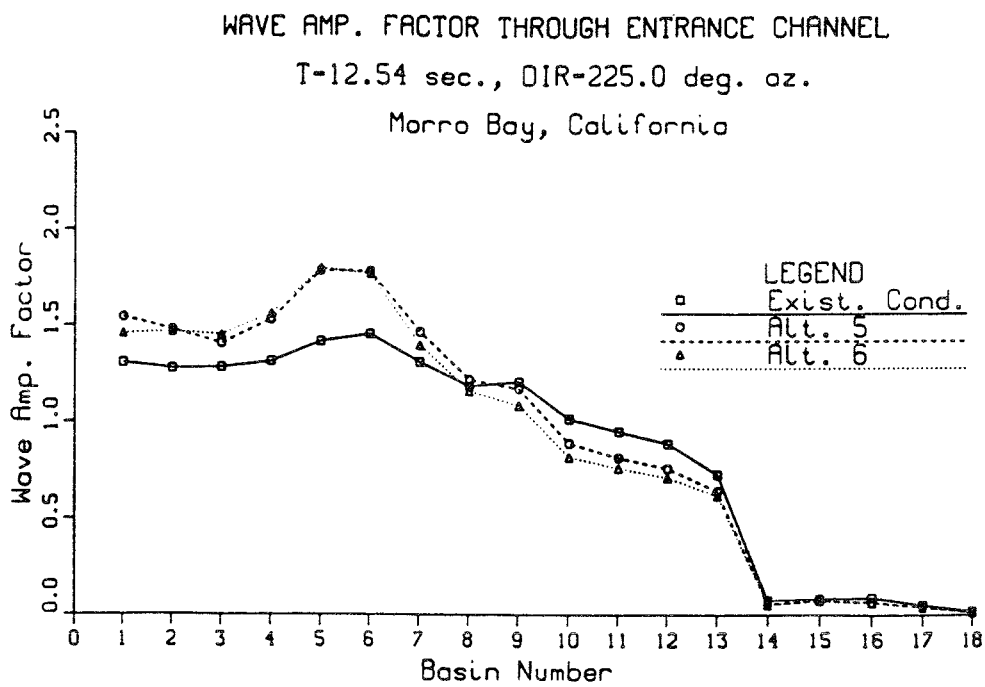

Figure B-10.

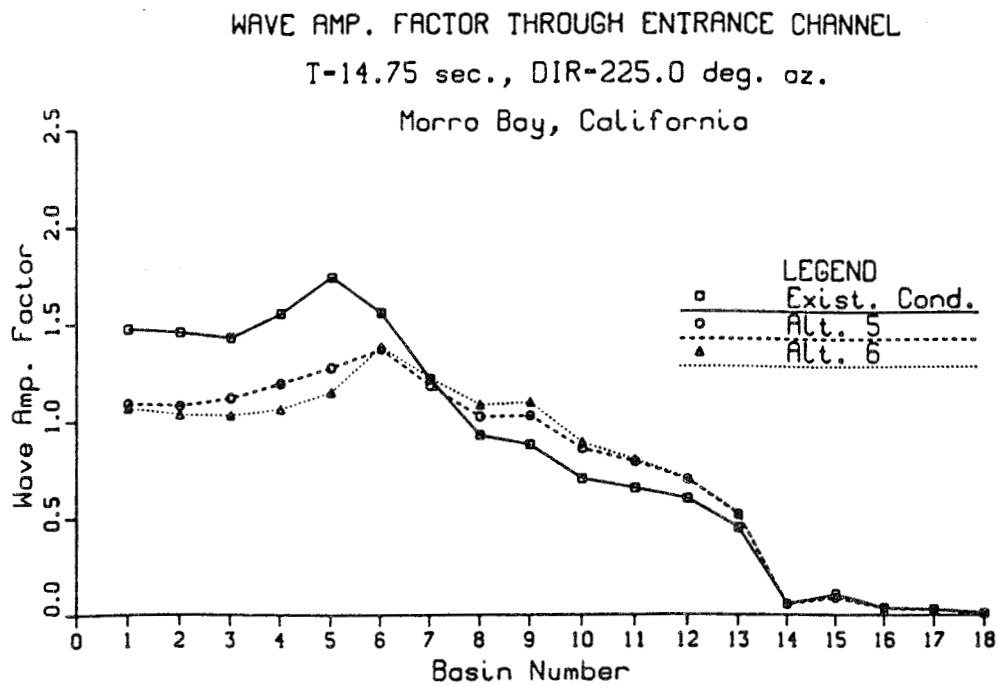

Figure B-11.

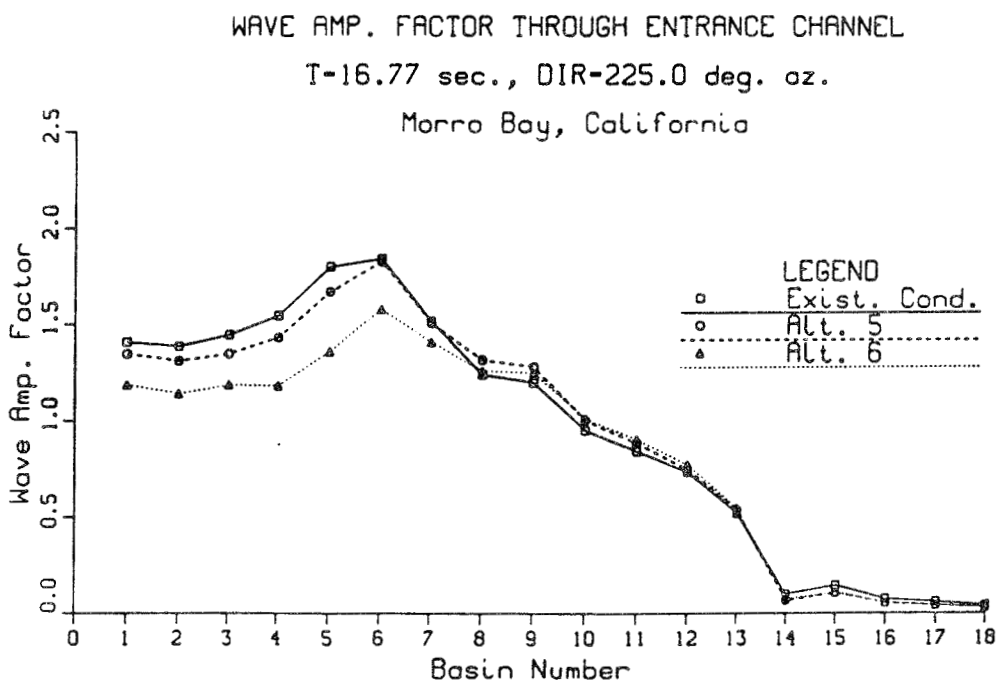

Figure B-12.

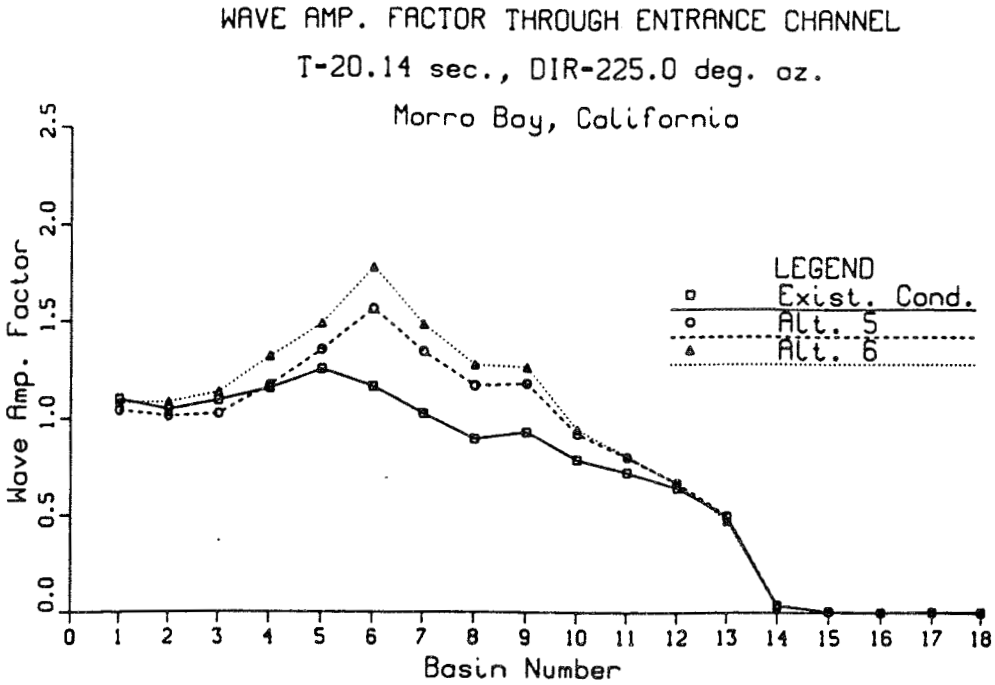

Figure B-13.

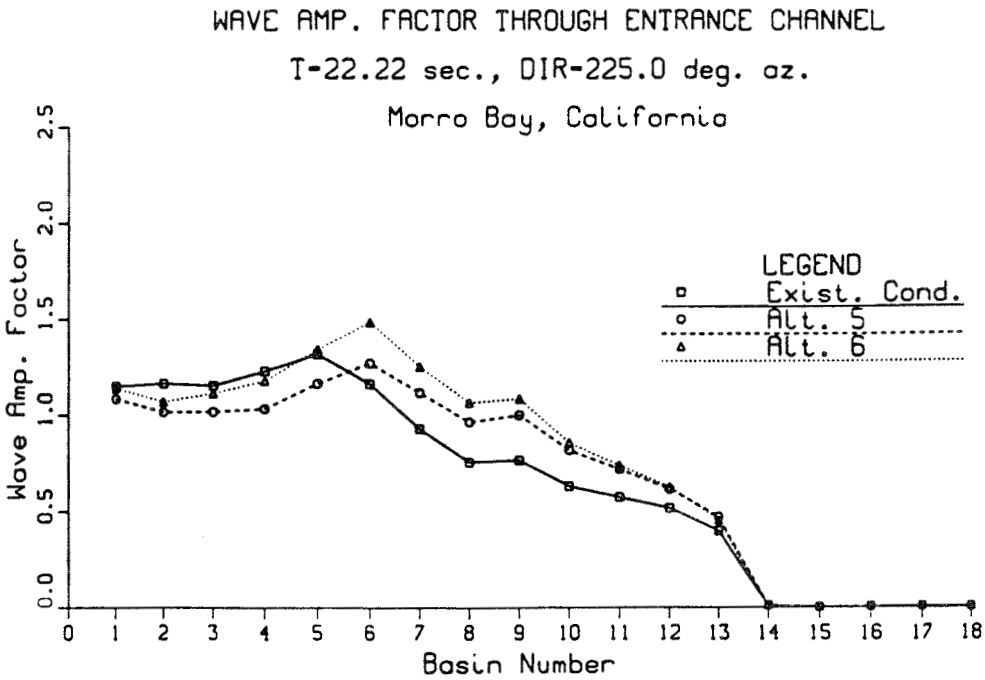

Figure B-14.

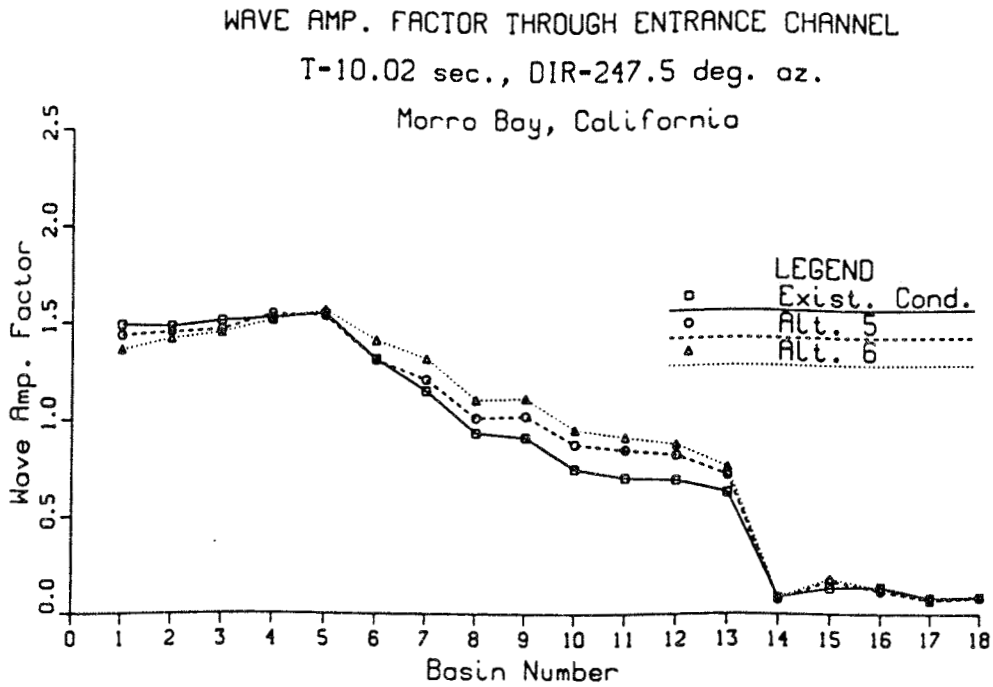

Figure B-15.

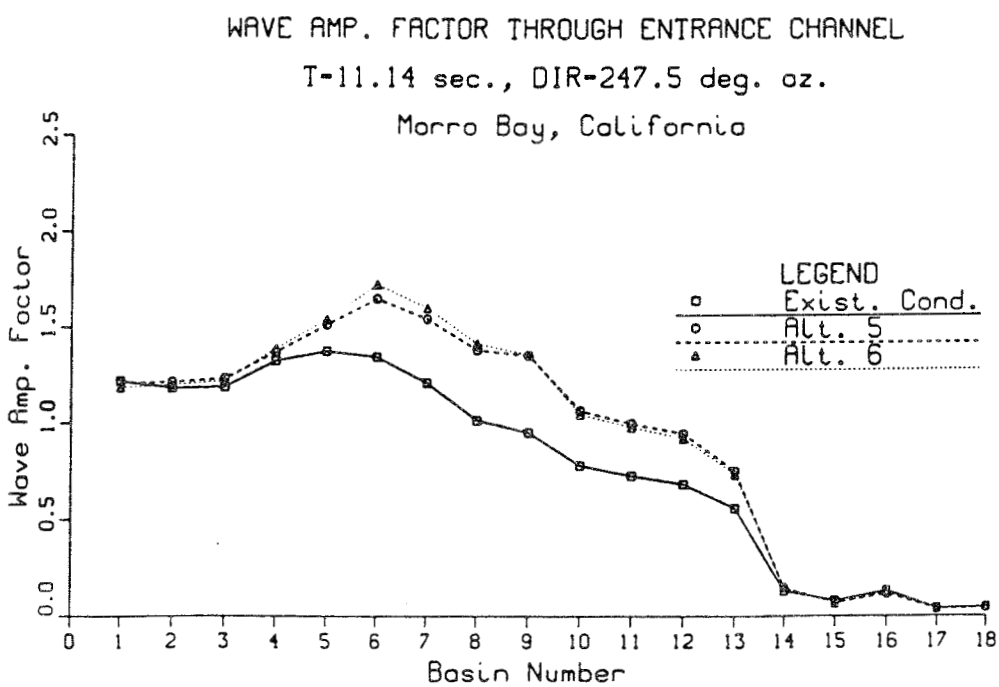

Figure B-16.

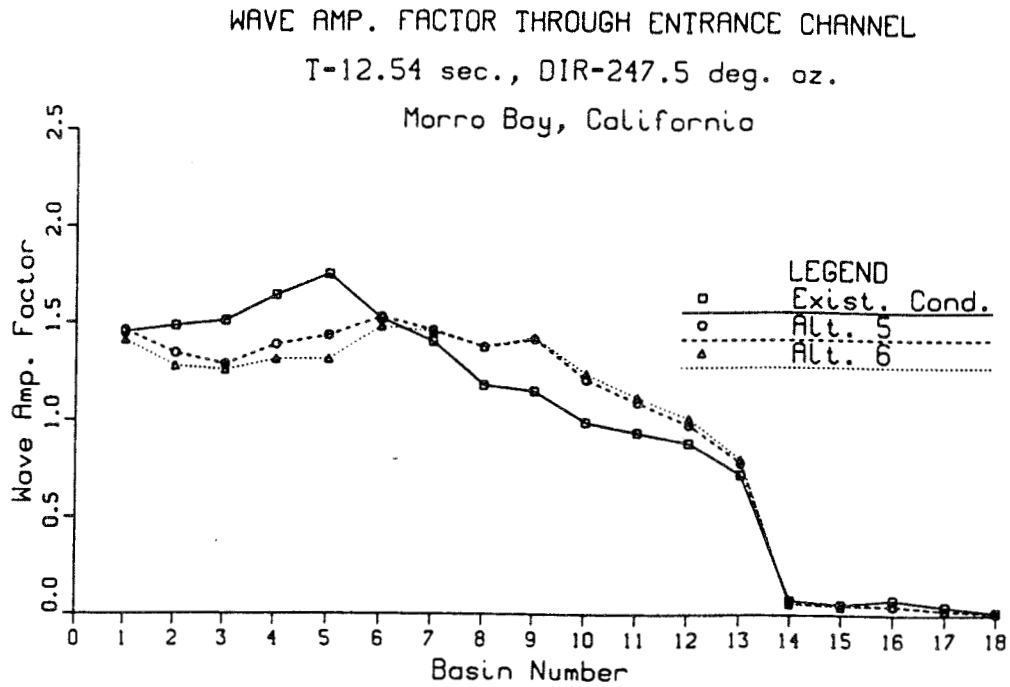

Figure B-17.

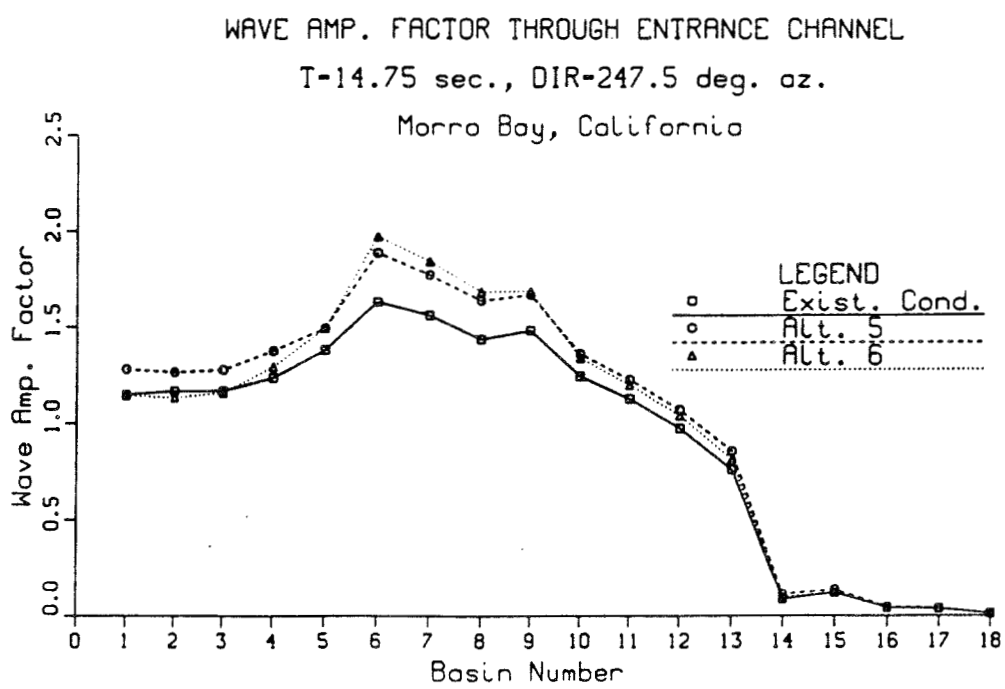

Figure B-18.

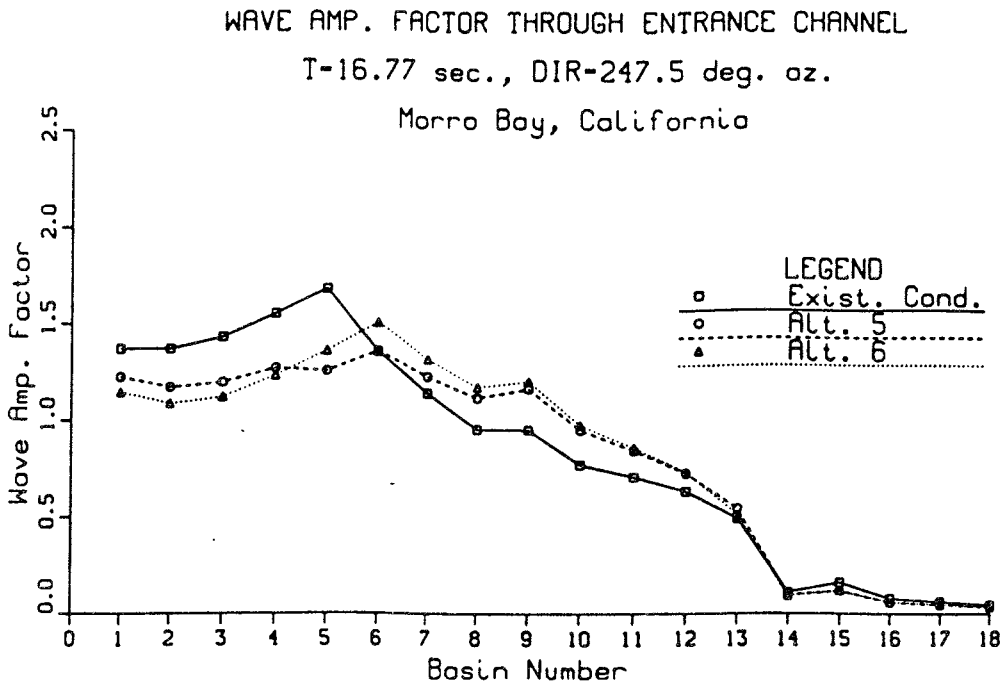

Figure B-19.

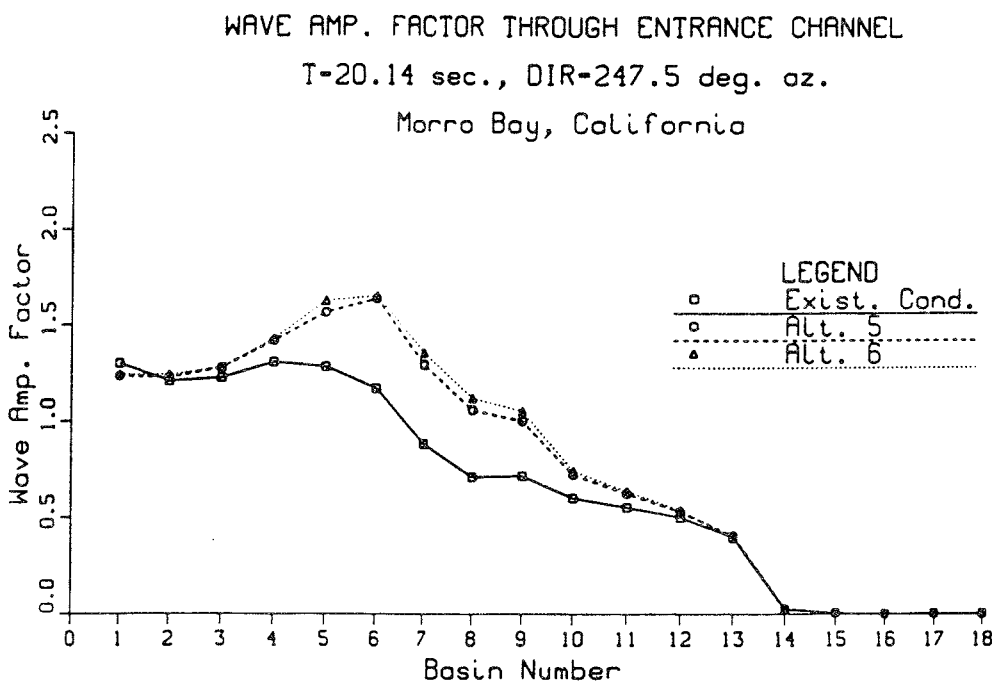

Figure B-20.

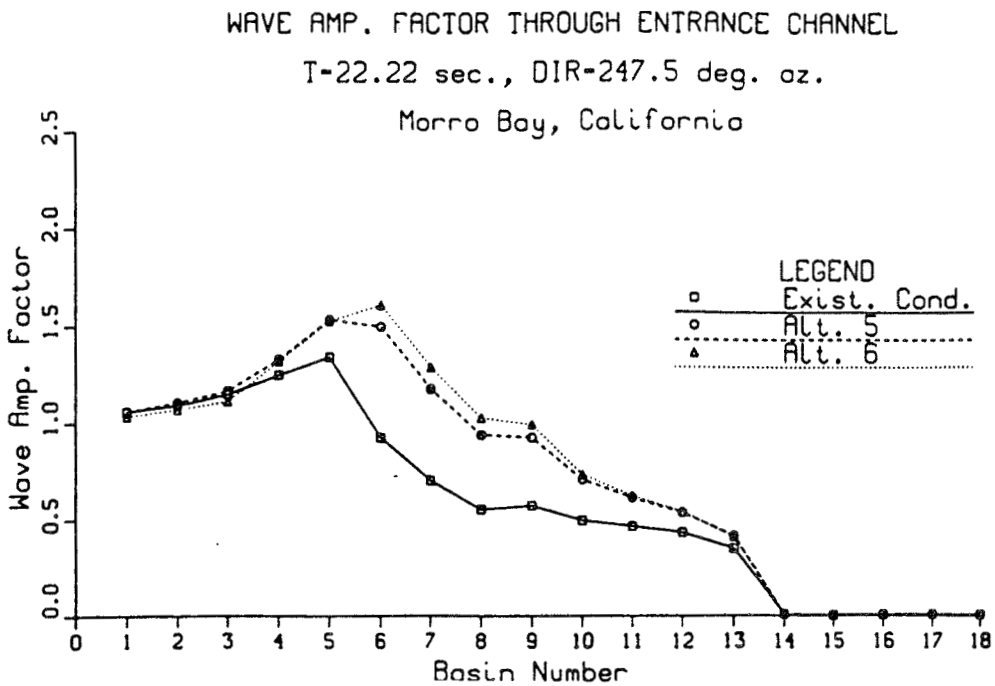

Figure B-21.

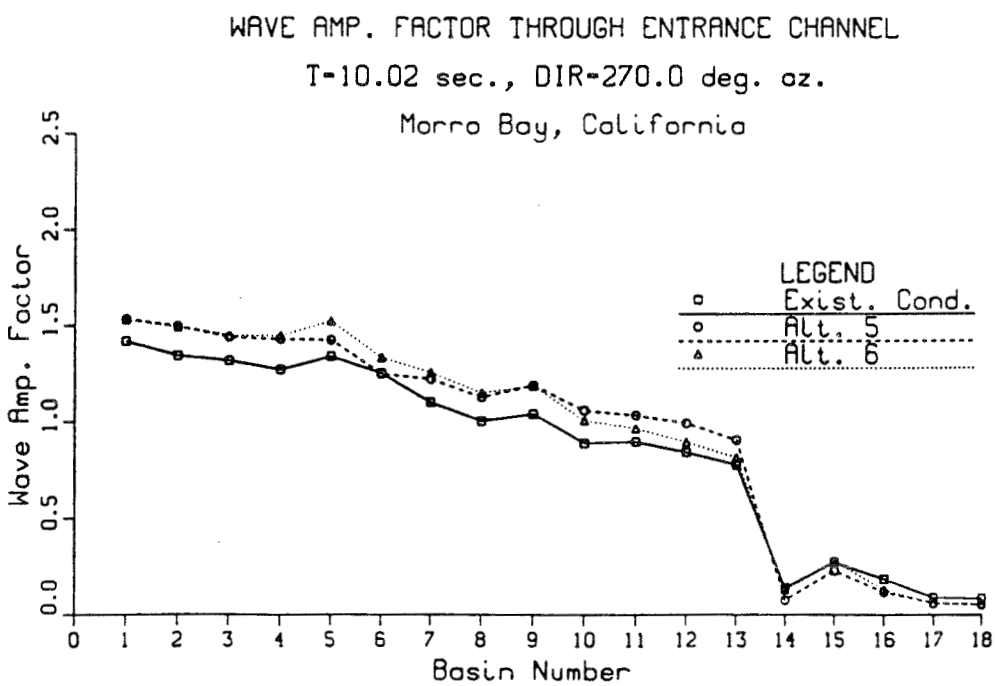

Figure B-22.

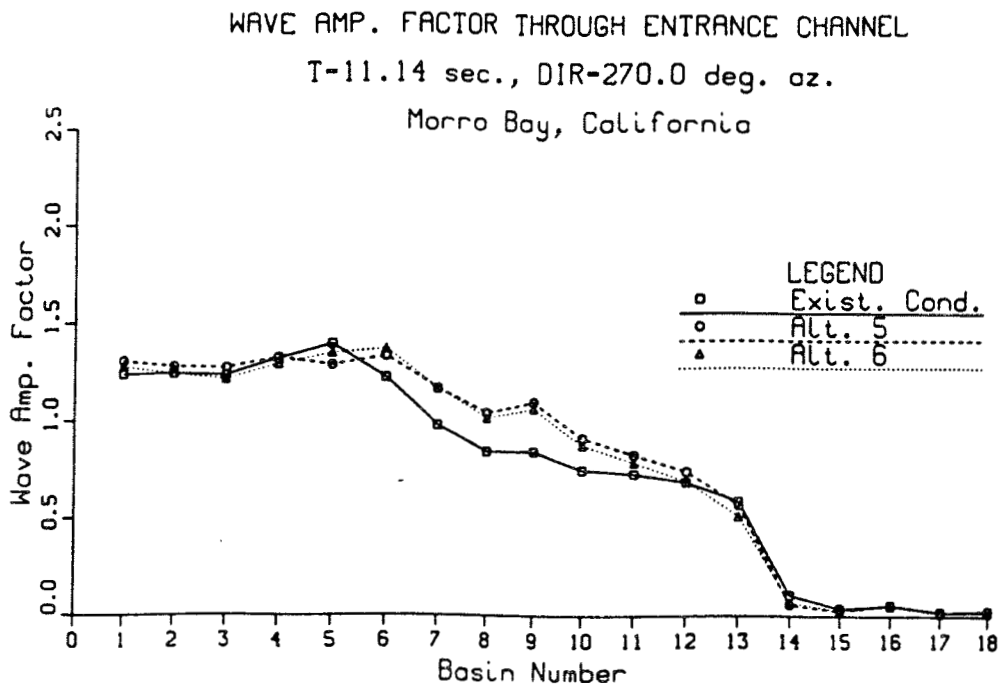

Figure B-23.

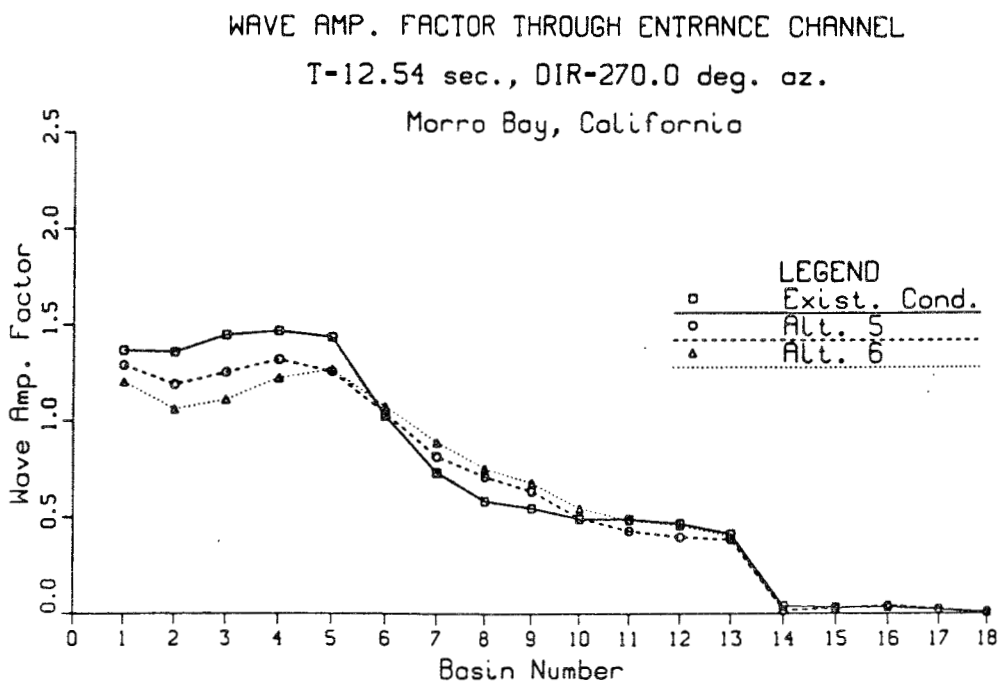

Figure B-24.

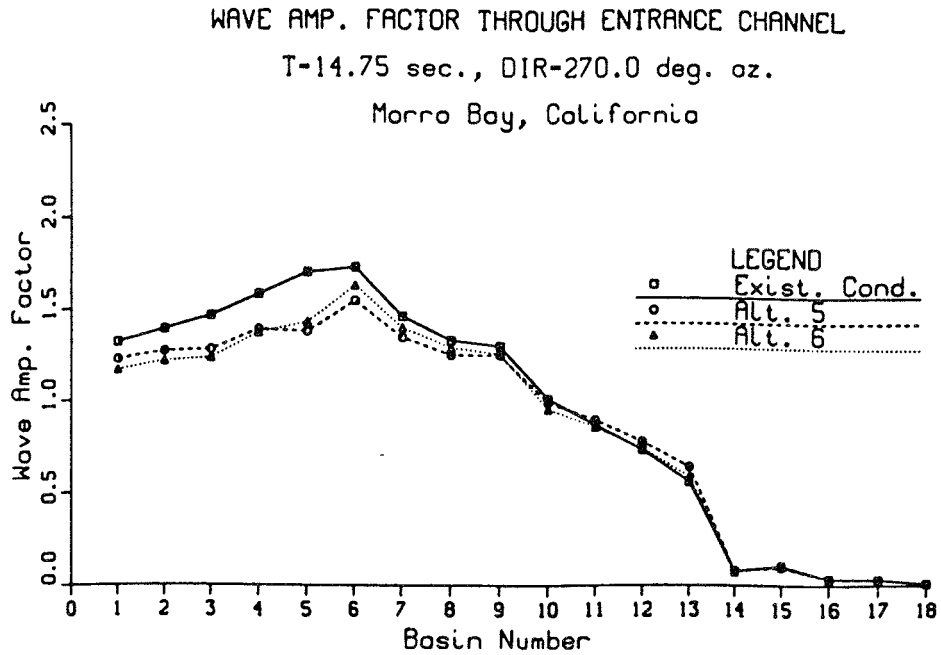

Figure B-25.

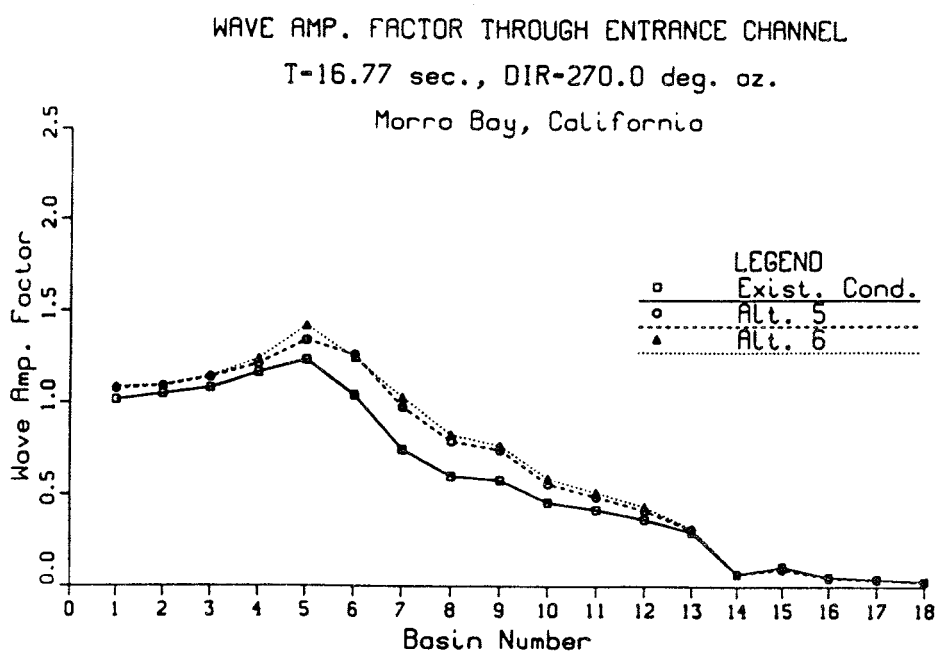

Figure B-26.

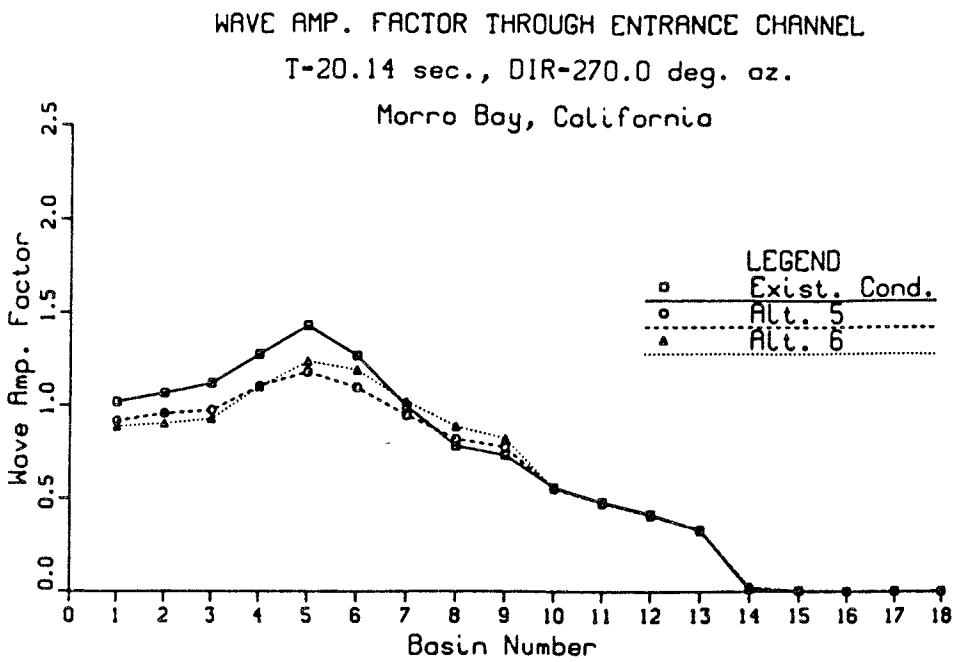

Figure B-27.

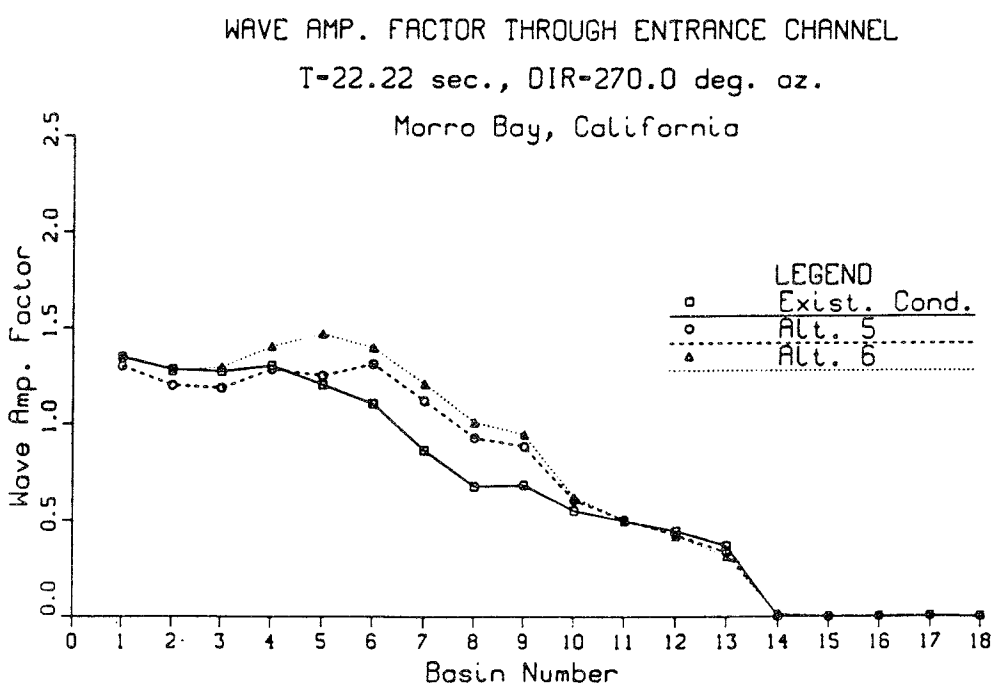

Figure B-28.

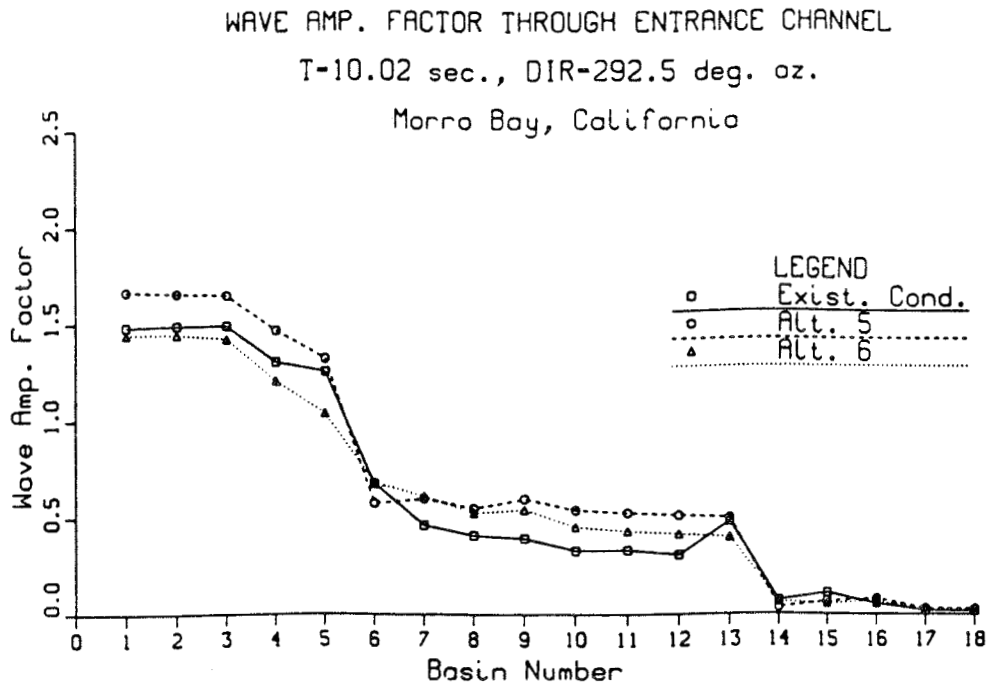

Figure B-29.

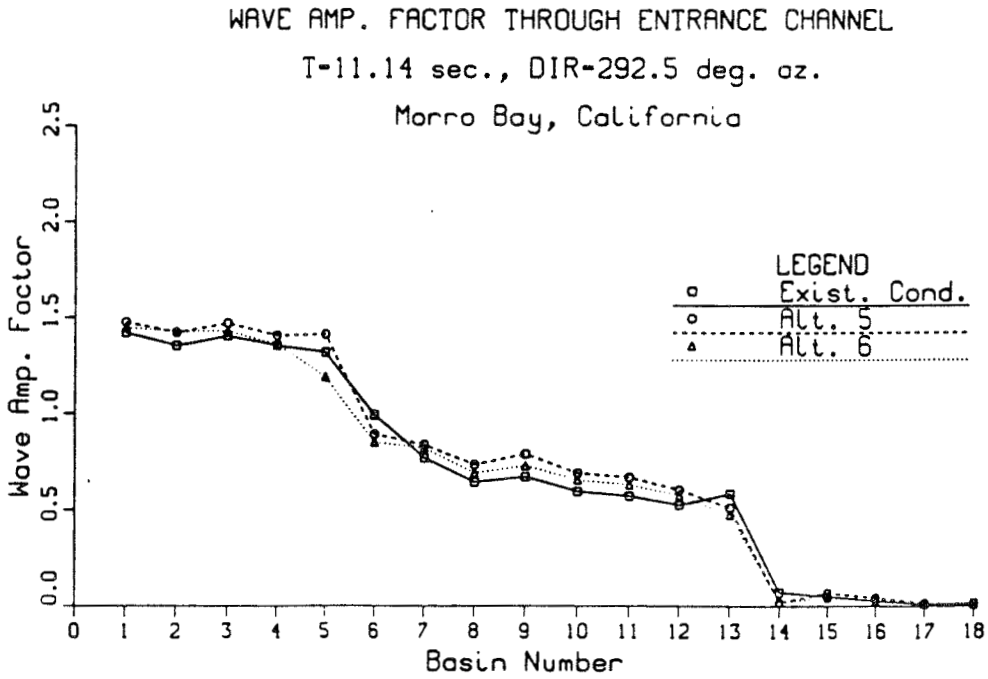

Figure B-30.

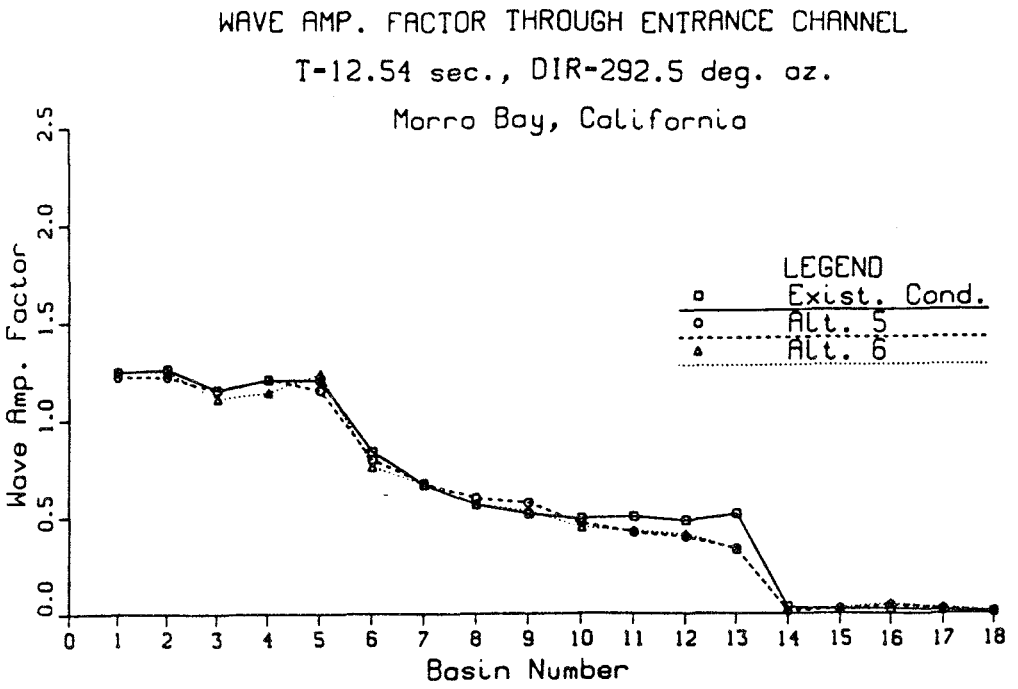

Figure B-31.

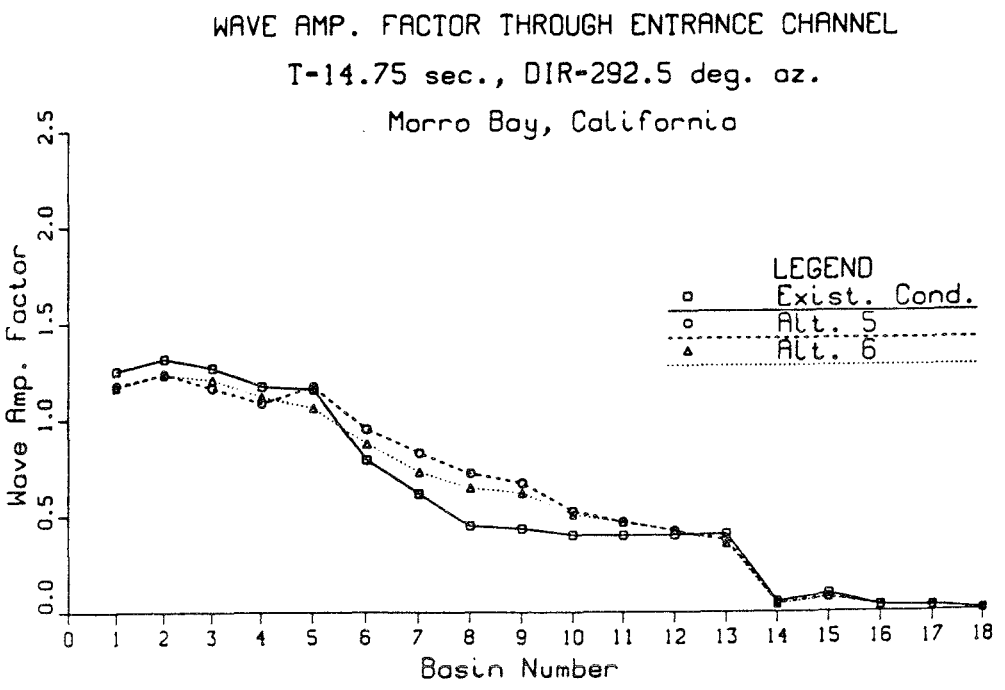

Figure B-32.

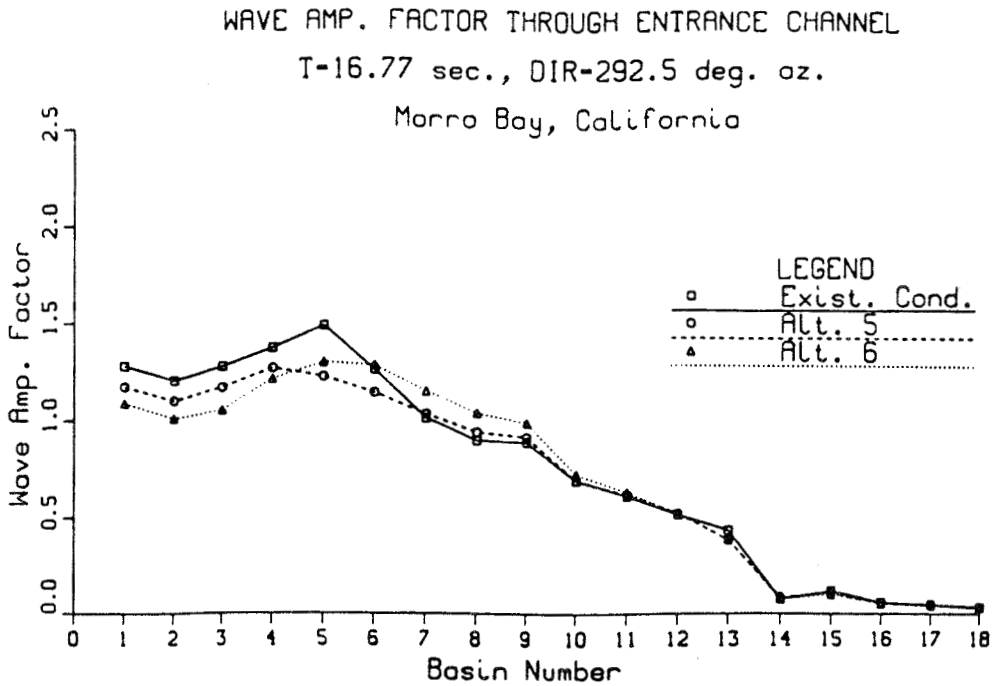

Figure B-33.

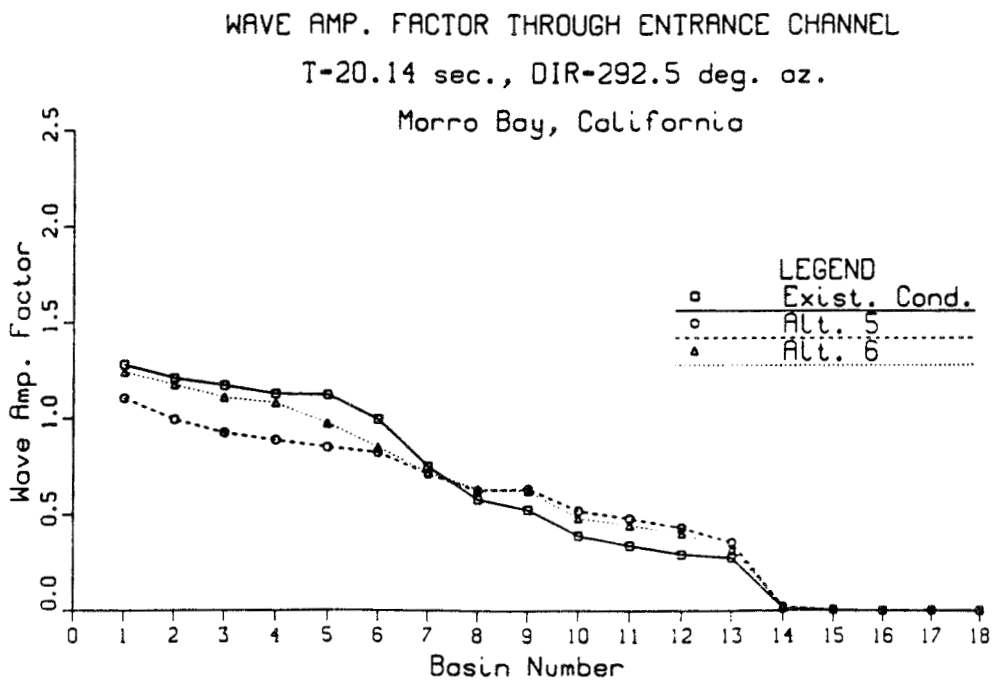

Figure B-34.

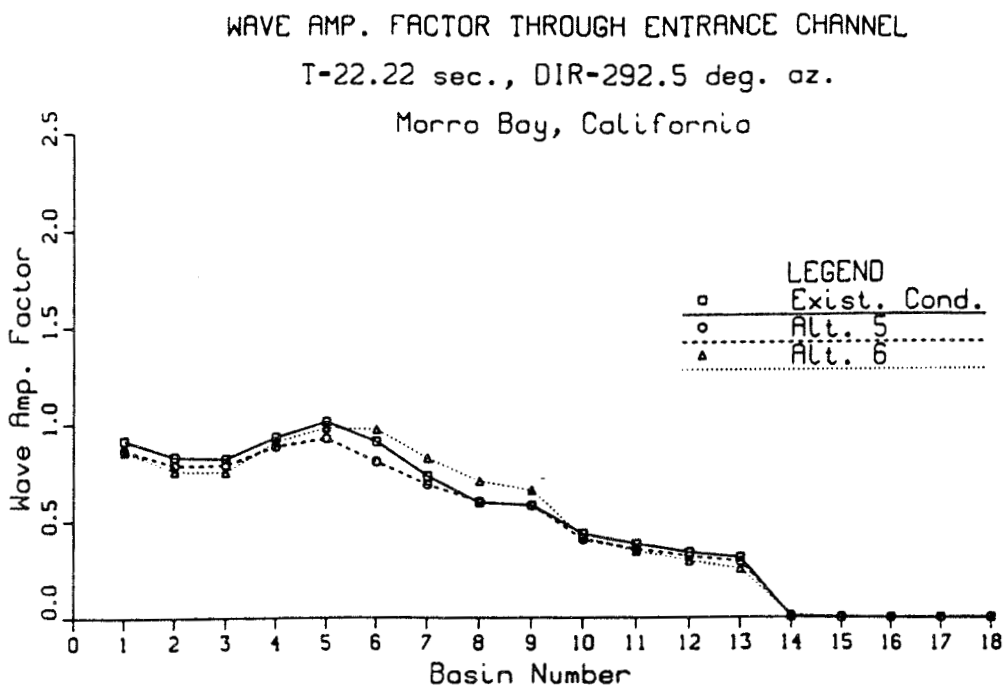

Figure B-35.

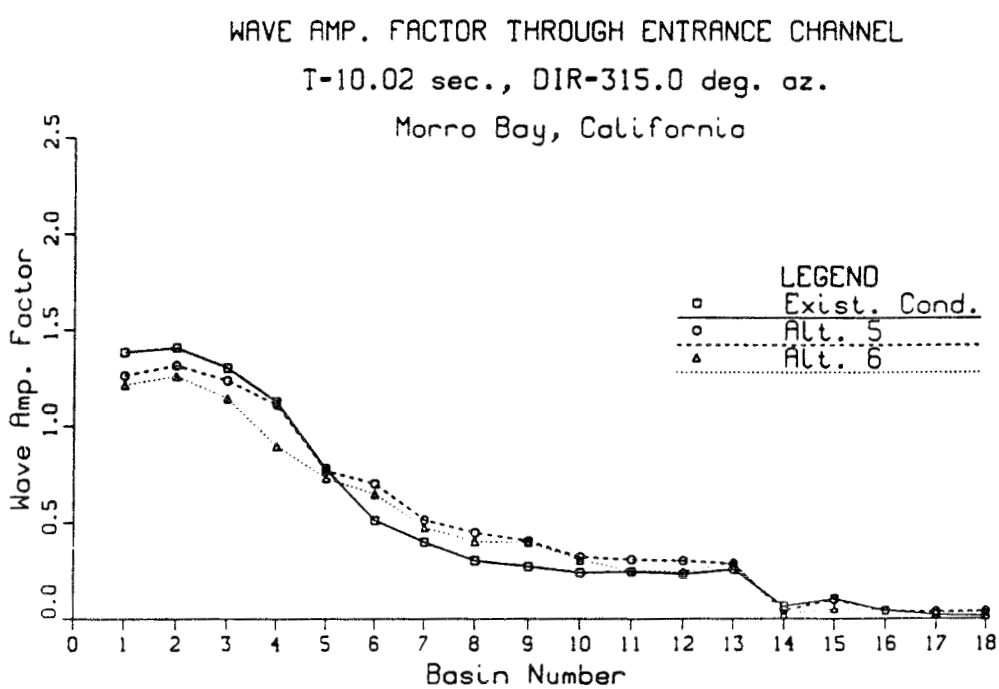

Figure B-36.

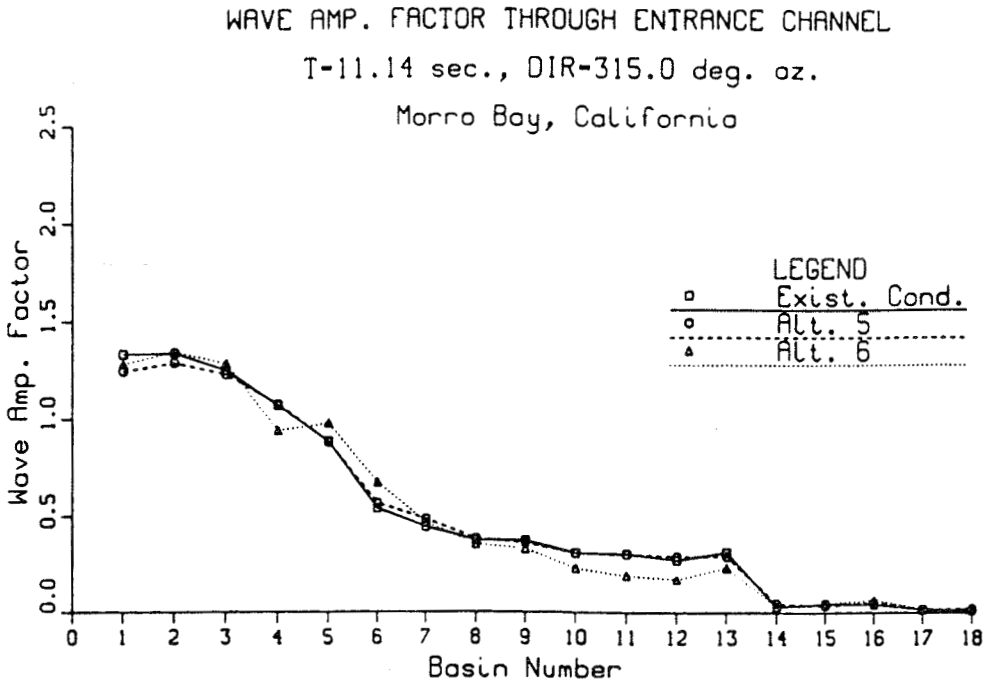

Figure B-37.

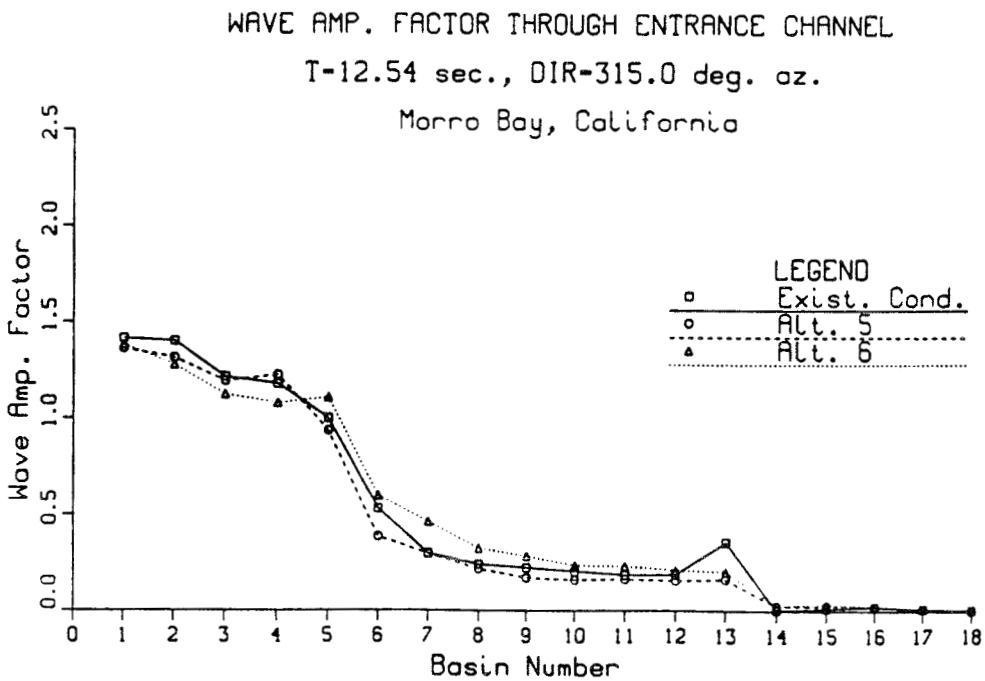

Figure B-38.

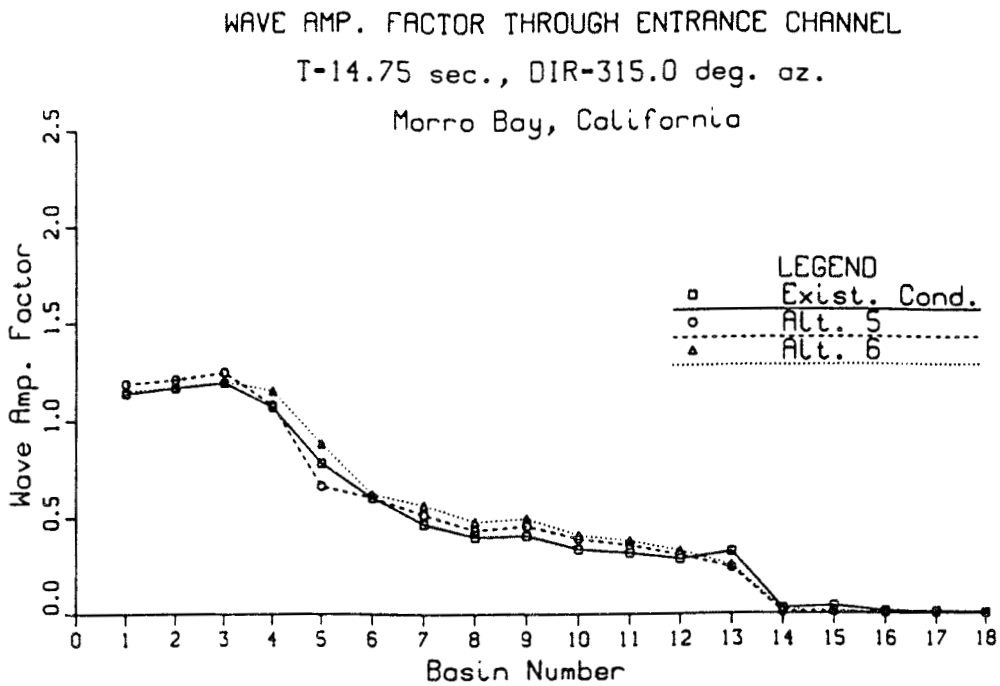

Figure B-39.

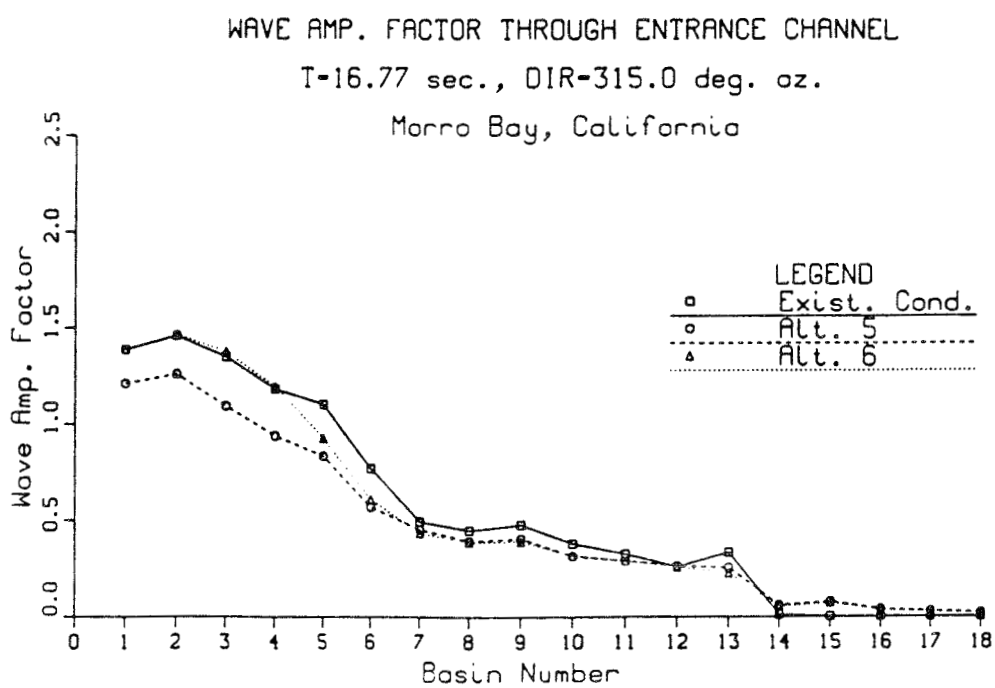

Figure B-40.

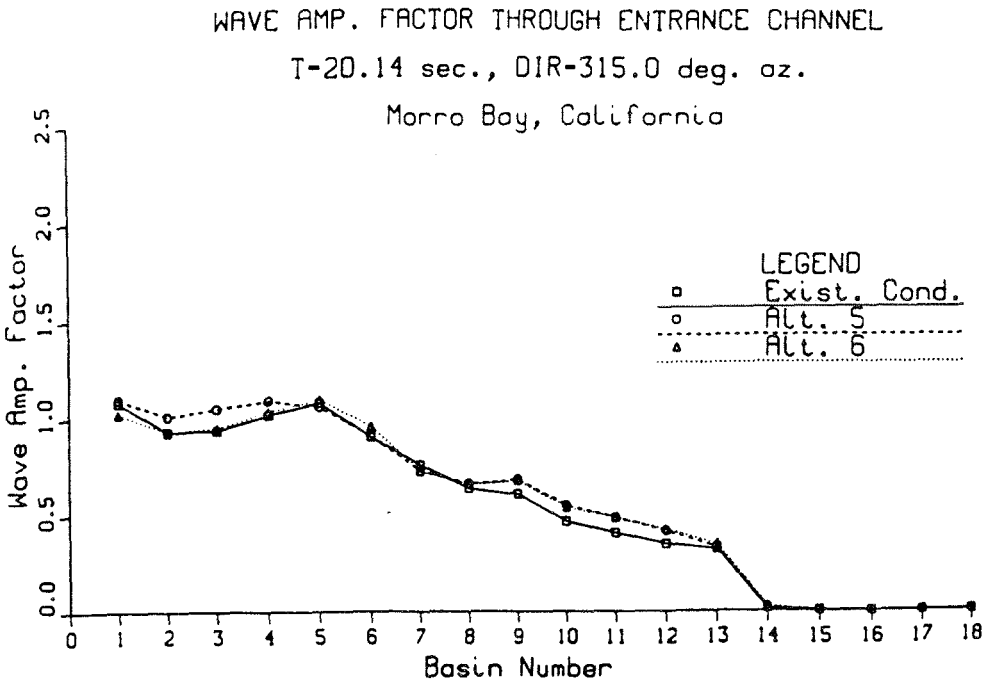

Figure B-41.

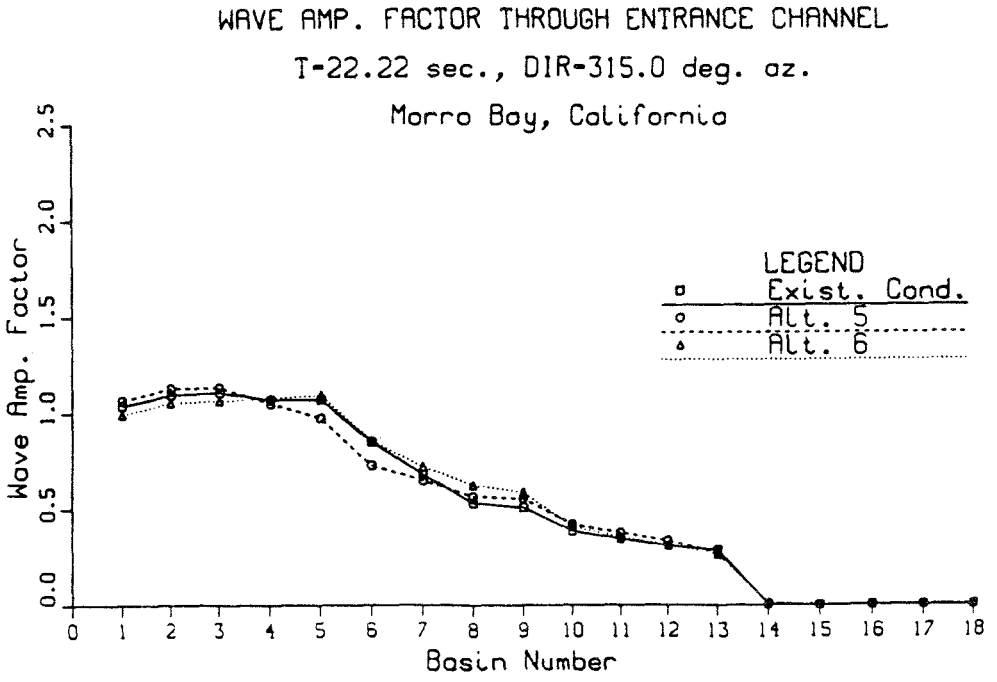

Figure B-42.

Table B-43

BREAKING DAYS PER YEAR THROUGH CHANNEL - JANUARY

Basin No.	Exist.	Alt. 5	Alt. 6
1	1.37	0.66	0.31
2	1.17	0.09	0.11
3	0.00	0.31	0.00
4	3.67	0.35	0.39
5	2.96	0.09	0.34
6	0.21	1.96	1.68
7	0.04	2.95	1.56
8	0.03	0.03	0.21
9	0.23	0.74	1.94
10	0.00	0.00	0.00
11	0.00	0.00	0.07

Table B-44

BREAKING DAYS PER YEAR THROUGH CHANNEL - FEBRUARY

Basin No.	Exist.	Alt. 5	Alt. 6
1	0.92	0.27	0.13
2	1.07	0.03	0.04
3	0.00	0.13	0.01
4	2.93	0.34	0.23
5	2.68	0.02	0.31
6	0.03	1.58	1.13
7	0.05	2.32	1.20
8	0.00	0.02	0.08
9	0.11	0.45	1.63
10	0.00	0.00	0.00
11	0.05	0.01	0.08

Table B-45

BREAKING DAYS PER YEAR THROUGH CHANNEL - MARCH			
Basin No.	Exist.	Alt. 5	Alt. 6
1	0.36	0.14	0.06
2	0.72	0.01	0.01
3	0.00	0.03	0.00
4	2.08	0.07	0.07
5	2.43	0.02	0.09
6	0.00	0.49	0.37
7	0.00	1.93	0.93
8	0.00	0.00	0.08
9	0.09	0.52	1.33
10	0.00	0.00	0.00
11	0.01	0.00	0.05

Table B-46

BREAKING DAYS PER YEAR THROUGH CHANNEL - APRIL			
Basin No.	Exist.	Alt. 5	Alt. 6
1	0.33	0.29	0.16
2	0.34	0.03	0.03
3	0.00	0.01	0.00
4	0.79	0.00	0.00
5	1.05	0.09	0.00
6	0.00	0.16	0.17
7	0.00	0.68	0.31
8	0.00	0.02	0.08
9	0.13	0.31	0.52
10	0.00	0.00	0.00
11	0.02	0.00	0.01

Table B-47

BREAKING DAYS PER YEAR THROUGH CHANNEL - MAY			
Basin No.	Exist.	Alt. 5	Alt. 6
1	0.02	0.09	0.01
2	0.06	0.00	0.00
3	0.00	0.00	0.00
4	0.01	0.00	0.00
5	0.08	0.00	0.00
6	0.00	0.00	0.00
7	0.00	0.00	0.00
8	0.00	0.00	0.00
9	0.01	0.08	0.06
10	0.00	0.00	0.00
11	0.00	0.00	0.04

Table B-48

BREAKING DAYS PER YEAR THROUGH CHANNEL - JUNE			
Basin No.	Exist.	Alt. 5	Alt. 6
1	0.00	0.02	0.00
2	0.02	0.00	0.00
3	0.00	0.00	0.00
4	0.00	0.00	0.00
5	0.03	0.00	0.00
6	0.00	0.00	0.00
7	0.00	0.00	0.00
8	0.00	0.00	0.00
9	0.00	0.00	0.00
10	0.00	0.00	0.00
11	0.00	0.00	0.00

Table B-49

BREAKING DAYS PER YEAR THROUGH CHANNEL - JULY			
Basin No.	Exist.	Alt. 5	Alt. 6
1	0.00	0.00	0.00
2	0.00	0.00	0.00
3	0.00	0.00	0.00
4	0.00	0.00	0.00
5	0.00	0.00	0.00
6	0.00	0.00	0.00
7	0.00	0.00	0.00
8	0.00	0.00	0.00
9	0.00	0.00	0.00
10	0.00	0.00	0.00
11	0.00	0.00	0.00

Table B-50

BREAKING DAYS PER YEAR THROUGH CHANNEL - AUGUST			
Basin No.	Exist.	Alt. 5	Alt. 6
1	0.00	0.00	0.00
2	0.00	0.00	0.00
3	0.00	0.00	0.00
4	0.00	0.00	0.00
5	0.00	0.00	0.00
6	0.00	0.00	0.00
7	0.00	0.00	0.00
8	0.00	0.00	0.00
9	0.00	0.00	0.00
10	0.00	0.00	0.00
11	0.00	0.00	0.00

Table B-51

BREAKING DAYS PER YEAR THROUGH CHANNEL - SEPTEMBER			
Basin No.	Exist.	Alt. 5	Alt. 6
1	0.00	0.00	0.00
2	0.00	0.00	0.00
3	0.00	0.00	0.00
4	0.00	0.00	0.00
5	0.01	0.00	0.00
6	0.00	0.00	0.00
7	0.00	0.00	0.00
8	0.00	0.00	0.00
9	0.00	0.01	0.00
10	0.00	0.00	0.00
11	0.00	0.00	0.00

Table B-52

BREAKING DAYS PER YEAR THROUGH CHANNEL - OCTOBER			
Basin No.	Exist.	Alt. 5	Alt. 6
1	0.10	0.03	0.01
2	0.13	0.00	0.00
3	0.00	0.02	0.00
4	0.62	0.05	0.02
5	0.68	0.00	0.05
6	0.03	0.16	0.09
7	0.00	0.56	0.16
8	0.00	0.00	0.01
9	0.03	0.10	0.50
10	0.00	0.00	0.00
11	0.00	0.00	0.02

Table B-53

BREAKING DAYS PER YEAR THROUGH CHANNEL - NOVEMBER			
Basin No.	Exist.	Alt. 5	Alt. 6
1	0.49	0.12	0.00
2	1.02	0.01	0.01
3	0.00	0.10	0.00
4	2.17	0.12	0.10
5	1.98	0.00	0.10
6	0.01	0.68	0.43
7	0.02	2.07	1.28
8	0.00	0.00	0.10
9	0.17	0.74	1.02
10	0.00	0.00	0.00
11	0.00	0.00	0.05

Table B-54

BREAKING DAYS PER YEAR THROUGH CHANNEL - DECEMBER			
Basin No.	Exist.	Alt. 5	Alt. 6
1	1.65	0.70	0.48
2	1.55	0.18	0.18
3	0.00	0.21	0.00
4	3.81	0.26	0.42
5	3.42	0.03	0.27
6	0.06	1.69	1.16
7	0.01	3.07	1.99
8	0.00	0.03	0.08
9	0.21	0.67	1.76
10	0.00	0.00	0.00
11	0.03	0.00	0.12

Table B-55

DAYS OF BREAKING - YEARLY SUMMARY			
Basin No.	Exist.	Alt. 5	Alt. 6
1	5.24	2.32	1.16
2	6.08	0.35	0.01
3	0.00	0.81	0.01
4	16.08	1.19	1.23
5	15.32	0.25	1.16
6	0.34	6.72	5.03
7	0.12	13.58	7.43
8	0.03	0.10	0.64
9	0.98	3.62	8.76
10	0.00	0.00	0.00
11	0.11	0.01	0.44

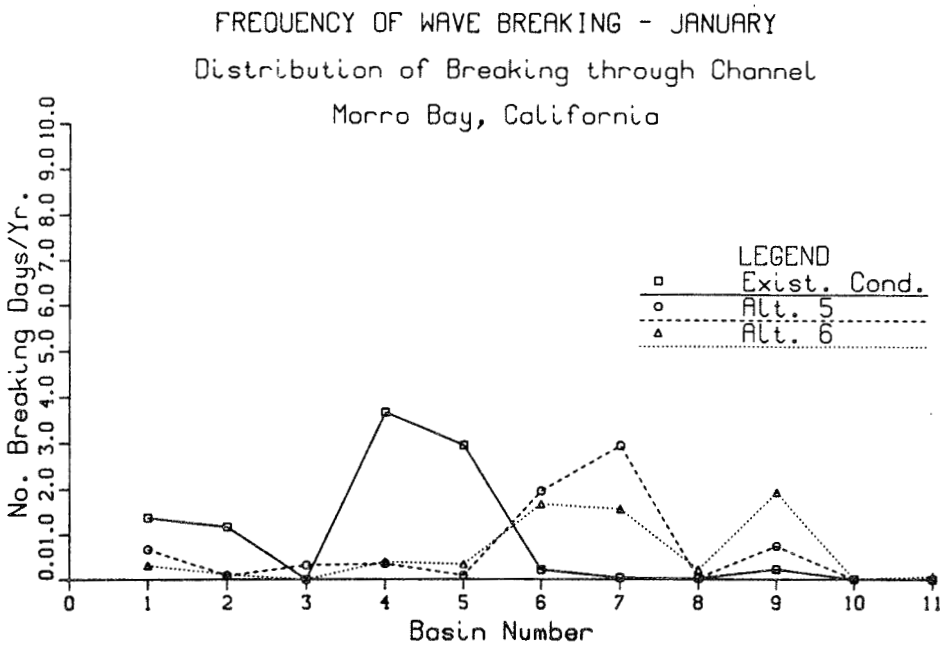

Figure B-43.

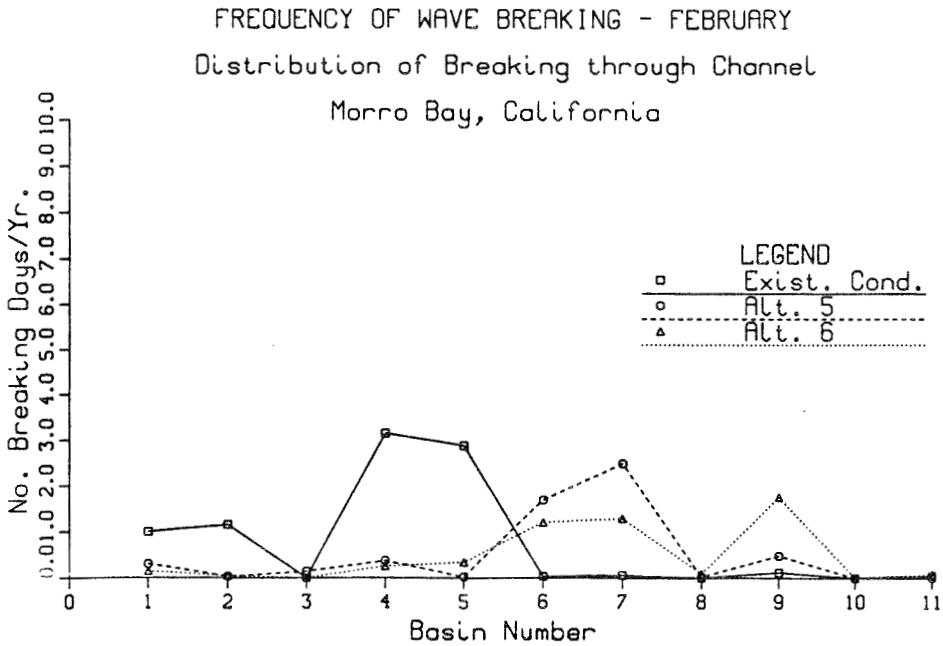

Figure B-44.

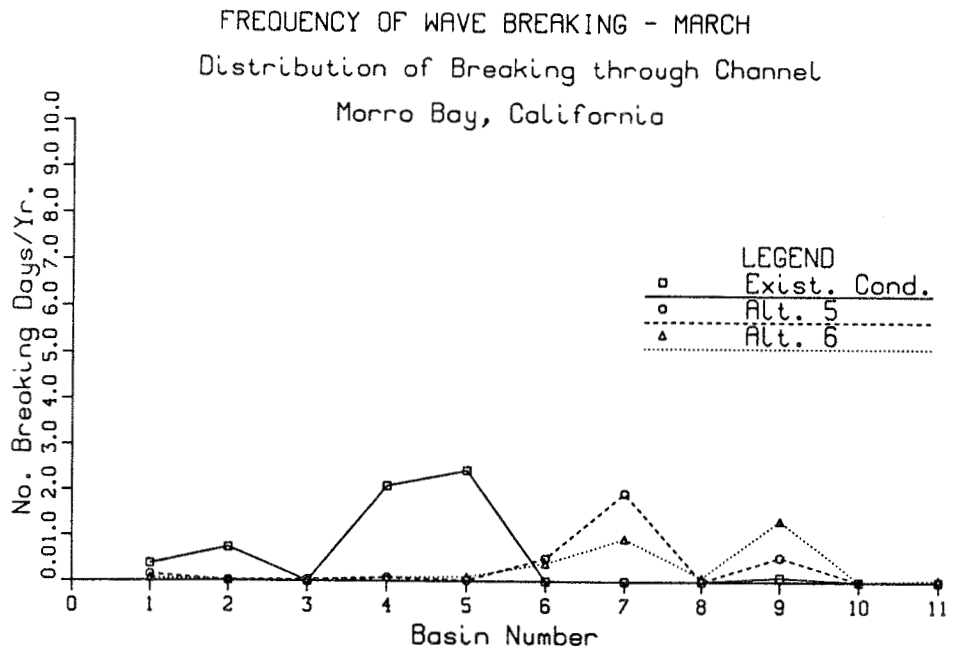

Figure B-45.

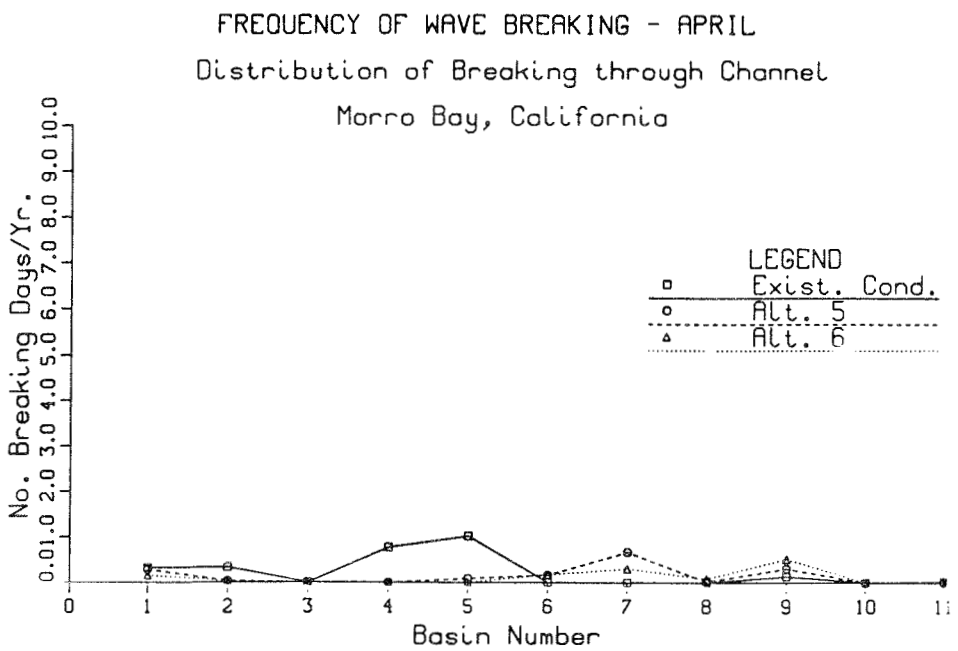

Figure B-46.

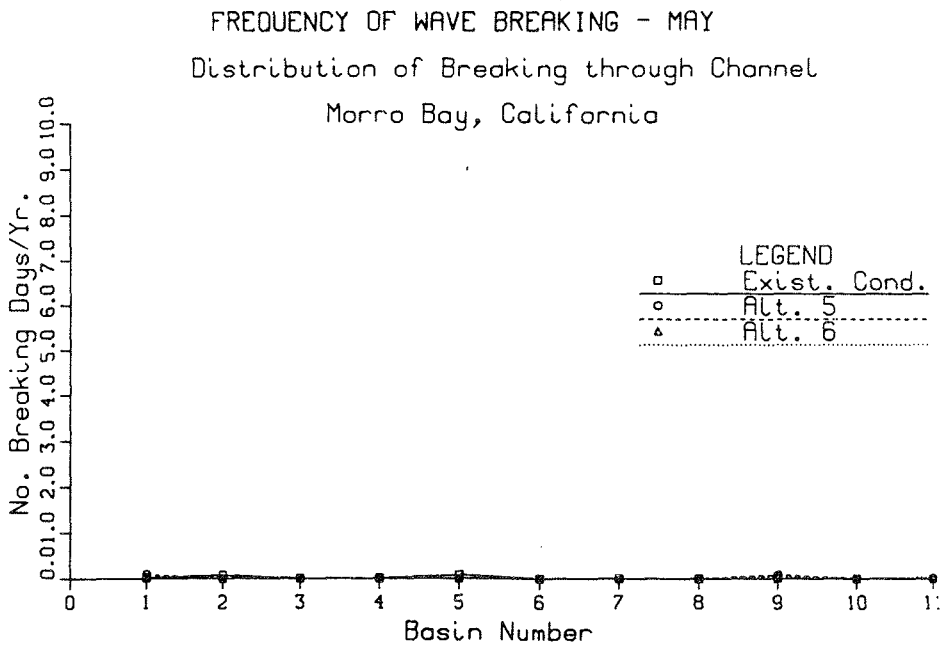

Figure B-47.

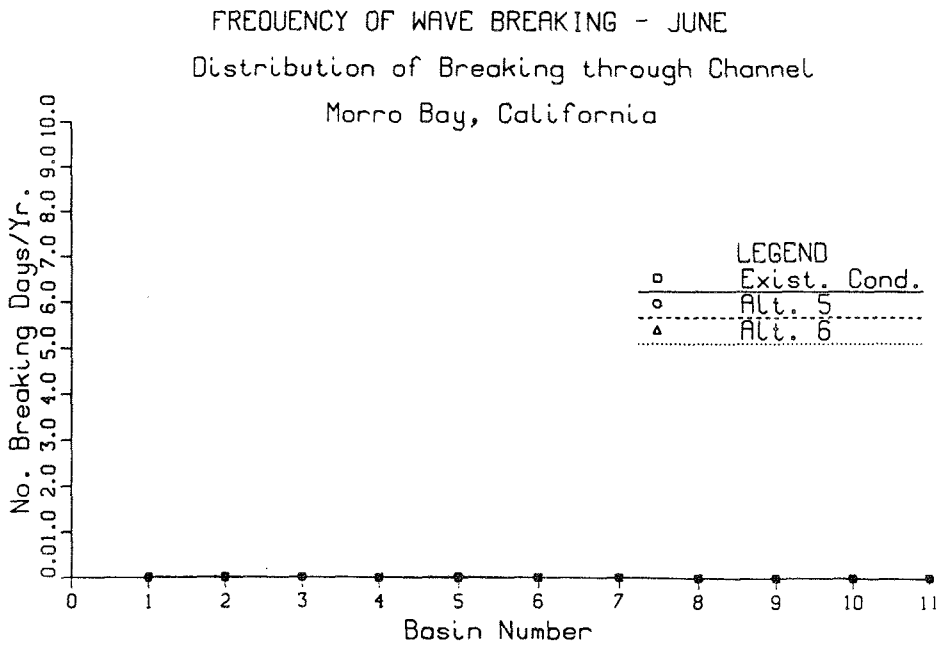

Figure B-48.

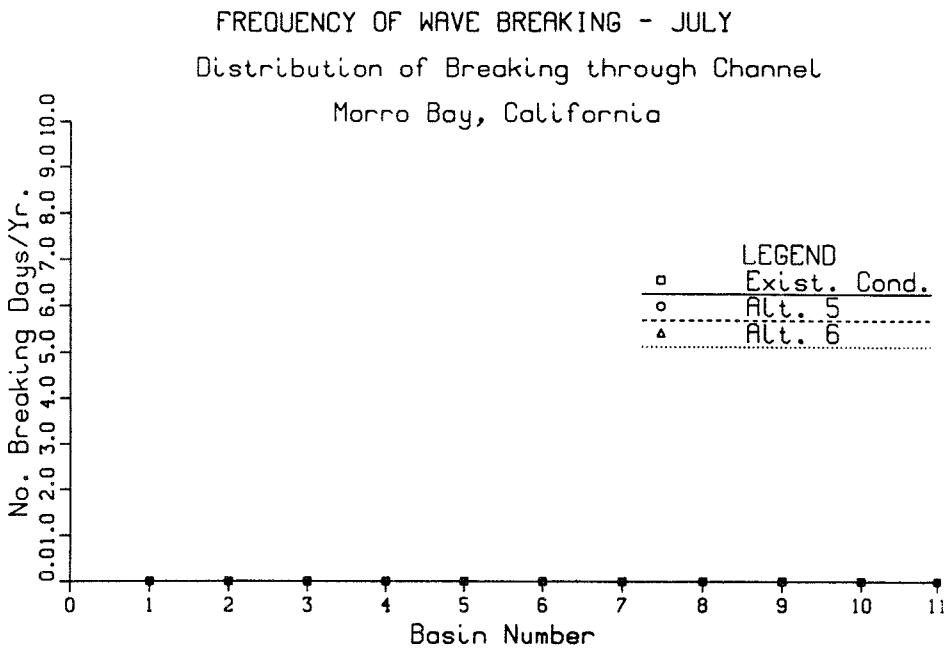

Figure B-49.

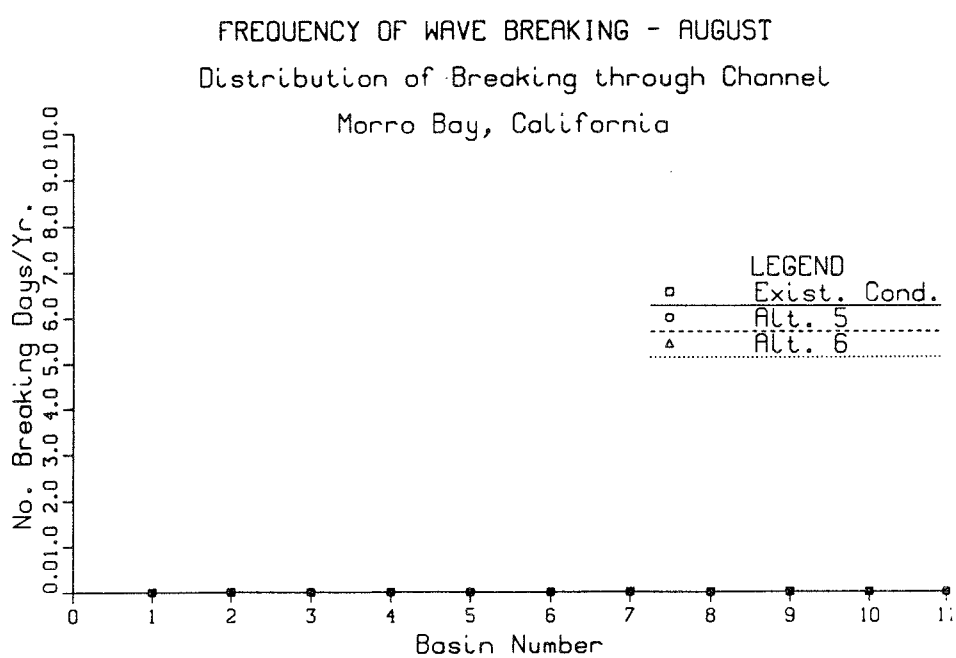

Figure B-50.

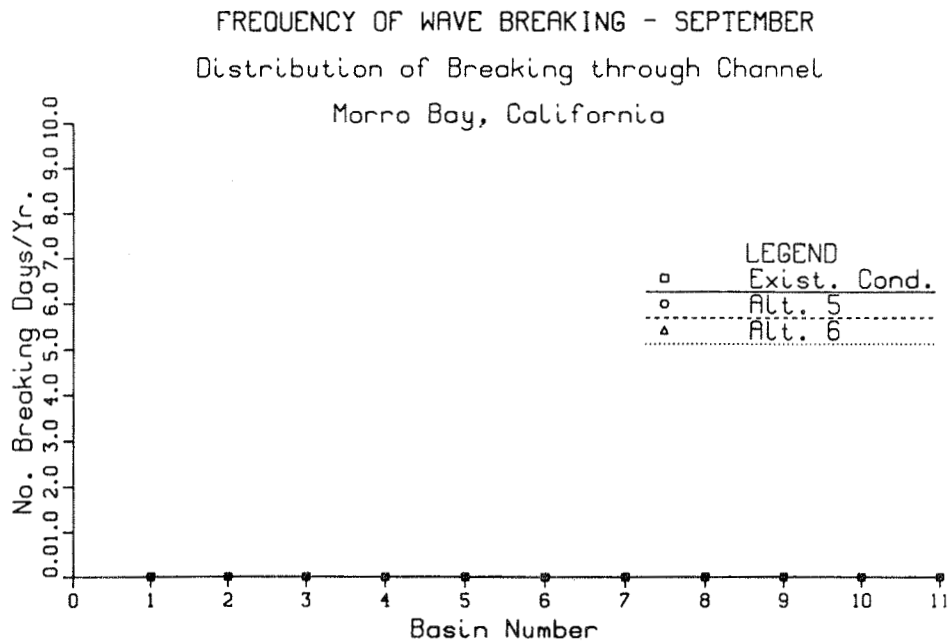

Figure B-51.

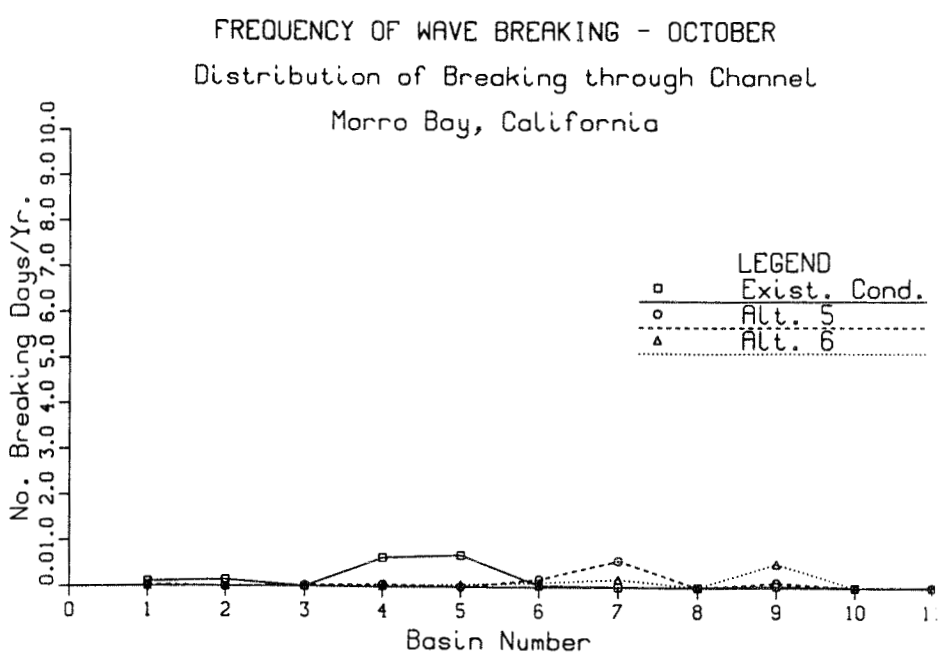

Figure B-52.

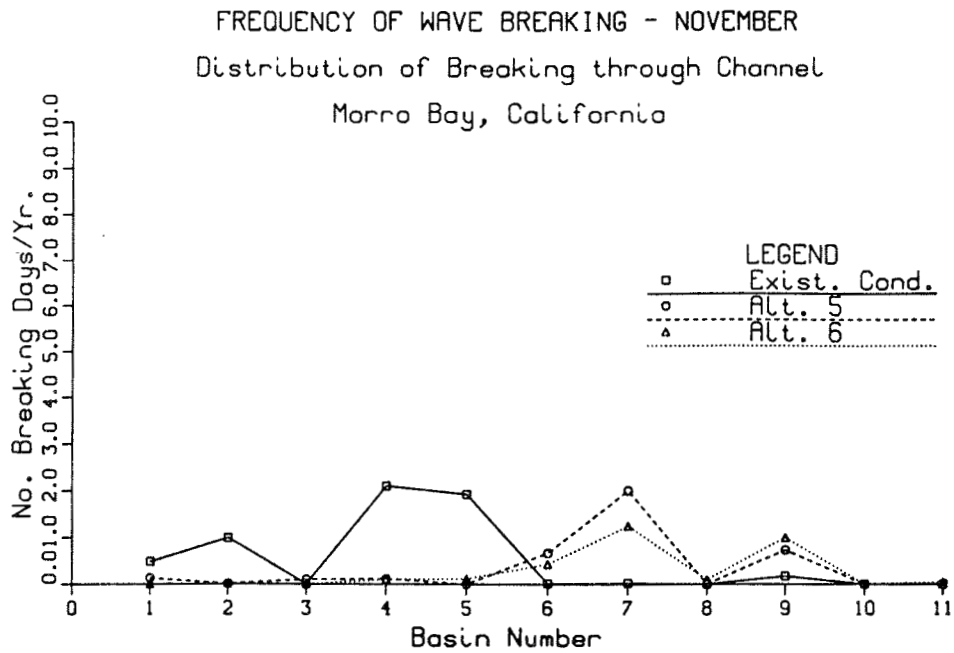

Figure B-53.

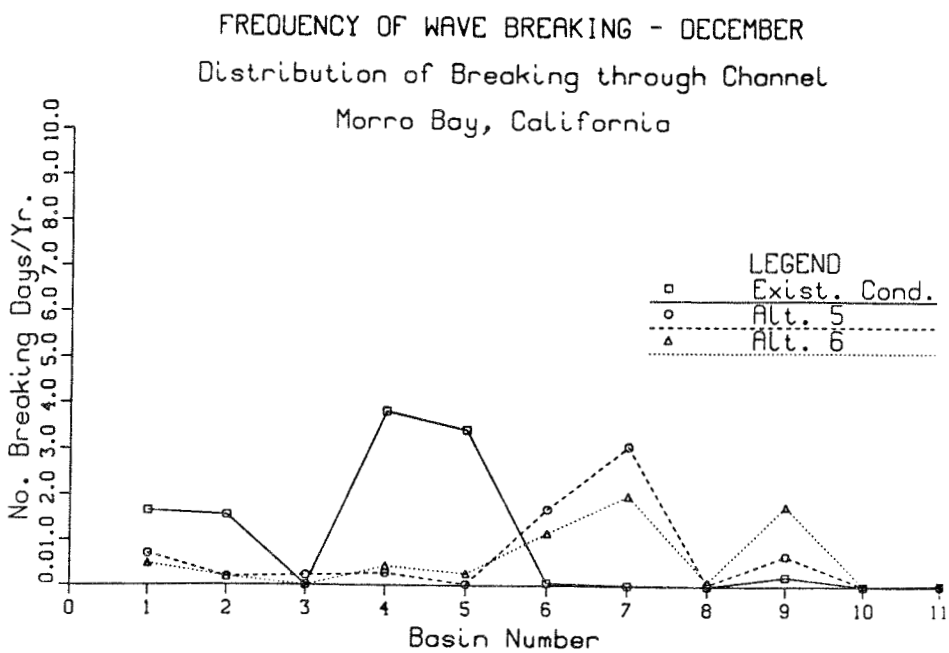

Figure B-54.

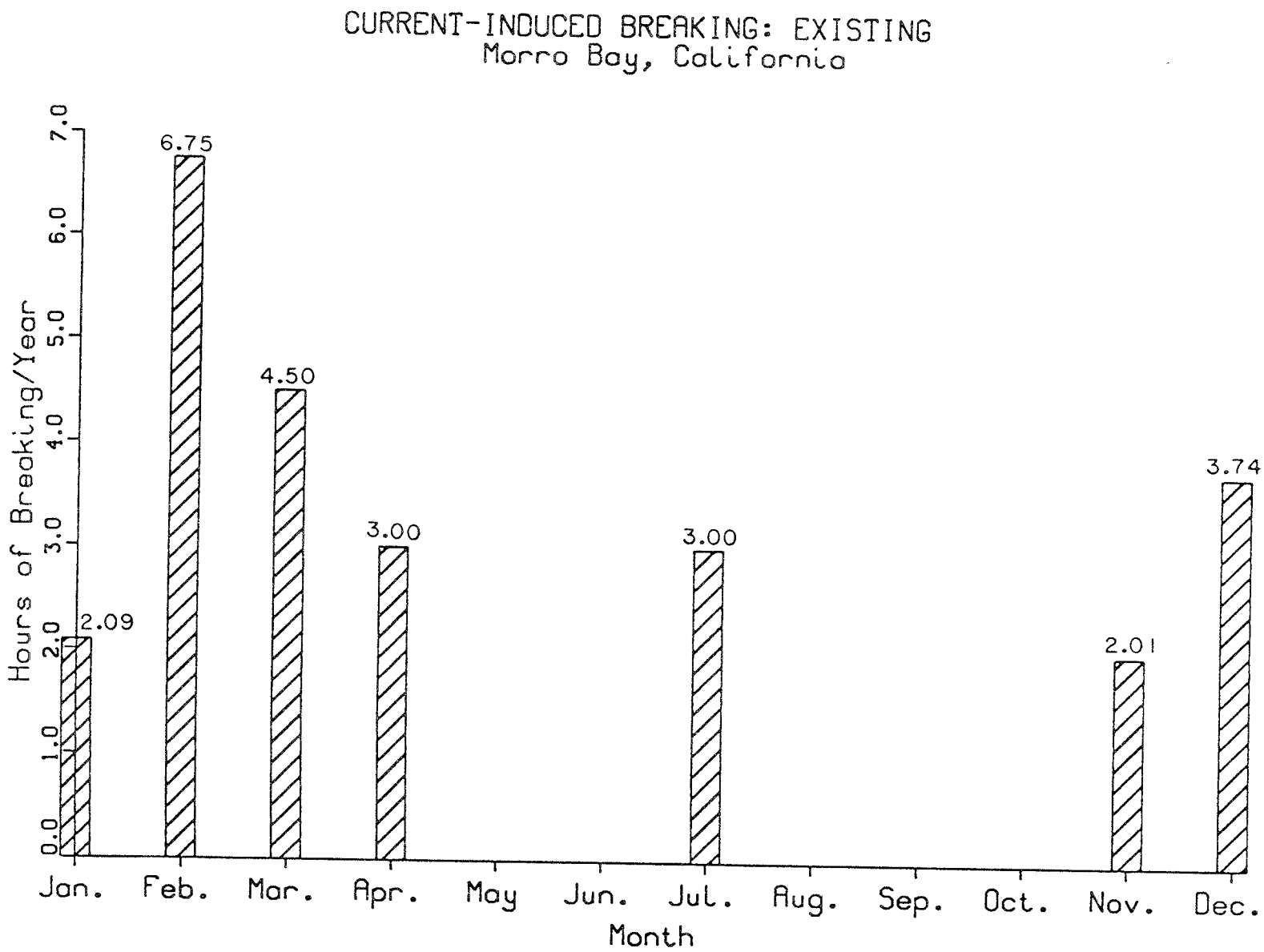

Figure B-55. Hours of Maximum Current-Induced Breaking - Ex. Cond.

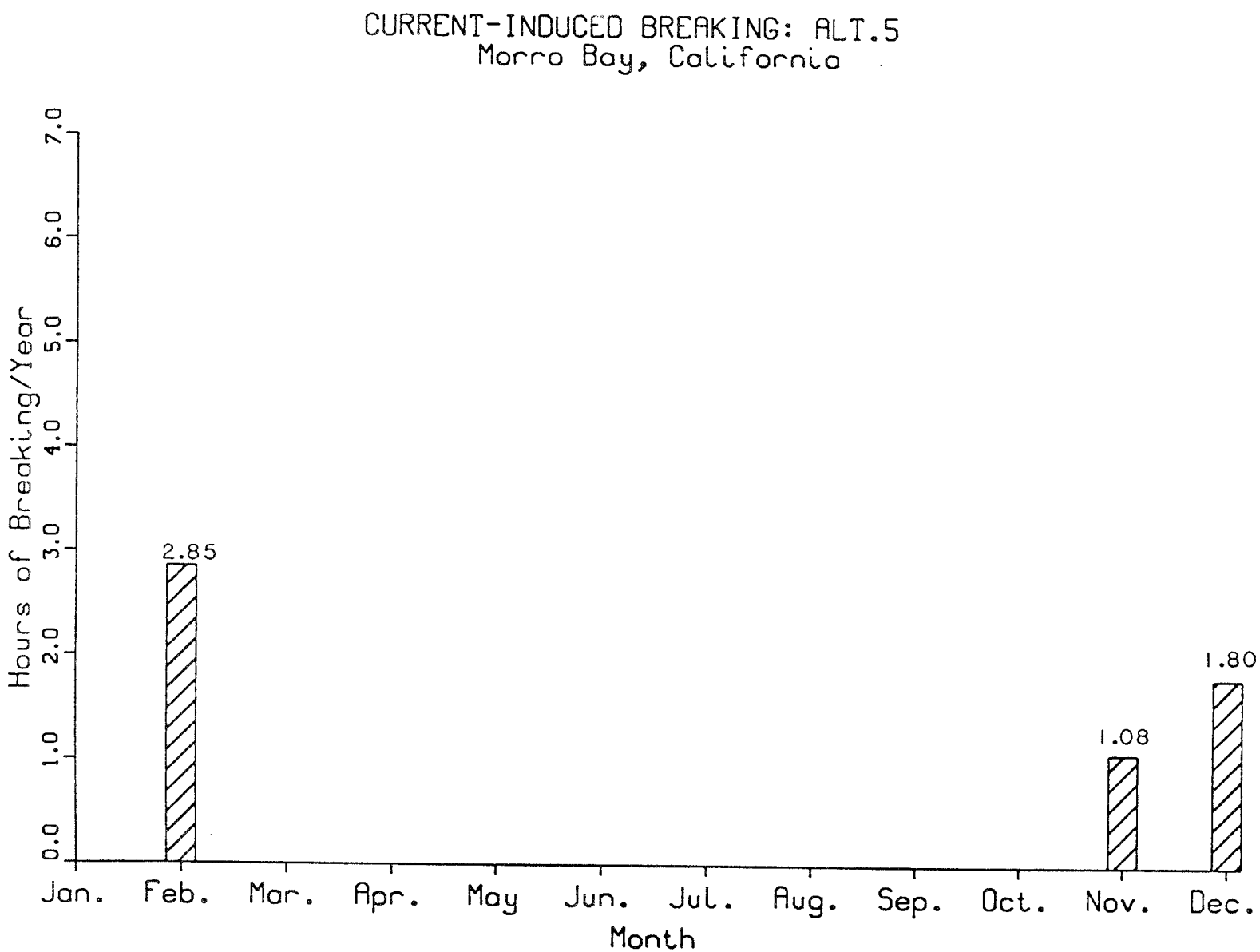

Figure B-56. Hours of Maximum Current-Induced Breaking - Alt. 5

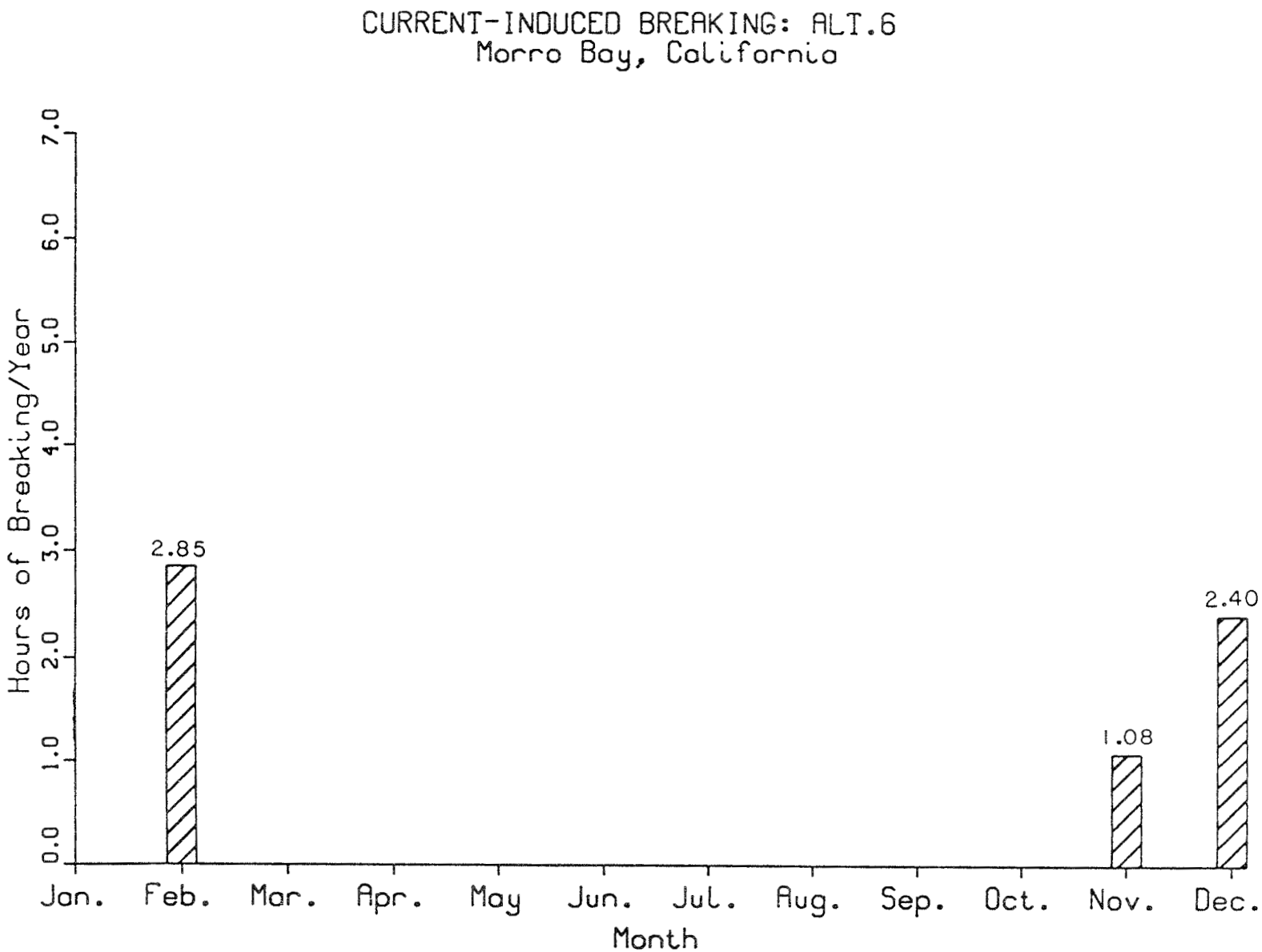

Figure B-57. Hours of Maximum Current-Induced Breaking - Alt. 6

APPENDIX C: LONGSHORE TRANSPORT ANALYSIS

Table C-1. Sediment Transport Analysis Results - North Beach

Potential Sediment Transport Rates - Morro Bay, Ca.
North Beach Source - Southerly Transport

Month	Sea Trans. (cu.yd./mo.)	Swell Trans. (cu.yd./mo.)	Southern Swell Trans. (cu.yd./mo.)
Jan.	6.79	0	0
Feb.	31.74	0	0
Mar.	2673.99	0	0
Apr.	6340.21	0	0
May	2074.81	0	0
Jun.	1501.10	0	0
Jul.	1562.91	0	0
Aug.	857.96	0	0
Sep.	73.28	0	0
Oct.	427.48	0	0
Nov.	72.97	0	0
Dec.	1050.91	0	0

Grand Total: 16674 cu. yd./yr. towards harbor

Table C-2. Sediment Transport Analysis Results - South Beach

Potential Sediment Transport Rates - Morro Bay, Ca.
South Beach Source - Northerly Transport

Month	Sea Trans. (cu.yd./mo.)	Swell Trans. (cu.yd./mo.)	Southern Swell Trans. (cu.yd./mo.)
Jan	41924.59	4304.43	46.24
Feb	49595.11	7363.09	34.04
Mar	17296.55	515.64	18.76
Apr	7841.21	14.09	398.79
May	438.71	18.15	1490.29
Jun	34.59	0.40	2042.04
Jul	27.24	0.00	2004.33
Aug	2.27	0.00	1564.15
Sep	835.78	6.58	2181.07
Oct	8791.72	148.43	199.34
Nov	8242.09	199.97	953.65
Dec	37059.14	1936.09	140.45

Grand Total: 197669 cu.yd./yr. towards harbor

APPENDIX D: NOTATION

A	Cross-sectional area
a	Wave amplitude function; also, breaking criterion parameter
a_o	Incident wave amplitude
b	Breaking criterion parameter
C	Wave celerity
C_g	Group celerity
E_a	Longshore energy flux in millions of ft-lb/day per foot of beach
g	Gravitational acceleration
H	Wave height
(H/L)	Maximum wave steepness
i	Offshore cell index; also imaginary number = $(-1)^{1/2}$
j	Longshore cell index
K_r	Reflection coefficient
k	Wave number = $2\pi/L$; also, index for the number of a wave in a set of W waves
L	Wavelength
M	Total number of offshore cells
N	Total number of waves breaking in cell j
n	Unit-normal vector directed outward from the water regions
P_{ls}	Longshore flux factor in lb-ft/sec per foot of beach
Q	Potential sediment transport rate
s	Wave phase function
T	Wave period
U	Current velocity
W	total number of waves in a set
wt_k	percent occurence of kth wave divided by 100

x	horizontal coordinate
y	horizontal coordinate
α	Reflective component of absorbing baoundary
β	Dimensionless bottom friction coefficient
γ	Phase difference between bottom friction and flow velocity
θ	Wave approach angle
λ	Complex bottom friction factor
π	3.14159.....
ρ	Mass density of sea water
σ	Wave frequency, intrinsic wave frequency
ϕ	Velocity potential
Ω	Absolute wave frequency

Subscripts:

A	Denotes stationary reference frame
"A-A"	Denotes application at cross-section "A-A" of Figure 1
b	Denotes conditions at breaking
ent	Denotes application at harbor entrance
I	Denotes moving reference frame

Mathematical symbols:

∂	Partial differentiation
∇	Gradient operator in two dimensions = $(\partial/\partial x + \partial/\partial y)$
$\sum$	Summation